AUTOMATED IMPACT DEVICE BASED ON PHASE SYNCHRONISATION ASSESSMENT FOR THE ENHANCEMENT OF IMPACT-SYNCHRONOUS MODAL ANALYSIS DURING OPERATION

LIM HONG CHEET

FACULTY OF ENGINEERING
UNIVERSITY OF MALAYA
KUALA LUMPUR

2018

AUTOMATED IMPACT DEVICE BASED ON PHASE SYNCHRONISATION ASSESSMENT FOR THE ENHANCEMENT OF IMPACT-SYNCHRONOUS MODAL ANALYSIS DURING OPERATION

LIM HONG CHEET

THESIS SUBMITTED IN FULFILMENT OF THE REQUIREMENTS FOR THE DEGREE OF DOCTOR OF PHILOSOPHY

FACULTY OF ENGINEERING
UNIVERSITY OF MALAYA
KUALA LUMPUR

2018

UNIVERSITY OF MALAYA

ORIGINAL LITERARY WORK DECLARATION

Name of Candidate: Lim Hong Cheet

Matric No: KHA 140095

Name of Degree: Doctor of Philosophy (PhD.)

Title of Project Paper/Research Report/Dissertation/Thesis ("this Work"):

Automated Impact Device based on Phase Synchronisation Assessment for the Enhancement of Impact-synchronous Modal Analysis during Operation

Field of Study: Engineering Design

I do solemnly and sincerely declare that:

(1) I am the sole author/writer of this Work;
(2) This Work is original;
(3) Any use of any work in which copyright exists was done by way of fair dealing and for permitted purposes and any excerpt or extract from, or reference to or reproduction of any copyright work has been disclosed expressly and sufficiently and the title of the Work and its authorship have been acknowledged in this Work;
(4) I do not have any actual knowledge nor do I ought reasonably to know that the making of this work constitutes an infringement of any copyright work;
(5) I hereby assign all and every rights in the copyright to this Work to the University of Malaya ("UM"), who henceforth shall be owner of the copyright in this Work and that any reproduction or use in any form or by any means whatsoever is prohibited without the written consent of UM having been first had and obtained;
(6) I am fully aware that if in the course of making this Work I have infringed any copyright whether intentionally or otherwise, I may be subject to legal action or any other action as may be determined by UM.

Candidate's Signature Date: 17 July 2018

Subscribed and solemnly declared before,

Witness's Signature Date:

Name:

Designation:

DEVELOPMENT OF AUTOMATED IMPACT DEVICE BASED ON PHASE SYNCHRONISATION ASSESSMENT FOR THE ENHANCEMENT OF IMPACT-SYNCHRONOUS MODAL ANALYSIS DURING OPERATION

ABSTRACT

Impact-synchronous Modal Analysis (ISMA) integrated with Impact-synchronous Time Averaging (ISTA) was introduced as a viable option for existing modal analysis techniques during operation. However, ISMA using manual impact hammer required a high number of impacts for better Frequency Response Functions (FRFs) estimation especially when the operating frequencies coincided with the natural modes. This finding has subsequently reduced the effectiveness and practicality of ISMA. Lack of control of impact timing using manual impact hammer has initiated phase synchronisation effect investigation and subsequent to the designs of auto impact device with different controlled impact events in order to fill the gaps from previous research. Firstly, phase synchronisation effect in ISMA during operation is investigated as in simulation studies and experimental testing. The assessment showed that a small amount of averaging, (i.e. up to 5 averages) is sufficient to eliminate the non-synchronous components by 98.48% on simulation and 95.22% on experimental modal testing under inconsistent phase condition. To enhance ISMA, it is known from the assessment that each impact applied must be non-synchronous with the periodic response of cyclic load. Thus, the auto impact device with non-synchronous impacts is designed where the impact frequency is a non-integer multiple of operating frequency. Implementation of this device in ISMA has reduced the dominant cyclic load component and second harmonic up to 45% and 17% respectively. Subsequently, all natural modes of interest are identified which is not achievable through manual impact hammer. Although the FRFs estimation is enhanced, a sharp peak originated from cyclic load is still observable. Hence, further reduction of cyclic load components is continued through a post-processing inconsistent phase

selection assessment. When the selected impacts are non-synchronous with the cyclic load components, i.e., two pairs of data where the selected impacts in each pair is 180° difference, four averages or impacts are sufficient to reduce the first and second harmonics up to 82% and 52% respectively. Thus, the estimated FRF is strongly enhanced and good correlation is observed between modal extraction data and benchmark EMA. Utilising the outcomes from the assessment, a feedforward Automated Phase Controlled Impact Device (APCID) is designed in such a way that it is capable to adapt the updated phase difference information based on the electrical pulse signal of tachometer in each triggered time block of signal and uses this information to control the correct timing to impart an impact at the correct time/phase which is always non-synchronous with respect to the periodic response of cyclic load. Applying impact on the crest or trough or any phase position of the sinusoidal response due to cyclic load is then possible. Implementation of APCID in ISMA has reduced the first and second harmonics up to 92% and 55% respectively. In overall, a reduced number of averages thereby expedite the overall operational modal testing procedure, an improved of FRFs estimation and a good correlation of modal extraction data with benchmark data shown in this research has highlighted the advantages of ISMA using auto impact device based on phase synchronisation assessment.

Keywords: Automated impact device, Harmonic component, Impact-synchronous modal analysis, Impact-synchronous time averaging, Modal parameters

PEMBANGUNAN ALAT IMPAK AUTOMATIK BERDASARKAN PENILAIAN KESEGERAKKAN FASA DALAM PENAMBAHBAIKAN IMPACT-SYNCHRONOUS MODAL ANALYSIS SEMASA KEADAAN OPERASI

ABSTRAK

Satu kaedah novel telah diperkenalkan, iaitu "Impact-synchronous Modal Analysis" (ISMA) dengan mengintegrasikan "Impact-synchronous Time Averaging" (ISTA) sebagai alternatif lain kepada teknik yang sedia ada dalam keadaan operasi. Walau bagaimanapun, kaedah ISMA yang menggunakan tukul impak manual memerlukan bilangan purata impak yang tinggi untuk menganggarkan "Frequency Response Functions" (FRFs) terutamanya apabila frekuensi operasi bertepatan dengan mod semula jadi. Kelemahan ini mengakibatkan kurangnya keberkesanan dalam penggunaan kaedah ISMA. Kurangnya kawalan ke atas masa impak sewaktu menggunakan tukul impak secara manual telah mencetus idea kepada penyiasatan ke atas kesan fasa segerak dan seterusnya mereka bentuk alat impak auto dengan ciri-ciri impak terkawal yang berbeza untuk mengisi jurang penyelidikan. Pertama, kesan fasa segerak dalam ISMA dalam keadaan operasi dikaji menerusi kajian simulasi dan ujian eksperimen. Penilaian ini menunjukkan bahawa bilangan purata impak yang kecil (sehinggga 5 purata impak) adalah mencukupi untuk menapis komponen-komponen yang tidak segerak dengan peningkatan sebanyak 98.48% dalam simulasi dan peningkatan sebanyak 95.22% dalam kajian fasa tidak konsisten. Hasil pernilaian ini telah menunjukkan untuk penambahbaikan ISMA, setiap impak yang diaplikasikan haruslah tidak segerak dengan respon dari beban kitaran. Dengan itu, alat impak auto direka bentuk di mana frekuensi impak adalah selain daripada gandaan frekuensi operasi. Penggunaan peranti ini telah mengurangkan komponen beban kitaran dominan dan harmonic kedua hingga 45% and 17%. Hasilnya, semua mod semula jadi dapat dikenal pasti di mana hal ini tidak dapat dicapai melalui tukul impak secara manual dan impak secara rawak dengan menggunakan

alat impak auto. Walaupun anggaran FRFs diperbaiki namun puncak tajam yang terhasil dari beban kitaran masih dapat dilihat. Oleh itu, pengurangan komponen-komponen beban kitaran diteruskan melalui penilaian pemilihan fasa pasca pemprosesan. Apabila impak yang dipilih tidak segerak dengan komponen-komponen beban kitaran, iaitu apabila dua pasang data dengan impak terpilih dalam setiap pasangan mempunyai perbezaan fasa 180°, empat purata atau impak adalah mencukupi untuk mengurangkan harmonik-harmonik pertama dan kedua sehingga 82% dan 52%. Oleh itu, FRFs yang dianggarkan berjaya diperbaiki dan hubungan yang lebih baik terhasil antara data pengeluaran "modal" dan hasil analisis kajian daripada penanda aras EMA. Hasil daripada ujikaji ini, satu peranti iaitu "Automated Phase Controlled Impact Device" (APCID) yang menggunakan kawalan "feedforward" telah direka, dimana peranti ini mampu menyesuaikan maklumat perbezaan fasa yang dikemaskini berdasarkan isyarat pulsa elektrik tachometer dalam setiap blok signal yang dicetuskan dan menggunakan maklumat ini untuk mengawal masa yang betul untuk mengaplikasikan impak yang tidak segerak dengan respon dari beban kitaran. Dengan ini, aplikasi impak pada puncak atau palung atau sebarang kedudukan fasa ke atas tindak balas sinusoidal yang disebabkan oleh beban kitaran dapat dijalankan. Penggunaan peranti ini dalam ISMA telah mengurangkan harmonik pertama dan kedua hingga 92% dan 55%. Akhirnya, hubungan yang lebih baik dapat diperolehi di antara data pengeluaran "modal" dengan hasil analisis kajian daripada penanda aras EMA. Secara keseluruhannya, pengurangan bilangan purata impak dapat mempercepatkan prosedur pengujian "modal operasi", malah, penambahbaikkan penganggaran FRF dan hasil hubungan yang lebih baik antara data pengeluaran "modal" dengan hasil analisis kajian penanda aras EMA telah berjaya menonjolkan kelebihan ISMA menggunakan alat impak auto berdasarkan penilaian kesan fasa segerak.

Kata kunci: Alat impak auto, Data pengeluaran “modal”, Impact-synchronous Modal Analysis, Impact-synchronous Time Averaging, Komponen harmonik

ACKNOWLEDGEMENTS

I would like to take this opportunity to express my heartfelt thanks to all the people who were instrumental in guiding me throughout this post-graduate study.

First of all, I would like to express my deepest appreciation to my supervisors Ir. Dr. Ong Zhi Chao, Prof. Dr. Zubaidah Binti Ismail and Dr. Khoo Shin Yee of University of Malaya, for their patience, guidance, motivation, invaluable assistance and encouragement throughout the course of this project and in the preparation of this thesis. Their taught and enlightenment will always be remembered and thankful of.

Many thanks to Mr. Lee Ching Heng, Mr. Kong Sung Chuan, Mr. Chew Yi of Mechanical Engineering Department for the collaboration, help in the measurement done and precious sharing of knowledge and experience. Not forgetting special thanks to all the staffs, fellow friends, technicians and clerks of Mechanical Engineering Department. I am grateful and wish to acknowledge the financial support and advice given by University of Malaya Research Grant (RP022D-2013AET), Fundamental Research Grant Scheme (FP010-2014A), Postgraduate Research Grant (PG011-2015A), Advanced Shock and Vibration Research (ASVR) Group of University of Malaya.

Lastly, I would like to thank my beloved family for all their support, love, care and patience. All their loves and trust has been an energy boost for me and enlightens my life.

TABLE OF CONTENTS

LIST OF FIGURES

LIST OF TABLES

LIST OF SYMBOLS AND ABBREVIATIONS

Symbol

ω	:	Angular frequency /cyclic load frequency
ω_{dr}	:	Damped natural frequency of mode r
β	:	Phase angle
β_1	:	Phase of the desired deterministic response signal due to impact
β_2	:	Phase of the undesired deterministic signal of the periodic response of cyclic load
Φ_a	:	Phase difference
Φ_p	:	Desired impact phase angle
σ_r	:	Decay rate of mode r
Δt	:	Time difference
a	:	Amplitude of the signature
a_r	:	Amplitude of mode r
A	:	Amplitude of the signature
A_r	:	Amplitude of mode r
b	:	Amplitude of the signature
b_r	:	Amplitude of mode r
BS	:	Block size
DC	:	Duty cycle
$e(t)$	:	Summation of deterministic signal of periodic response of cyclic load with random ambient noises
f	:	Measured input disturbance
f_1	:	Amplitude of the undesired deterministic signal of the periodic response of cyclic load

f_{impact}	:	Impact frequency
f_{square}	:	Frequency of the square wave
g_1	:	Amplitude of the undesired deterministic signal of the periodic response of cyclic load
i_{rise}	:	Array index of rising edge
k	:	Number of impact/averages
L_{exp}	:	Experimental impact location (set-point)
L_{real}	:	Impact location (process output)
n	:	Maximum number of modes
n_{lc}	:	Number of load cycles added
n_{square}	:	Number of cycle of square wave in a time block
n_{tbl}	:	Number of time block length
N	:	Total number of impacts
N_{active}	:	Number of block which is active pulse
$p(t)$	:	Sinusoidal signature
$q(t)$	:	Desired deterministic response signal due to impact
r	:	Number of natural mode
R_2	:	Amplitude of the undesired deterministic signal of the periodic response of cyclic load
SR	:	Sampling rate
S_{comp}	:	Compensate sample (value of 1)
S_{ext}	:	Extracted samples from the end of time block
t_{block}	:	Time response block
t_{exp}	:	Experimental impact time before offset adjustment
t_{on}	:	Solenoid ‘On’ time

t_{pulse}	:	Length of time for active pulse
t_{real}	:	Real impact time observed in the response signal
T_0	:	Time interval between impacts
$T_{counter}$	:	Actual counter time
T_{cycle}	:	Time interval of load cycles
$T_{desired}$	:	Time interval of desired impact
T_{impact}	:	Impact interval
T_{lag}	:	Lag time
T_{offset}	:	Time delay taken by the impact device to impart on the surface of structure after "On" signal
T_{square}	:	Period of the square wave
T_{trig}	:	Triggering interval
T_{Φ}	:	Phase difference time
$x(t)$	:	Vibration signal in time domain/total time response
$y(t)$	:	Averaged vibration signal in time domain

Abbreviation

3D	:	Three Dimensions
APCID	:	Automated Phase Controlled Impact Device
ARMA	:	Autoregressive Moving-average
CE	:	Complex Exponential
CEFD	:	Complex Exponential Frequency Domain
DAQ	:	Data Acquisition
DOF	:	Degree of Freedom
DSPI	:	Direct System Parameter Identification
EFDD	:	Enhanced Frequency Domain Decomposition

EMA	:	Experimental Modal Analysis
ERA	:	Eigensystem Realization Algorithm
ERA-FD	:	Eigensystem Realization Algorithm in the Frequency Domain
FDD	:	Frequency Domain Decomposition
FFT	:	Fast Fourier Transform
FRF	:	Frequency Response Function
GSH	:	Gaukroger-Skingle-Heron
IRF	:	Impulse Response Functions
ISMA	:	Impact-synchronous Modal Analysis
ISTA	:	Impact-synchronous Time Averaging
ITD	:	Ibrahim Time Domain
LSCE	:	Least Squares Complex Exponential
MAC	:	Modal Assurance Criterion
NExT	:	Natural Excitation Technique
NI	:	National Instruments
NN	:	Neural Network
ODS	:	Operating Deflection Shape
OMA	:	Operational Modal Analysis
OMAH	:	Operational Modal Analysis with eXogenous Inputs (Harmonic Excitation)
OMAX	:	Operational Modal Analysis with eXogenous Inputs
OSK	:	Optimized Spectral Kurtosis
p-TOMA	:	Polyreference Transmissibility Measurement based Operational Modal Analysis
PDF	:	Probability Density Function
PolyMAX	:	Poly-Least Squares Complex Frequency Domain

PP	:	Peak-picking
PRCE	:	Polyreference Complex Exponential
PRFR	:	Polyreference Frequency Domain
RD	:	Random Decrement
RFP	:	Rational Fraction Polynomial
SISO	:	Single Input Single Output
SLDV	:	Scanning Laser Doppler Vibrometry
SNR	:	Signal to Noise Ratio
SSI	:	Stochastic Subspace Identification
SSTD	:	Single Station Time Domain
TFDD	:	Time-frequency Domain Decomposition
TOMA	:	Transmissibility Measurement based Operational Modal Analysis
TSA	:	Time Synchronous Averaging
UM	:	University of Malaya
USB	:	Universal Serial Bus

LIST OF APPENDICES

CHAPTER 1: INTRODUCTION

1.1 Introduction

The chapter begins with Section 1.2 by presenting the background on the evolution of modal analysis techniques, i.e., from classical Experimental Modal Analysis (EMA), to Operational Modal Analysis (OMA) and so to Impact-synchronous Modal Analysis (ISMA). Section 1.3 has identified the problem statement from previous works which is then became the motivation for this research study and the novelty of the study is shown in Section 1.4. Section 1.5 has listed four objectives to be achieved and the contributions from each objective are elaborated in Section 1.6 and lastly, the thesis outline are shown in Section 1.7.

1.2 Background

Common problems related to vibrations occur due to inherent unbalance in the engines for prime movers, in blade and disk vibrations on turbines, and in reciprocating machines, etc. Vibration problems are often extra serious when the frequency of the excessive vibration coincides with the natural frequency of the structure. In this case, the response of the structure is amplified causing excessive deflections which in some cases can cause immediate failure. Thus, it is valuable to know how an operating system responds to a harmonic excitation. In general, the response of a structure to harmonic vibration coinciding with a natural frequency, depends on three factors which are; (i) the amount of damping, (ii) the excitation frequency, and (iii) the relationship between the mode shape coefficients in the excitation and the response points (William, 1998).

Modal analysis is an important and established tool in various engineering fields that can be used to address such vibration cases. Engineers utilise the modal parameters obtained from modal analysis which are natural frequencies, damping ratios, and mode shapes (Avitabile, 2001; Fayyadh & Razak, 2013) in designing structures or machines to

get the desired characteristics, as well as to obtain high efficiency during operation. The two most widely used modal analysis techniques are EMA and OMA. EMA describes the dynamic characteristics of the system based on measured input and output data. The analysis can be carried out either in the time domain or frequency domain, depending on user convenience. However, there is a significant constraint of using this technique as the systems or machines are not allowed to operate. In the oil and gas industry, for example, production downtime can equate to hundreds of thousands dollar loss per day, and thus it is not feasible to shut down the machinery under testing to perform EMA.

In practice, when the structure is excited by external or internal dynamic forces, e.g. a wind excited building or bridge, engine vibration excited cars or machines, OMA is preferred over EMA. OMA, also known as output-only modal analysis or ambient modal analysis, is a suitable technique when a machine or system cannot be shut down for EMA purposes. OMA does not require the input excitation to be measured, but only the output responses. Thus, the total time and cost required for the modal analysis test are greatly reduced. A limitation with OMA for the purpose of achieving the sensitivity of a structure to harmonic loading is that it does not result in scaled mode shapes, and thus cannot answer what a machine's sensitivity is to a particular (harmonic) force.

A method, namely ISMA using Impact-synchronous Time Averaging (ISTA) was introduced as an alternative to EMA and OMA. ISTA reduces the asynchronous signals, i.e., cyclic load component and its harmonics and random noise, while preserving the desired responses due to impact in the time window. The major difference between ISMA and other techniques is that the input excitation force is measurable while performing modal testing during operation. This ensures that all the important system characteristics are recorded. In the post-processing analysis stage, ISMA utilises the same modal parameters extraction technique as in EMA. Thus, ISMA is a sort of hybrid between EMA

and OMA, possessing the positive characteristics of both. As reported in (Ong et al., 2016; Rahman et al., 2014), the effectiveness of ISMA is governed by four parameters, i.e., exponential windowing function, impact force level, number of averages, and phase synchronisation effect.

1.3 Problem Statement and Motivation

Previous research experimentally demonstrated that the number of averages or impacts had a very important effect when applying ISMA on structures with dominant periodic responses of cyclic loads and ambient excitation (Rahman et al., 2014). However, it was found that at operating frequencies that coincided with the natural modes, ISMA with random impacts required a high number of impacts to determine the dynamic characteristics of the system. This is probably due to the lack of information of phase angles with respect to impact and it has subsequently reduced the effectiveness and practicality of ISMA. Remark that although phase synchronisation effect was first reported in (Ong, 2013), this pioneering work was merely proven in the simulation study. A more-thorough study of phase synchronisation on the effectiveness of ISMA during operation has not been reported so far.

Nowadays, it is quite common to use automated impact device in modal testing. In fact, this excitation device can guarantee three conditions which are almost impossible to achieve by using manual impact hammer; (i) consistent impact force and impact location, (ii) reduced human error such as double impact, and (iii) reduce human power since it is fully automated. A literature by the similar author on the use of automated impact device was shown in (Ong & Lee, 2015). In this literature, an automated impact device was introduced for the purpose of improving the practicality in ISMA through continuously imparting non-synchronous impacts. This literature looked into several important characteristics, i.e., impact period, impact level, impact contact time, isolation effect of

the device, and found that this device is effective, precise, robust, and reliable in the experimental testing during static condition. Nevertheless, this device has yet to be tested in operational modal testing. All in all, the effect of phase synchronisation on the effectiveness of ISMA is still an open question and remains to be investigated. Table 1.1 has summarised the research gap between previous research and current research.

Table 1.1: Research Gap between Current Study and Previous Study

No	Subject	Previous Research	Research Gap	Current Research
1	Modal analysis technique	EMA required the complete shutdown of the system while OMA is applicable only to the operating system. Besides, the advancement of these methods is shown in the post-processing of signals, e.g., modal identification algorithms. The effectiveness of ISMA on the static system was encapsulated in (Ong & Lee, 2015).	The effectiveness of modal analysis technique which focuses on the digital signal processing upstream of the collected data rather than the modal identification algorithm has not been fully validated especially on the operating system.	Intensive study on the effectiveness of ISMA on the operating system in the presence of dominant harmonic disturbances/components.
2	Phase synchronisation effect	Focus on parameters, i.e., number of averages, windowing function, and impact force, on the effectiveness of ISMA (Ong et al., 2016; Rahman et al., 2014).	A thorough study of phase synchronisation effect on the effectiveness of ISMA has not been reported.	Intensive study of phase synchronisation effect on the effectiveness of ISMA. This includes integrating the findings into both post-processing inconsistent phase selection assessment

Table 1.1: Continued

				and real-time manner (automated impact device with controlled impact events).
3	Excitation device in EMA and ISMA	Existing automated impact devices controlled by a simple "On" and "Off" state has proven to be a viable alternative to manual impact hammer in static condition in the effort to improve measurement accuracy, for instance, human error such as double impact could be avoided (Jannifar et al., 2017; Ong & Lee, 2015).	These devices have not been tested so far on the operating system, particularly in the effort to eliminate the dominant harmonic disturbances/ components, (i.e., cyclic load component and its harmonic) and random noise.	Implementation of automated impact device with non-synchronous impacts and Automated Phase Controlled Impact Device (APCID) using feedforward control in ISMA during operation.

1.4 The Novelty

It is most meaningful where less time, reduced human error, and expense are required to obtain complete and clean data when compared to existing modal analysis technique. At the end of this research, ISMA method may be expected to apply to a broad range of applications in various engineering disciplines, for example, damage identification, finite element model updating, force identification, structural dynamic modification, etc., to whether the system is in static or operating condition.

1.5 Research Objectives

The focus of this study is to enhance the effectiveness of ISMA during operation through the investigation of phase synchronisation effect and subsequently with the use of automated impact device. There are four objectives in conjunction with the problem statements mentioned in Section 1.3 which are listed below:

i. To investigate the phase synchronisation effect in ISMA during operation.
ii. To validate the effectiveness of ISMA during operation using automated impact device with non-synchronous impacts.
iii. To propose a post-processing inconsistent phase selection assessment for the enhancement of ISMA during operation.
iv. To develop an automated impact device with inconsistent phase selection capability, i.e., APCID and to validate the effectiveness of ISMA during operation using APCID.

1.6 Research Contributions and its Significance

This section provides the reader with a comprehensive understanding on the contributions and significance of each objective.

i. In the first objective, the aim is to demonstrate the significance of phase angle with respect to impact in the determination of dynamic characteristics. Basically, there are only two situations to be considered, i.e., consistent and inconsistent phase condition. The contribution from this objective is that it forms a fundamental idea throughout the research in which synchronisation of phases between responses due to impact and the periodic responses of cyclic loads should be avoided to enhance the effectiveness of ISMA.
ii. In the second objective, an automated impact device with controlled impact event, i.e., non-synchronous impacts excitation is introduced in ISMA in

accordance with the findings from objective one. The device is designed so that the impact interval is a non-integer multiple of the operating frequency in the effort to filter out all the non-synchronous components. Remark that this is the very first time to implement such device in operational modal testing, particularly in the effort to reduce the harmonic disturbances.

iii. In the third objective, a post-processing inconsistent phase selection assessment is proposed aiming to find a detailed relationship tailored between the phase angle of the cyclic load component with respect to impact applied for subsequent elimination of dominant cyclic load component as well as its harmonics. The assessment allows selection of responses due to impact based on phase position on the periodic response of cyclic load. By a careful selection of the responses due to impact in conjunction with the fundamental concept, i.e., two identical waves with 180 degrees out of phase (anti-phase) will completely cancel each other in block averaging, the assessment could provide some insight not only on reducing the dominant cyclic load component, but also its harmonics.

iv. In the fourth objective, a feedforward control automated impact device namely APCID is designed utilising the findings from objective three. This device is capable to adapt the updated phase difference information based on the electrical pulse signal of the tachometer in each triggered time block of signal and uses this information to control the correct timing to impart an impact. This represents an additional advantage where applying impact on the crest or trough or any phase position of the sinusoidal response due to cyclic load is then possible. Thus, implementation of this device in ISMA is thus a key breakthrough where harmonic disturbances could be eliminated with minimal average in a real-time manner.

1.7 Thesis Outline

The thesis consists of five chapters. Chapter 1 introduces the problem statements and main motivation of this research from three main subjects, i.e., modal analysis technique, phase synchronisation effect, and excitation device. Subsequently, four objectives are set and the contributions from each objective are further elaborated. Also, the novelty of this study is included in this chapter. Chapter 2 discusses on previous literature that is related to current study, for example, the limitations of EMA, OMA, OMAX and ISMA, as well as some mechanical vibration, modal testing theories. Lastly, the mathematical background for different control strategies of automated impact device, i.e., non-synchronous impact excitation and feedforward control, are explained. Chapter 3 has elaborated on the software, equipment and experimental procedure for EMA, ISMA during operation using different excitation devices, and post-processing inconsistent phase selection assessment. The results corresponding to each of the objective are collected, analysed and discussed in Chapter 4. Basically, the parameters to be compared in this chapter between ISMA and benchmark data are FRFs estimations, natural frequencies, damping ratios and correlation of mode shape. Finally, conclusions and recommendations are made in Chapter 5 based on the research objectives in this study.

CHAPTER 2: LITERATURE REVIEW

2.1 Introduction

The chapter begins with Section 2.2 which provides the interested reader with a comprehensive review of the four modal analysis methods, usually distributed over a large number of publications. Next, background theories for Impact-synchronous Modal Analysis (ISMA) are explained in Section 0. Lastly, the parameters used for controlling of automated impact device, i.e., non-synchronous impacts excitation and Automated Phase Controlled Impact Device (APCID), are introduced in Section 2.4.

2.2 Overview of Modal Analysis

Modal analysis is a framework used in investigating the dynamic behaviour of linear and time-invariant systems. This study enables an enhanced understanding and identification of the root cause of the vibration phenomena encountered in engineering by describing a system with its modal parameters, namely the natural frequencies, natural damping and natural modes (Rossmann, 1999; H. Wang et al., 2010). These three parameters comprehensively define the dynamic characteristics of a system. The methods used for the modal identification are many and varied and can be classified as belonging to the time domain or the frequency domain. Time domain methods use measured time response data. These include the Complex Exponential (CE) method (Brown et al., 1979; Spitznogle et al., 1971; Spitznogle & Quazi, 1970), the Polyreference Complex Exponential (PRCE) method (H. Vold et al., 1986; H. Vold et al., 1982), the Ibrahim Time Domain (ITD) method (Ibrahim & Mikulcik, 1973, 1976, 1977), the Single-Station Time Domain (SSTD) method (Zaghlool, 1980), the Random Decrement (RD) method (Vandiver et al., 1982), the Least-Squares Complex Exponential (LSCE) method (Brown et al., 1979), the natural excitation technique (NExT) typically combined with the Eigensystem Realization Algorithm (ERA) (James et al., 1992; Juang & Pappa, 1985; Juang & Suzuki, 1988), the Autoregressive Moving-average (ARMA) method (Andersen

et al., 1995), the Stochastic Subspace Identification (SSI) method (Overschee, 1996; Peeters & De Roeck, 2000), the Frequency Domain Decomposition (FDD) method (Brincker, Zhang, et al., 2000), the Enhanced Frequency Domain Decomposition (EFDD) method (Jacobsen et al., 2006), and the Direct System Parameter Identification (DSPI) method (Leuridan, 1984; Leuridan & Vold, 1983).

On the other hands, the methods belonging to the family of frequency domain identification based on measured FRFs are the Peak-picking (PP) method (Bendat & Piersol, 1993; Felber, 1994), the Circle Fit (Kennedy and Pancu) method (Ewins, 1984), the Inverse FRF method (Dobson, 1985), the poly-Least Squares Complex Frequency Domain (PolyMAX) method (Peeters et al., 2004), the Dobson's (or "Bendent") method (Dobson, 1987), the Gaukroger-Skingle-Heron (GSH) method (Gaukroger et al., 1973), the Ewins-Gleeson method (Ewins & Gleeson, 1982), the Frequency Domain Prony method (Brittingham et al., 1980), the Complex Exponential Frequency Domain (CEFD) method (Schmerr, 1982), the Eigensystem Realization Algorithm in the frequency domain (ERA-FD) method (Juang & Suzuki, 1988), the Rational Fraction Polynomial (RFP) method (Richardson & Formenti, 1982), the Global RFP (extension of RFP) method (Richardson, 1986; Richardson & Formenti, 1985; Vanderauweraer & Leuridan, 1987), the Global method (Fillod et al., 1985), and the Polyreference Frequency Domain (PRFR) method (L. Zhang & Kanda, 1986; L. Zhang et al., 1985; L. Zhang et al., 1986).

Currently, the two techniques used to extract these parameters are the classical Experimental Modal Analysis (EMA) and Operational Modal Analysis (OMA). The philosophy and theoretical insights of this framework were reported in numerous books and significantly flourished to this day (Avitabile, 2017; Brincker & Ventura, 2015; Ewins, 2000; Fu & He, 2001; Maia & Silva, 1997). EMA has attracted attention and grown rapidly in popularity since the advent of the digital Fast Fourier Transform (FFT)

analyser in the early 1970's. In the modal data acquisition stage of EMA, the responses of a linear, time-invariant system are measured along with a known excitation, often out of its normal service environment. This process normally takes place in a closely-controlled condition, where the test structure is artificially excited by using traditional single impact hammer test or shaker. However, it is known that single impact hammer test can yield unreliable results especially for large structure due to low signal to noise ratio and low-energy input while for shaker test, it can be expensive and inconvenient for on-site testing. For that, a random impact test described by a stochastic model was introduced in (Zhu et al., 2006) which has the combined the advantages of single impact hammer and shaker test, i.e., the number of force pulses is modelled as a Poison process with stationary increments which have an arbitrary, deterministic shape function and random arrival times and amplitudes. Performing FFT on the measured signal will yield the Frequency Response Functions (FRFs) estimation. Then, the FRFs are subjected to a range of modal identification algorithms in an attempt to find the mathematical model which provides the closest description of the actually observed response by the system.

In this paragraph, the applications of modal analysis in recent years and in various fields is briefly discussed. In material engineering (Mansour et al., 2016), a three steps modal testing method was proposed to investigate the modal characterisation of viscoelastic composite materials which was rarely reported previously. This involved the use of analytical-experimental transfer function integrated with genetic algorithm for optimisation purpose. Good agreement of elastic modules was observed between the proposed method (non-destructive method) and the static tensile tests (destructive method). In civil engineering, the dynamic characteristics of a building are varied at different construction stages. In (Turker & Bayraktar, 2017), OMA was conducted to study the effects of construction stages (brick-walled, bare frame and coated cases) on the modal parameters of reinforced concrete buildings. The outcomes show that the natural

frequencies were affected by the number of stories and brick walls. The study is important and could be used for later assessment such as updating and calibrating analytical modes, on line damage identification and condition monitoring of buildings at construction stage. Modal analysis on fluid engineering is possible and it was shown in (Mikota et al., 2017). In this literature, hydraulic modal theory was first extensively validated where EMA was conducted on the hydraulic pipelines, i.e., a straight pipe line, same pipe line with single branch, and a pipeline system with three sides branches, in fluid power systems to investigate the dynamic characteristics of the fluid. The study is essential as the fluid power systems can take advantage of the modal characterisation that is well established in structural acoustics and mechanics with respect to cavitation and structural safety of the hydraulic system. Accurate modal parameters are important for model correlation between experimental results and finite element model. In spacecraft engineering, the body rates induced by launcher will alter the trajectories of target vehicles at egress and subsequently affect the successful execution of flight test missions. A model correlation procedure with a set of correlation criteria was used in conjunction with extracted modal parameters to improve the accuracy of finite element model. The literature showed that after several iterations in the model correlation process, the finite element model was able to regenerate the dominant dynamic behaviors as observed in the experiment testing, especially at the key location of the launcher tip (Couch et al., 2016). Another similar research on liquid rocket engine nozzle, i.e., model updating using experimentally determined modal parameters, but was focused on using 3D Scanning Laser Doppler Vibrometry (SLDV) to overcome poor mode shape precision by traditional modal test (Yan et al., 2017). Furthermore, model updating is essential for structural health monitoring in civil engineering. Ideally, for ambient vibration testing, the response from a system is modelled as a stationary signal but in most of the real cases, the response could be non-stationary, for example, a series of wind gusts or in the case of measured

seismic response. In (Ka-Veng. et al., 2002), a Bayesian time-domain approach was presented which is based on an approximation of the probability distribution of the response to a non-stationary stochastic excitation. It allows one to obtain not only the most probable values of the updated modal parameters and stochastic excitation parameters but also their associated uncertainties using only a single set of output response data. Modal parameters of fruits is also an important information especially during the transportation stage. In (F. Wang et al., 2017), a frequency sweep test and modal analysis through finite element model were carried out to determine the natural frequency of Xinong No.8 watermelon cultivar. The end results of this study were aiming to reduce loss/damage of watermelon during the delivering stage and to provide a guideline for the design of watermelon transportation device design to avoid resonance. The literature that gives guidance to the user on how to perform modal analysis in automotive engineering, particularly on large body is shown in (Fan et al., 2015). In this study, modal analysis was performed on a developing truck cab body using pseudo-random signal excited at multiple points along the x, y, z directions. Comparison of modal parameters was then made between experimental and finite element method. The improved measured were put forward to reduce vibration noise, avoid modal coupling and to enhance local stiffness in the car body.

With the academic principles of system identification, EMA has aided the engineers to get more physical insight from the identified dynamic characteristics of the system. Through the continuously evolving its application base, modal analysis is today successfully applied in material engineering, (material properties identification and modification and non-linearity identification) (Mansour et al., 2016; Mishra & Chakraborty, 2015; Zhou et al., 2017a, 2017b), civil engineering, (e.g. buildings, dams, off-shore platforms, bridges, wind mills, etc.) (Ding et al., 2008; Garcia-Perez et al., 2013; Hameed & Pavic, 2016; Li et al., 2010; Magalhaes et al., 2012; Reynders et al., 2010;

Turker & Bayraktar, 2017; H. Wang et al., 2016; Wong, 2004), industry machinery, (e.g. pipeline systems, turbines, compressors, pump, diesel engine, etc.) (L. He et al., 2014; L. Z. He et al., 2014; Mikota et al., 2017), spacecraft engineering, (e.g. satellites, solid panels, antennas, launchers, etc.) (Couch et al., 2016; Wickramasinghe et al., 2013), aerospace engineering, (e.g. in-flight tests, control surfaces, landing gear, ground vibration test, etc.) (Böswald et al., 2017; Yan et al., 2017), food engineering, (e.g. transportation) (F. Wang et al., 2017), and automotive engineering, (e.g. fully trimmed cars, body-in-white, suspension system, engine, etc.) (Fan et al., 2015; Hou et al., 2013; Lee et al., 2015).

However, conventional EMA has limitations; (i) simplified rather than exact boundary conditions of the system in a real situation are simulated in laboratory testing, (ii) FRF or Impulse Response Functions (IRFs) are hard to measure in practice, especially on large and complex systems and (iii) it requires the system to be in a complete shutdown state; which means no unaccounted excitation force will be induced into the system. In industrial applications, especially in petrochemical plants, the downtime cost is crucial and thus it is not practical to shut down the machinery under testing to perform EMA.

While EMA has been used successfully for many systems, it is difficult to perform on large and highly complex civil structures such as buildings and bridges as it is very difficult to excite the structure artificially. Besides, in some practical situations where the system cannot be shut down completely, OMA is preferred. OMA, also known as ambient vibration testing or output-only analysis, is a system identification process based solely on the output only data. It has drawn great attention in various engineering field due to many advantages; (i) the analysis procedure is fast and cheap in the absence of artificial exciter and simulation of boundary condition can be avoided, (ii) dynamic characteristics of a complete system are measured instead of component, and (iii) linearization of the

system characteristics by using the broadband random excitation is possible and (L. M. Zhang et al., 2010). The performance comparisons of EMA and OMA were reported in (Giraldo et al., 2009; Ibrahim & Mikulcik, 1976; Lauwagie et al., 2006; Orlowitz & Brandt, 2017; Thibault et al., 2012). Note that while performing OMA, assumptions are made about the nature of the loads exciting the system, i.e., Gaussian white noise input (Brincker & Ventura, 2015).

However, the lack of knowledge of the input forces does affect the parameters extracted. Mode shapes obtained from OMA cannot be normalised accurately, which affects the development of mathematical models thereafter. Knowing the mass normalised mode shapes is essential, as one can use this information for certain applications, for example, damage detection, health-monitoring applications, force estimation, model updating and structural modification. For that, additional procedure to compute the scaling factors is needed. Two approaches in the early stage, i.e., finite element model approach given a priori details on material characteristics of the test structure and the approach making restrictive assumptions on the excitation at specific measurement points was reported in (Doebling & Farrar, 1996; Randall et al., 1999). Many investigations have been done for scaling mode shape particularly involve only the output response data. These methods can be split into four main categories; (i) methods that dependent on highly accurate FE model (Aenlle & Brincker, 2013), (ii) methods that dependent on OMA test where specific dynamic systems, for example, tuned mass damper, is coupled with the test structure (Brownjohn & Pavic, 2007; Hwang et al., 2006; Porras et al., 2012), (iii) methods that dependent on OMA test with exogenous inputs (OMAX and OMAH) (Brandt et al., 2017; Cara, 2016; Reynders et al., 2010), where the unknown excitation is complemented by a known excitation from external actuator and (iv) methods that dependent on repetition of OMA tests with different layouts on the structure in term of stiffness, mass, or both (Aenlle et al., 2012; Aenlle et al., 2010; Bernal,

2004, 2011; Fernandez et al., 2011; Khatibi et al., 2012; Parloo et al., 2002; Yu & Song, 2017).

There is a fundamental assumption on the characteristic of the non-measured excitation in OMA, i.e., Gaussian white noise with flat spectrum (at least at the frequency band of interest). For that, all natural modes in the frequency band of interest are assumed to be equally excited and the corresponding modal parameters can be correctly identified. This is often true when dealing with most of the civil engineering structures, for example, towers, bridges, buildings are mainly excited by seismic micro-tremors, traffic or wind. Unlike civil engineering structures, it is well-known that harmonic components (deterministic inputs) are often present in mechanical engineering structures in operation. The harmonic excitations could be originated from the ambient environment including floors vibration or rotating parts like pulleys, gears, shafting, of prime movers like diesel motors, internal combustion engines, etc. As a consequence, the excitation to the system becomes coloured instead of pure white noise and lead to general OMA methods failure (Manzato et al., 2014).

There are three different ways where failure can happen. Firstly, it is possible that the operational modes due to harmonic excitations are identified as natural modes even though both of these modes are well separated in the spectrum. Secondly, when the harmonic components are close to the natural modes, the modal parameters extracted is affected by the presence of close harmonic components. Typically, a poor estimate of the modal damping is inevitable. A third failure mechanism occurs in the case of the operational modes and natural modes concurrence and subsequently inhibits the identification of the natural modes.

For that, many approaches have been proposed to tackle this limitation, i.e., the concern for non-white excitation in OMA. Generally, these approaches fall into four

categories. The first category is known as statistics driven identification of the harmonics where statistical measurement known as Probability Density Function (PDF) and kurtosis is used determine a peak in a spectrum is a natural mode or operational mode (Brincker, Andersen, et al., 2000; Brincker, Zhang, et al., 2000). This approach, however, is limited to lightly damped operational mode. For heavily damped operational mode this approach may fail as the operational mode will be identified as natural mode (Motte et al., 2015). Besides, a Time-frequency Domain Decomposition (TFDD) was proposed which serve the same purpose. The technique utilised mother wavelet filter prior to perform histogram and kurtosis analysis for well-separated structural and operational mode (Le & Argoul, 2015). The second category involves the removal of harmonic components from the measured signal in the pre-processing stage by using time-synchronous averaging, cepstrum editing, non-parametric estimate of the harmonic frequency, a joint use of the "entropy" and Hilbert transform properties or random decrement technique (Agneni et al., 2012; Dion et al., 2013; Modak et al., 2010; Peeters et al., 2007; Pintelon et al., 2008, 2010; Randall et al., 2012). Furthermore, an automatic method combining Optimized Spectral Kurtosis (OSK) and Kalman filter was proposed to remove modulated sinusoidal components presents in the measured signal (Dion et al., 2013).

In (Mohanty & Rixen, 2004a, 2004b, 2004c, 2006), it was shown that existing approaches, i.e., LSCE, ERA, ITD method, was modified to explicitly incorporate the harmonic component in the modal identification process. However, these approaches require some prior knowledge about the harmonic frequencies and it must be noted that a slight difference in the harmonic frequency assumptions compared to exact harmonic frequency could violate the whole modal identification process. The last category is known as input spectrum independent techniques, for instance, the transmissibility measurement based OMA (TOMA) and polyreference TOMA (p-TOMA), in which the modal parameters extraction is independent on the type of input excitation to whether or

not the excitation is white noise or coloured noise (Devriendt et al., 2009; Weijtjens, De Sitter, et al., 2014; Weijtjens, Lataire, et al., 2014).

The fact that the ambient forces are sometimes confined to a narrow frequency band is another shortcoming of OMA. As a consequences, not all the natural modes are excited or they are extracted with low quality. To overcome the limitations of OMA, a combined used of EMA and OMA approach therefore has been proposed namely OMAX (Guillaume et al., 2006). In OMAX, both the unknown ambient excitations and measurable artificial excitation are available. Note that the measurable artificial excitation can be stochastic as well as deterministic. The main difference between classical EMA and OMAX is that the unknown ambient excitation is included in the system model identification: they are threatened as useful excitation instead of ambient noises. For that, the artificial excitation can has amplitude equal to, or even lower, than the amplitude of the unknown ambient excitation. This is, of course, a very importance information for modal testing on civil engineering structures. Instead of using hydraulic or electromechanical shakers which are difficult to transport and heavy, small actuator is sufficient to provide the required artificial excitation. The feasibility of OMAX so far has been explored in modal identification of footbridges where an in-depth comparison with numerical models and EMA and OMA test was performed. As reported in (Reynders et al., 2010; Reynders et al., 2008), modal parameters from OMAX test was good, sometimes even superior, quality, than the classical EMA and OMA. In addition, the mode shapes obtained through this approach could be scaled to unity modal mass. Another work by the similar author was shown in (Reynders et al., 2010). In this study, the results from OMAX tests were used to update finite element model for structural damage identification purpose. With OMAX tests, more or higher modes can be identified (compared to OMA) and this eventually solved one of the limitations in FE model updating technique, i.e., the ability to identify enough modal parameters with sufficient

accuracy (identification problem). However, large discrepancies of modal parameters were observed for FE model updated with the OMAX for additional detected modes. The authors commented that this is probably due to modelling problems in the FE model. Prior to this work, the literature presented was on white noise excitation. Up to this point the works have been focused on white noise excitation (ambient excitation). In actual situation, however, the excitation may be coloured or composed of different patterns, such as harmonic excitations from those rotating parts in mechanical. In (Devriendt et al., 2012), it was proposed to combine TOMA and OMAX which can be considered as a new methodology in the field of OMA. The idea is to tackle the case when the unknown ambient excitation is coloured since transmissibility measurement is the ratio between two responses, and thus it can be computed without the information of the input excitation. The proposed idea was validated through simulation and flight flutter test data by using a proper weighting. However, the efficiency of OMAX on mechanical systems particularly rotating machinery in the presence of dominant harmonic excitations has not been reported so far.

For these reasons, there has been an increasing interest during the last few years towards combined modal testing techniques to deal with mechanical systems during operation. A method, named ISMA that utilises Impact-synchronous Time Averaging (ISTA) was proposed (Rahman et al., 2011a, 2011b). This modal analysis technique focuses on the digital signal processing upstream of the collected data rather than the modal identification algorithm. In the commonly used time domain synchronous averaging technique, signal acquisition from a rotating machine is triggered at the same rotational position of the shaft using a tachometer for every cycle. The time block, i.e., the block of vibration data captured in time series of averaged signals, eliminates all the non-synchronous and random components, leaving behind only components that are integer multiples of the running speed. In ISMA, the same and simple averaging concept

is used but only to achieve the reverse, i.e., to filter out all the speed synchronous and random signatures. It is effective in filtering out the cyclic load component, the harmonics, and noises, which are non-synchronous with the impacts. ISMA has the advantages of the OMA and EMA combined. It carries out the analysis while the system is in operation, and at the same time it is able to provide the actual input forces in the transfer functions, thus allowing for better modal extractions and mathematical model development. This novel technique has been successfully applied in both rotor and structural dynamic systems to determine the dynamic characteristics of structures without disturbing operations(Rahman et al., 2014; Rahman et al., 2011a, 2011b).

The effectiveness of ISMA is governed by four important parameters, i.e., number of averages, impact force, windowing function and phase synchronisation effect. In (Rahman et al., 2014), it was concluded that; (i) at low operating frequency, high number of averages was sufficient to extract the modal parameters, (ii) at high operating frequency, the extraction of modal parameters was difficult even though with high number of averages and (iii) for operating frequency that was far away from the natural mode, moderate number of averages was sufficient to determine the dynamic characteristics. On the other hands, the effects of windowing function and impact force were reported in (Ong et al., 2016). Proper selection of decay rate in the exponential window aids in eliminates or minimises leakage due to truncated response signal on a low damped structure and also filters out all the responses contributed by the unaccounted forces in a time record window block. Besides, low impact forces may not be adequate to excite the structure's natural modes, while excessive impacts may result in non-linearity of the system. Thus, if the information of the cyclic force is known in advance, suitable amount of impact force to be applied to the system can be determined to overcome the dominant cyclic load effect. Lastly, the phase sychronisation effect was only investigated through a simulation study and results showed that synchronisation between responses

due to impact and periodic responses of cyclic load should be avoided for better performance of ISMA method (Ong, 2013).

When performing ISMA on operating structures with dominant periodic responses of cyclic loads and ambient excitation, a high number of averages are needed to eliminate the harmonic disturbances. The effect of number of averages on ISMA is proven in the previous study (Rahman et al., 2014) where impacts were applied randomly on the operating structure using manual impact hammer as the phase angles information with respects is an unknown. An important finding showed that when the operating frequencies coincided with the natural modes, ISTA required a high number of averages to eliminate the harmonic disturbances in obtaining a better FRFs estimation prior to dynamic characteristics identification. But, this is a time consuming and labour intensive process. Lack of knowledge and control of impact with respect to phase angle of the harmonic disturbances using conventional impact hammer in ISMA has limited the effectiveness and practicality of this novel technique. The effect of the phase angle of the harmonic disturbances with respect to the impact is found to be a key factor in enhancing the effectiveness of ISMA when performing modal testing on structures with dominant periodic responses of cyclic loads.

For many years there has been increasing interest in using automated impact device as a replacement for manual impact hammer in EMA. In (Sharma et al., 2016), pneumatic exciter embedded with force transducer which can generate uncorrelated impact has been tested on simple static structure whereas an eletromechanically driven solenoid coupled with force sensor was found in (Jannifar et al., 2017). There is also electric impact hammer available in the market sold by the manufacturer, The Modal Shop. All the devices discussed are actually serving the same purposes which are to overcome the limitations when using manual impact hammer. This device can guarantee three

conditions; (i) consistent impact force and impact location, (ii) reduced human error such as double impact and (iii) reduce human power since it is fully automated. Thus, these devices are simply controlled by an "On" and "Off" state.

In (Ong & Lee, 2015), a portable and calibrated automated impact device was introduced in ISMA. The device was designed in such a way that it is able to impart impacts at consistent impact interval but always non-synchronous with the periodic response of cyclic load and it was successfully applied in modal testing during static condition. Since the device is equipped with this additional feature, its application is thus not only limited to static condition, but also favourable for operational modal testing.

In summary, ISMA method is still in evolution in the digital signal processing aspects, particularly upstream of the collected data. This simply means that continuous efforts have to be made in order to clean up the vibration signal prior to applying FFT to estimate the FRFs followed by modal parameters extraction. While ISMA was successfully applied during static condition, its effectiveness on rotating systems still requires a further investigation and validation. Moreover, previous research has shown that high number of averages were required for accurate extraction of modal parameters especially when the operating frequency coincided with the natural mode. This is probably due to the lack of information of phase angles with respect to impact and it has subsequently reduced the effectiveness and practicality of ISMA. Thus, a more-thorough study of phase synchronisation effect is needed for enhancement of ISMA method. Lastly, another long-sought goal is the investigation on whether the implementation of automated impact device in ISMA during operation is an additional benefit compared to manual impact hammer in conjunction with the findings from phase synchronisation effect, typically in the elimination of harmonic disturbances.

Table 2.1: Overview of Modal Analysis

Modal analysis	Description	Limitation	Application
EMA	1. Can be performed using conventional manual impact hammer or shaker 2. Input force and output response are measured 3. Required complete shutdown of system	1. Impractical due to high downtime costs especially in petrochemical plants 2. Difficult in simulating actual bounday conditions 3. FRF estimations for large structures are hard to measure	Material properties identification, finite element model updating, active and passive vibration control, damage detection, force identification, food transport engineering etc
OMA	1. System identification only required only output response from actual operating system 2. Linearization of the system characteristics is possible 3. Dynamic characteristics of the whole system are measured instead of individual components	1. Normalisation of mode shapes remains a problem due to the lack of input force information 2. Presence of harmonic excitations is inevitable in most of the real cases 3. Not applicable for static system	
OMAX	1. Unknown ambient excitations is included in the system model identification 2. Artificial excitation, e.g., from shaker, is applied to the system 3. Normalisation of the mode shapes is possible	1. Modelling problems in the FE model have led to the large discrepancies of modal parameters 2. Not applicable for static system	
ISMA	1. Input force and output response are measured 2. Can be performed on static and operating system	1. High number of averages are required to filter out dominant cyclic load component	

Table 2.1: Continued

	2. Use ISTA to filter out non-synchronous components	3. Synchronisation between response due to impacts and periodic response from cyclic load is unavoidable when using manual impact hammer	

2.3 Background Theory

The following sections have covered the averaging technique used in ISMA as well as the parameters that govern the effectiveness of ISMA from previously published works.

2.3.1 Impact-synchronous Modal Analysis

ISMA was introduced in a recent year which allows the modal extraction to be carried out during operation. This modal analysis technique focuses on the digital signal processing upstream of the collected data rather than the modal identification algorithm. In the commonly used time domain synchronous averaging technique, signal acquisition from a rotating machine is triggered at the same rotational position of the shaft using a tachometer for every cycle. The time block, i.e., the block of vibration data captured in time series of averaged signals, eliminates all the non-synchronous and random components, leaving behind only components that are integer multiples of the running speed. In ISMA, the same and simple averaging concept is used but only to achieve the reverse, i.e., to filter out all the speed synchronous and random signatures. It is effective in filtering out the cyclic load component, the harmonics, and noises, which are non-synchronous with the impacts. ISMA has the advantages of the OMA and EMA combined. It carries out the analysis while the system is in operation, and at the same time it is able to provide the actual input forces in the transfer functions, thus allowing for better modal extractions and mathematical model development. This novel technique has been successfully applied in both rotor and structural dynamic systems to determine the

dynamic characteristics of structures without disturbing operations. In general, the effectiveness of ISMA is governed by four important parameters, i.e., phase synchronisation effect, number of averages, impact force, and windowing function. This will be discussed in the following sections.

2.3.2 Impact-synchronous Time Averaging

ISTA relies on the Time Synchronous Averaging (TSA) technique where the averaging process is done in the time domain prior to performing FFT. In TSA, the reference signal is the running speed of the motor triggered by the tachometer, therefore, the signal which is not synchronous will be eliminated and leaving only the running speed component. In comparison, in ISTA, the reference signal is the input excitation which triggers the acquisition of time block signal. Block averaging is performed on both the force and response due to impact signal for each time block captured. Thus, by taking sufficient number of averages, the harmonic disturbances are no longer in phase for every triggered time block of signal. The harmonic disturbances and random noise will be gradually filtered out and the desired signal, i.e., response due to impact which is synchronous to the repetitive impact force is preserved. Figure 2.1 shows the effect of ISTA where the running speed is eliminated. The governing equation of ISTA is given by

$$y(t) = \frac{1}{N}\sum_{k=0}^{N-1} x(t + rT_0) \tag{2.1}$$

where $y(t)$ is the averaged vibration signal in time domain, N is the total number of impact, $x(t)$ is the vibration signal in time domain, k is the number of impact/averages and T_0 is the time interval between impacts.

A discrete number of FRFs are then obtained from the ratio of averaged responses due to impact and input excitation force signals. It is worth mentioning that the force transducer performs dual tasks in ISMA. Firstly, it acts as a trigger in ISTA for capturing

responses due to impact and secondly, it is used to measure input excitation force signal for the subsequent signal processing operation, e.g., cross spectrum and auto spectrum.

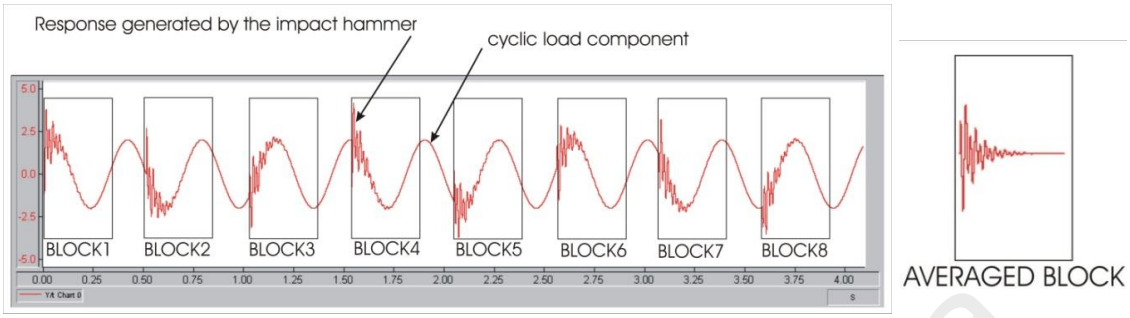

Figure 2.1: Elimination of Running Speed with ISTA (Ong, 2013)

2.3.3 Effect of Phase Synchronisation in Impact-synchronous Modal Analysis

In ISTA, a series of time blocks, each triggered by an impact force signal, use the fact that all other responses are non-synchronous with the impacts. Performing ISTA on a number of blocks would result in eliminating all these non-synchronous components, leaving behind only the structure's responses due to impact. The effect of the phase angle with respect to impact in ISTA can be described as follows.

The sinusoidal signature is given by

$$p(t) = Asin(\omega t + \beta) = acos\omega t + bsin\omega t \tag{2.2}$$

where A is the amplitude of the signature, ω the angular frequency (or cyclic load frequency), and β the phase angle. When $p(t)$ is captured in each individual block of time series at different β, the values a and b are different for each individual block of time series even though the amplitude A does not change corresponding to that individual block of time series. However, block averaging of this time series, i.e., all the individual blocks captured, will result in values of a and b diminishing to zero, subsequently reducing A to zero as well. To keep a and b consistent, $p(t)$ has to start at the same point for every block captured; i.e., β has to be consistent.

In the event of performing modal testing during operation, the total time response, (i.e., vibration signal in time domain), $x(t)$, is captured in a time block with respect to a specific trigger condition (Phillips & Allemang, 2003). The $x(t)$ measured consists of two types of signals, i.e., $q(t)$ and $e(t)$, as follows:

$$x(t) = q(t) + e(t) = \sum_{r=1}^{n} A_r e^{-\sigma_r t} sin(\omega_{dr} t + \beta_r) + R_2 sin(\omega t + \beta_2) \tag{2.3}$$

where $q(t)$, a desired deterministic response signal due to impact consisting of the summation of all the modes r, is synchronous with every impact force applied, and $e(t)$ is the summation of the undesired deterministic signal of the periodic response of cyclic load with frequency of ω in addition with random ambient noises. Parameter σ_r is the decay rate, ω_{dr} is the modal frequency, n is the maximum number of modes, A_r is the amplitude of mode r for the desired deterministic response signal due to impact, R_2 is the amplitude of the undesired deterministic signal of the periodic response of cyclic load, β_1 is the phase of the desired deterministic response signal due to impact, and β_2 is the phase of the undesired deterministic signal of the periodic response of cyclic load.

Eq. (2.3) can be written as

$$x(t) = \sum_{r=1}^{n} e^{-\sigma_r t} [a_r cos\omega_{dr} t + b_r sin\omega_{dr} t] + f_1 cos\omega t + g_1 sin\omega t \tag{2.4}$$

Signal $x(t)$ is triggered consistently with the impact force and is thus synchronous with phase β_1 in a time block (i.e., 4096 samples). Small variations in a_r and b_r would average to amplitude A_r in block averaging. However, the periodic response of cyclic load and random ambient noises, $e(t)$, is non-synchronous with every impact force applied, causing the phase value of β_2 to change for every individual block of time series captured and thus leading to different values of f_1 and g_1 corresponding to that individual block of time series. Because the values of f_1 and g_1 keep changing in all individual

blocks, performing block averaging on all the individual blocks captured in a time domain tends to diminish these non-synchronous components, i.e., f_1 and g_1, and subsequently reduces R_2 to zero as well. In short, performing ISTA on the total response signal $x(t)$ will filter out the signal $e(t)$ and the desired signal $q(t)$ will reinforce for every time block recorded over time. Note that this is similar to the response due to the impact signal obtained in modal testing during a stationary condition. It is worth mentioning that the cyclic load component can still be filtered out even if the ω equals one of the ω_{dr}. In summary, preservation of signatures during time averaging depends on the consistency of their β on every time block but not necessarily on their ω (Maia & Silva, 1997; Timoshenko et al., 1974).

2.3.4 Effect of Number of Average in Impact-synchronous Modal Analysis

Synchronisation of phases between responses due to impact and harmonic disturbances should be avoided in order to obtain a better representation of the dynamic characteristics for a system when performing ISMA. To achieve this, impacts can be applied randomly with a high number of averages. Applied random impacts can prevent the responses due to impact being synchronised with the harmonic disturbances. Thus, the total response measured after performing ISTA is the desired response due to impact. From previous research, a moderate amount of averages were sufficient to obtain a better FRFs estimation at a lower operating frequency as shown in Figure 2.2. For higher operating frequency and subsequently gradually increase the vibration amplitude, even performing ISMA with high number of averages, the cyclic load component still remained dominant in the FRFs estimation as shown in Figure 2.3 (Ong, 2013; Rahman et al., 2014). Eventually, the dominant cyclic load component will cover up the nearby natural modes and subsequent modal identification process could be difficult.

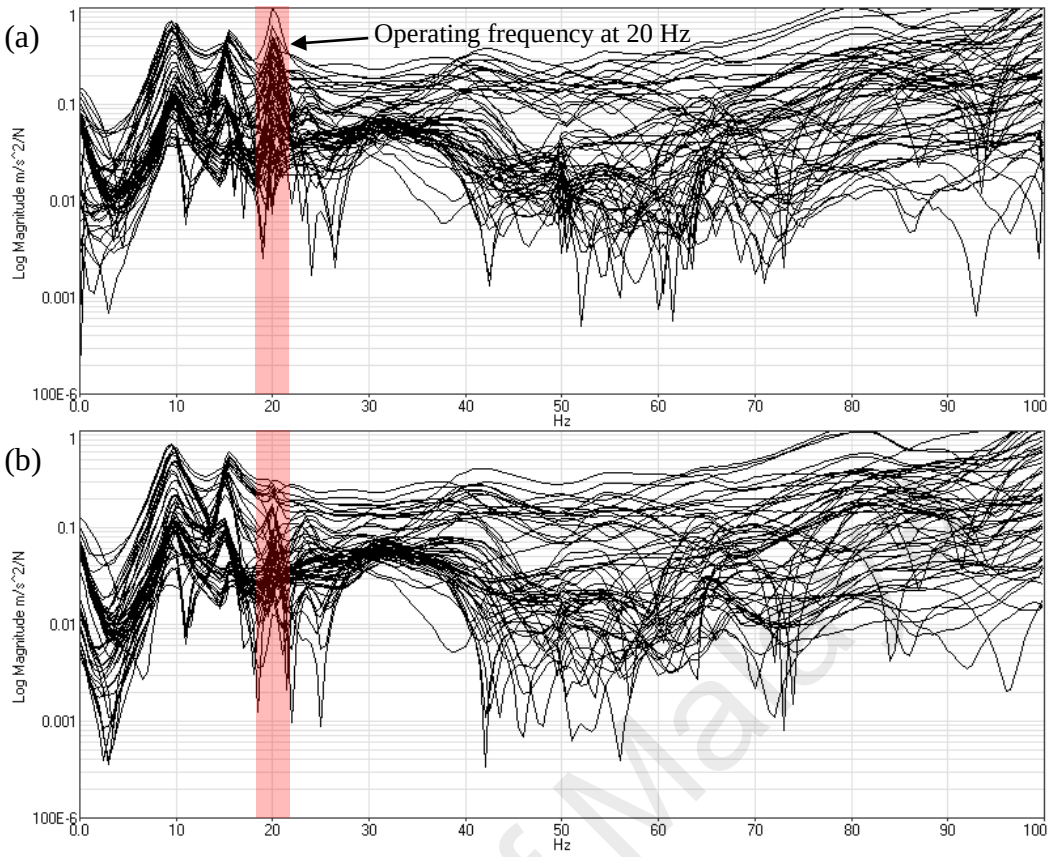

Figure 2.2: FRFs Estimation for 20 Hz: (a) 5 Averages, (b) 50 Averages (Rahman et al., 2014)

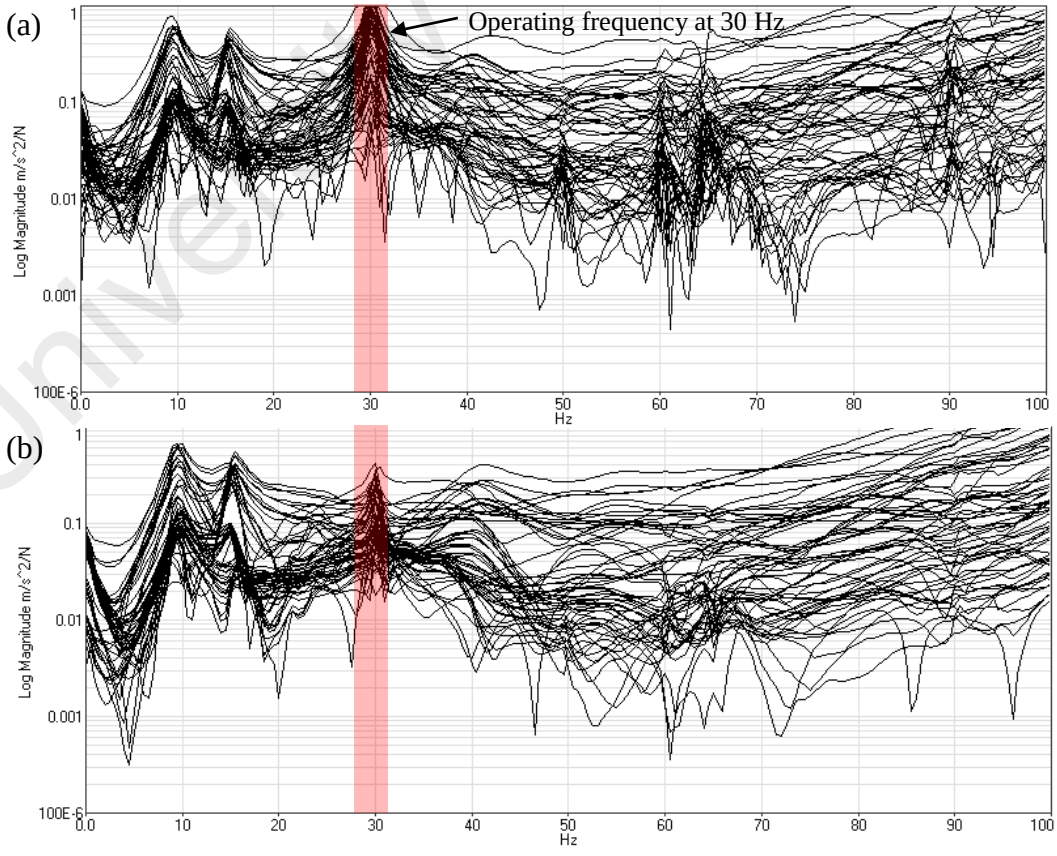

Figure 2.3: FRFs Estimation for 30 Hz: (a) 5 Averages, (b) 250 Averages (Rahman et al., 2014)

2.3.5 Effect of Impact Force in Impact-synchronous Modal Analysis

Besides, the impact force is another concern in performing ISMA on dominant operating cyclic loads typically on practical usage. Low impact forces may not be adequate to excite the natural modes, while excessive impacts may result in non-linearity. Thus, if the information of the cyclic force is known in advance, suitable amount of impact force to be applied on the system can be determined in order to overcome the dominant cyclic load effect subsequently all the natural modes in the frequency range of interest are excited. Figure 2.4 has depicted the comparison of using low and high impact force and its effect on the FRFs estimation. It is clearly observed that suppression of dominant cyclic load component is more successful with high impact force. (Ong, 2013; Ong et al., 2016).

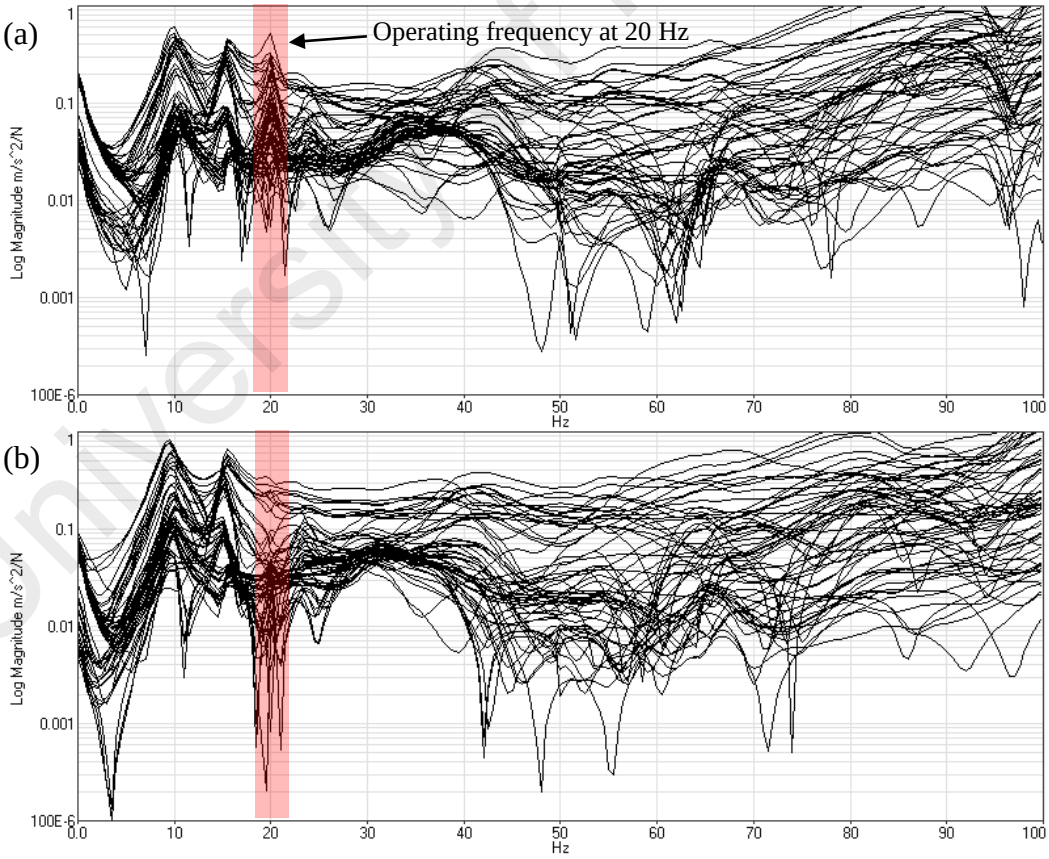

Figure 2.4: FRFs Estimation for 20 Hz: (a) Low Impact Force, (b) High Impact Force (Ong et al., 2016)

2.3.6 Effect of Windowing Function in Impact-synchronous Modal Analysis

Generally, exponential windowing function has an important effect when performing ISMA on structures with dominant periodic responses of cyclic loads and ambient excitation. It attenuates the amplitude of the response signal exponentially from a factor of one to a small value. This is very effective especially in performing modal testing during operation where the periodic responses of cyclic loads are dominant during the entire measured response time history. In ISTA, the exponential window performs a dual task. It minimises leakage due to truncated response signal especially on a low damped structure and also suppresses all the responses contributed by the unaccounted forces in a time record window block. However, proper selection of decay rate in exponential window is essential when performing ISMA. For instance, if the decay rate is too high, the natural modes will be severely damped and do not seem to appear in the FRFs estimation. Figure 2.5 has depicted the FRFs estimation obtained without and with a decay rate of 3 rad/s. The reduction of dominant cyclic load component is clearly observed for the case of using exponential window (Ong, 2013; Ong et al., 2016).

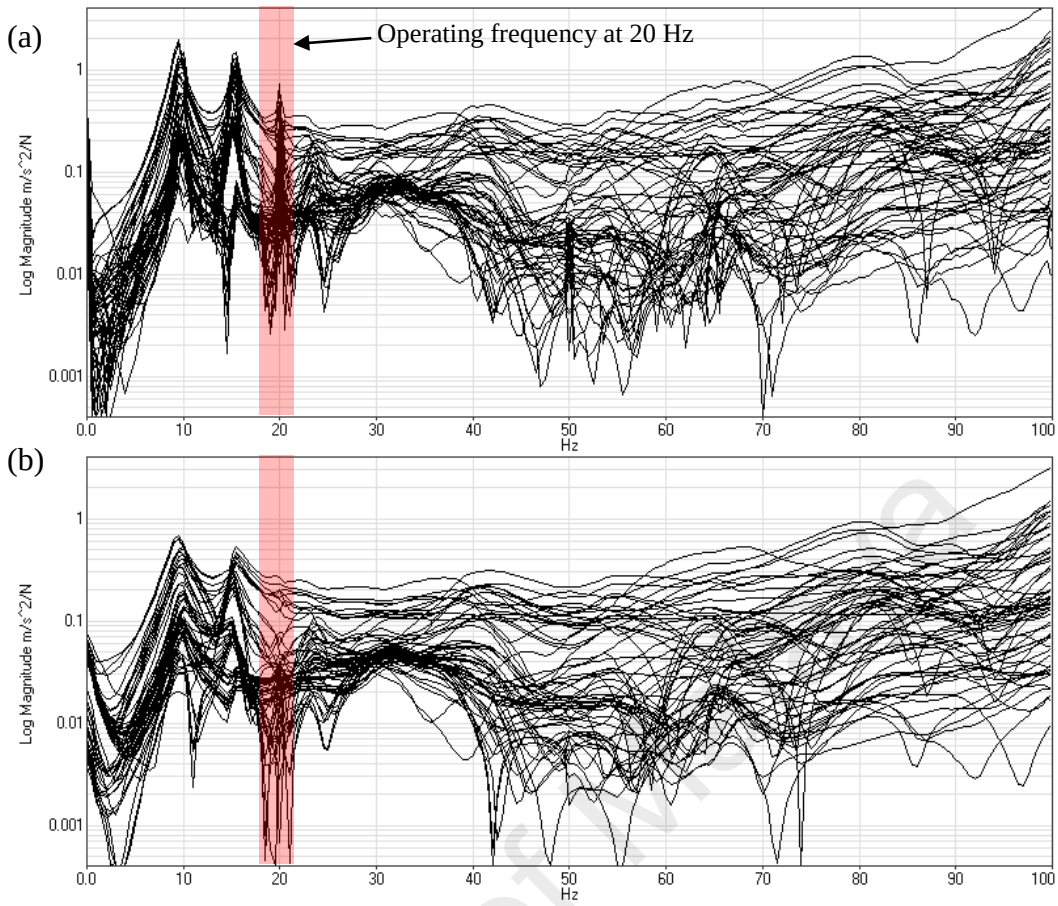

Figure 2.5: FRFs Estimation for 20 Hz: (a) No Exponential Window, (b) 3 rad/s (Ong et al., 2016)

2.4 Control of Automated Impact Device

In general, the development of automated impact device is not merely for automation, indeed there are many more advantages. Firstly, the impact frequency adjustable. This is particularly significant where synchronisation of response due to impact with periodic response of cyclic load can be avoided as long as the impact frequency is a non-integer multiple of the operating frequency. Since the impact force level is important in performing ISMA (Ong et al., 2016), the automated impact device is able to generate consistent and controllable forces which are difficult to achieve by using manual impact hammer. Lastly, the advantage of automated impact device over manual impact hammer is that it helps to reduce human power and human errors such as double impacts.

2.4.1 Automated Impact Device with Non-synchronous Impacts

A mathematical model has been developed in previous research to control the automated impact device in performing modal testing with a controlled impact interval (Ong & Lee, 2015). The automated impact device has yet to be tested in operational modal testing. Based on the mathematical model, which consists of a digital square wave signal, the 'On' and 'Off' state of the automated impact device is controlled by the crest and trough of the signal, respectively, as shown in Figure 2.6. The parameters that are involved in the control of the automated impact device are frequency (f_{square}) or period (T_{square}) of the square wave, sampling rate (SR), block size (BS), duty cycle (DC), time of response block (t_{block}), number of cycles of square wave in a time block (n_{square}), length of time for active pulse (t_{pulse}), time difference (Δt), number of blocks for active pulse (N_{active}), solenoid 'On' time (t_{on}), impact interval (T_{impact}) and impact frequency (f_{impact}). The parameters to be manipulated to get different impact profiles are BS, SR, DC, and f_{square} or T_{square} of square wave.

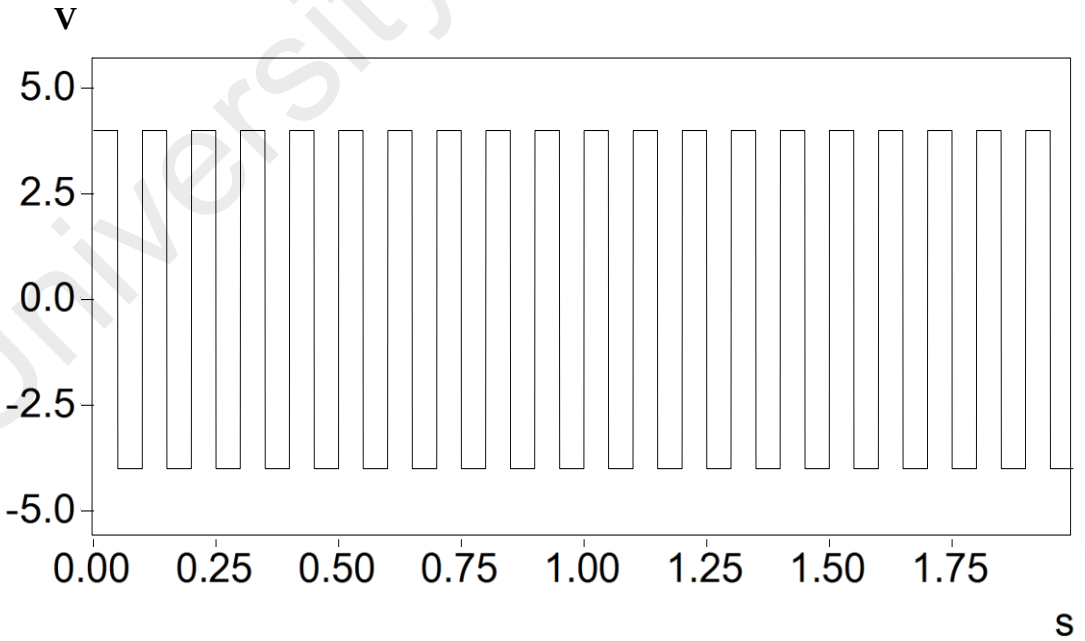

Figure 2.6: Digital Square Wave Input Signal

i. *Frequency or period of square wave*

The digital square wave signal is a fixed input given to the program with a specific f_{square} or T_{square} pre-set by the user. The f_{square} is given by

$$f_{square} = \frac{1}{T_{square}} \tag{2.5}$$

ii. *Duty cycle*

DC is defined as the percentage of the peak in a complete cycle of a waveform (square wave). A symmetric square wave has 50% of DC where the crest and trough have the same interval. Therefore, the length of pulse (t_{pulse}) can actually vary by setting different value of DC. The DC can be expressed as

$$DC = \frac{t_{pulse}}{T_{square}} \times 100\% \tag{2.6}$$

iii. *Block size and sampling rate*

BS is the number of samples taken within a time block while SR is the number of samples taken per second. For example, if the BS is 1024, that means there are 1024 data samples per time block data record. Meanwhile, if the SR is 50000, it simply means that the program will take 50000 data samples per second.

iv. *Time response block*

The time response block, t_{block} is the time taken for capturing one block of signal before undergoing any signal processing stages which is expressed by

$$t_{block} = \frac{BS}{SR} \tag{2.7}$$

v. *Number of cycle of square wave in a time block*

The number of cycle of square wave, n_{square} in a time block is given by

$$n_{square} = \frac{t_{block}}{T_{square}} \tag{2.8}$$

It represents the part of the original square wave which will be displayed on the generated time response block. It is important to note that n_{square} can be any integer starting from 1.

vi. *Length of pulse*

The length of time, t_{pulse} for an active pulse in one period of square wave is the length of the peak or the pulse in the generated time response block is given by

$$t_{pulse} = DC \times T_{square} \tag{2.9}$$

vii. *Time difference*

Time difference, Δt is very important as it defines how much the block will jump. It is defined as

$$\Delta t = t_{block} - n_{square} T_{square} \tag{2.10}$$

viii. *Number of block which is active pulse*

Number of block which is active pulse, N_{active} can be any integer and if it is not an integer, it must be truncated, e.g. 2.84 ≅ 2.00. It is evaluated by dividing t_{pulse} by Δt and this gives

$$N_{active} = \frac{t_{pulse}}{\Delta t} \tag{2.11}$$

ix. *Solenoid 'On' time*

The solenoid 'On' time, t_{on} is the time where the automated impact device will move downward to knock the structure. Note that t_{on} has to be as short as possible in order to yield a comparable impact contact time between automated impact device and manual impact hammer. t_{on} is defined as

$$t_{on} = \frac{t_{pulse}}{\Delta t} \times t_{block} = N_{active} \times t_{block} \tag{2.12}$$

x. *Impact interval and impact frequency*

Impact interval, T_{impact} is the time interval between two knocks and the inverse of impact interval is the impact frequency, f_{impact}. The equation for impact interval and impact frequency is given by

$$T_{impact} = \frac{T_{square}}{\Delta t} \times t_{block} \tag{2.13}$$

$$f_{impact} = \frac{1}{T_{impact}} \tag{2.14}$$

An excitation signal will be sent to the automated impact device when the crest of the digital square signal appears at the vertical axis/y-axis of a time block and vice versa. There are two possible cases when Δt is equal to zero; (i) the impact tip in contact with the surface of the system almost forever or (ii) automated impact device will not be "On". Thus, it is crucial to make sure that parameters are properly set; (i) there is motion of the peak towards the vertical axis caused by the displacement of subsequent block to the preceding block as shown in Figure 2.7 and Figure 2.8 (Δt must not be equal to zero) and (ii) the f_{impact} must be a non-integer multiple of the operating frequency of the system.

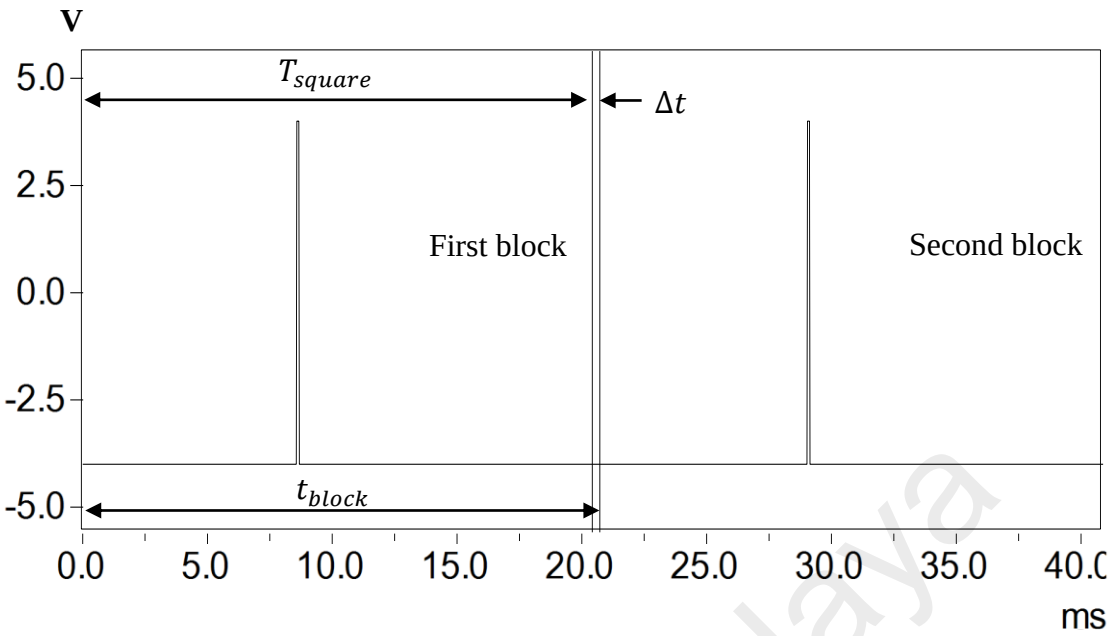

Figure 2.7: Input Square Wave after Applying Duty Cycle

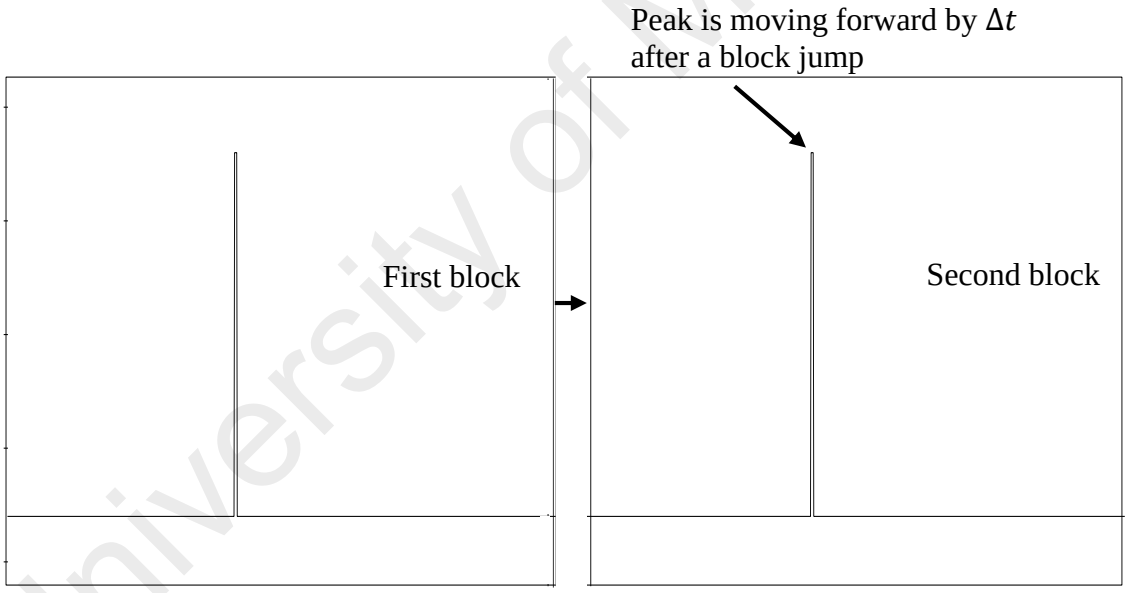

Figure 2.8: Displacement of the First Block with Second Block

2.4.2 Automated Phase Controlled Impact Device using Feedforward Control

The proposed impact device relates a control system that utilises accelerometer and tachometer in phase selection of sinusoidal response due to cyclic load, and more particularly, to a reference input element for adjustment of the sinusoidal signal to substantially eliminate the response due to cyclic load component through ISTA. When the system under testing is in operation, both tachometer and accelerometer give the same

frequency/running speed with a constant phase/time difference. Cross power spectrum is applied and the phase difference between tachometer speed component and cyclic load component can be obtained. The impact device is designed in such a way that it is capable to adapt the updated phase difference information in each triggered time block of signal and uses this information to control the correct timing to impart an impact based the electrical pulse signal of tachometer. Applying impact on the crest or trough or any phase position of the sinusoidal response due to cyclic load is then possible. Tachometer pulse signal is preferable in phase position selection because it is cleaner (just an on-off state) as compared to acceleration sinusoidal signal which usually consists of random noises. In general, the control system can be divided into 2 stages.

i. *Stage 1: Triggering*

It is worth to mention that triggering interval, T_{trig} should lie between 2 and 12 s, particularly around 6 s. Such time range gives ample time for the test structure to restore to its initial condition after the previous knock and also to give time for complete data acquisition process to take place. The triggering interval is determined by

$$T_{trig} = n_{tbl}\, x\, \frac{BS}{SR} \tag{2.15}$$

where n_{tbl} is the number of time block length, BS is the block size and SR is the sampling rate.

ii. *Stage 2: Feedforward controller for the APCID*

Feedforward control is based on the measurement of an input disturbance of arbitrary time dependence to the control system as an additional information to improve its performance. This input disturbance which acts as "early warning" that the controlled variable will be upset anytime in the future. With this warning, the feedforward controller

has the opportunity to define a new manipulated variable so that the controlled variable maintains at its set-point. In other words, feedforward control aids to reduce the influence of input disturbance to the control system. It is worth mentioning that this control strategy is independent of the process output.

Figure 2.9 shows the control approach of APCID using feedforward method. The control objective is the maintenance of the impact location (process output) denoted by L_{real} very close to its set-point, and the manipulated variable is the impact timing for the impact device to impart an impact. The set-point here is the experimental impact location, e.g., crest and trough on the periodic response of cyclic load represented by L_{exp}. The challenge is to reduce or, in the ideal case, eliminates the effect of the disturbance on the desired impact location by adjusting the impact timing of the impact device.

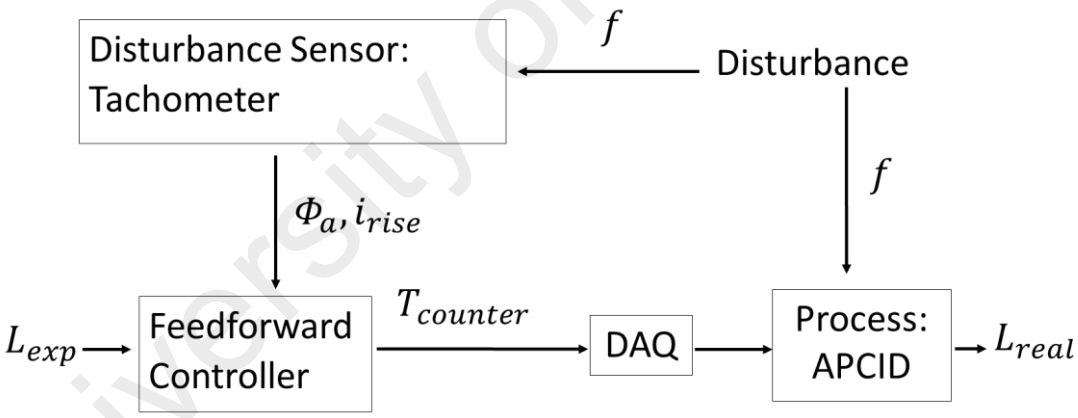

Figure 2.9: Block Diagram of Feedforward Control for APCID. The Variables Indicated are the Set-point, L_{exp}; the Control Signal, $T_{counter}$; the Process Output, L_{real}; the Measured Input Disturbance, f

The performance of the APCID is directly affected by the measured input disturbance, f, which is the operating frequency of a system, where in an ideal case, its performance is the best at constant operating frequency. However, when dealing with actual operating machinery, the measured f may vary slightly over time and sufficient to disturb the accuracy of the impact device. For incorporating such uncertainties in f, feedforward

control is implemented adapting real-time f from the structures at each triggered time block of signal by using tachometer.

Parameters for controlling the impact device are known as phase difference (degree), Φ_a, and array index of rising edge, i_{rise}, which can be derived from measured tachometer pulse signal. With this information, i.e., f, Φ_a, and i_{rise}, one can compute the phase difference time, T_Φ, time interval of load cycles, T_{cycle} which is the time corresponding number of load cycles added (n_{lc}), time interval of desired impact, $T_{desired}$ and lag time, T_{lag}. T_{lag} is introduced defining the time interval between the last rising edge of the tachometer speed component and the end of time block right after the impact is triggered. Thus, the governing equations are given by

$$T_\Phi = \left[-\frac{\Phi_a}{360°}\right] \times \frac{1}{f} \tag{2.16}$$

$$T_{cycle} = n_{lc} \times \frac{1}{f} \tag{2.17}$$

$$T_{desired} = \left[-\frac{\Phi_p}{360°}\right] \times \frac{1}{f} \tag{2.18}$$

where Φ_p is the desired impact phase angle and

$$T_{lag} = \left[S_{ext} + S_{comp} - i_{rise}\right] \times \frac{1}{SR} \tag{2.19}$$

where S_{ext} is the extracted samples from the end of time block and S_{comp} is the compensate sample (value of 1). The compensate sample is added to the equation as the phase difference time is calculated from the center of the tachometer speed component. Note that the time range of extracted samples must greater than the period of operating frequency so that at least one peak of tachometer speed component is observable in the extracted sample. An illustration of Φ_a, Φ_p, n_{lc}, S_{ext}, S_{comp}, and i_{rise} are shown in Figure 2.10 and Figure 2.11.

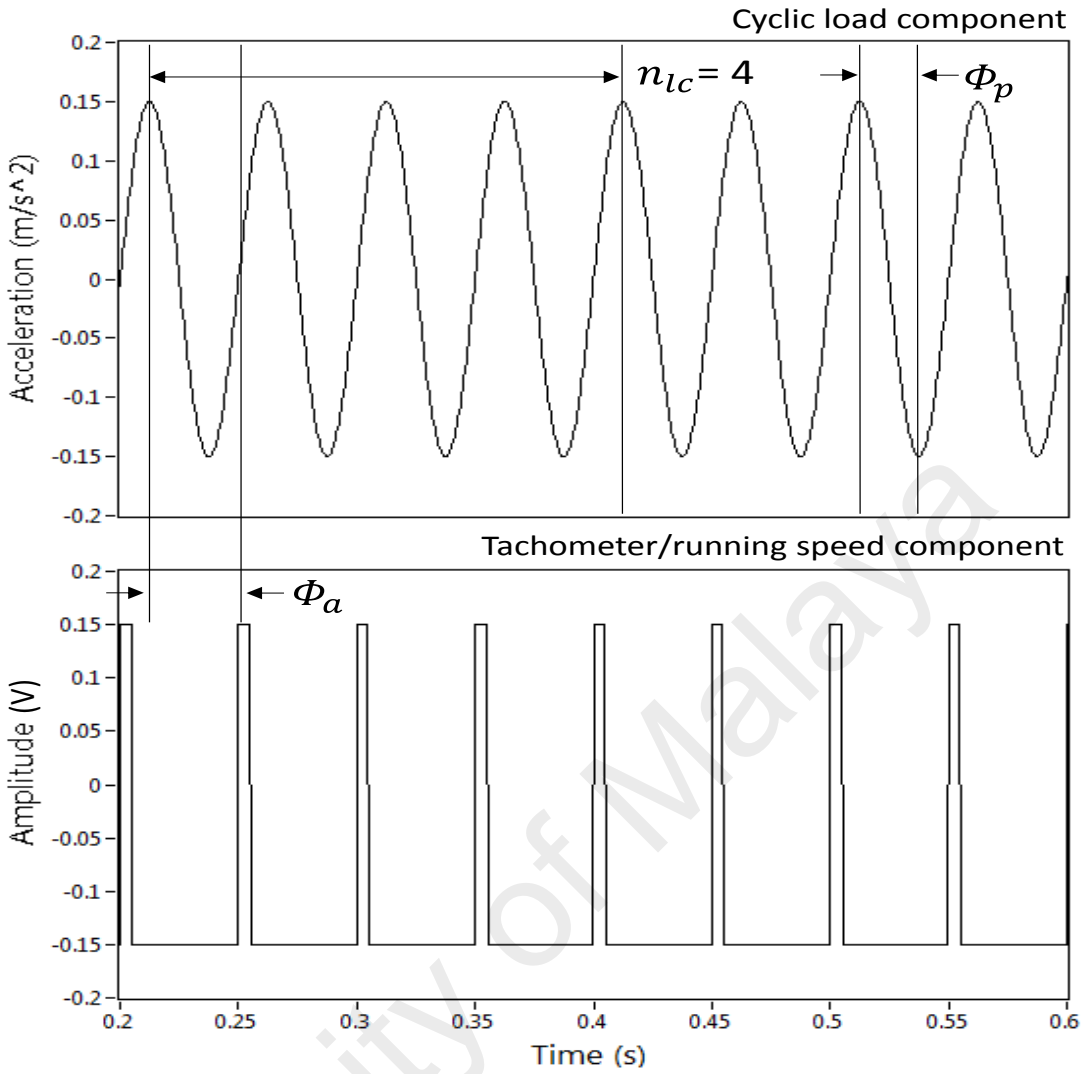

Figure 2.10: Illustration of Φ_a, Φ_p and n_{lc}

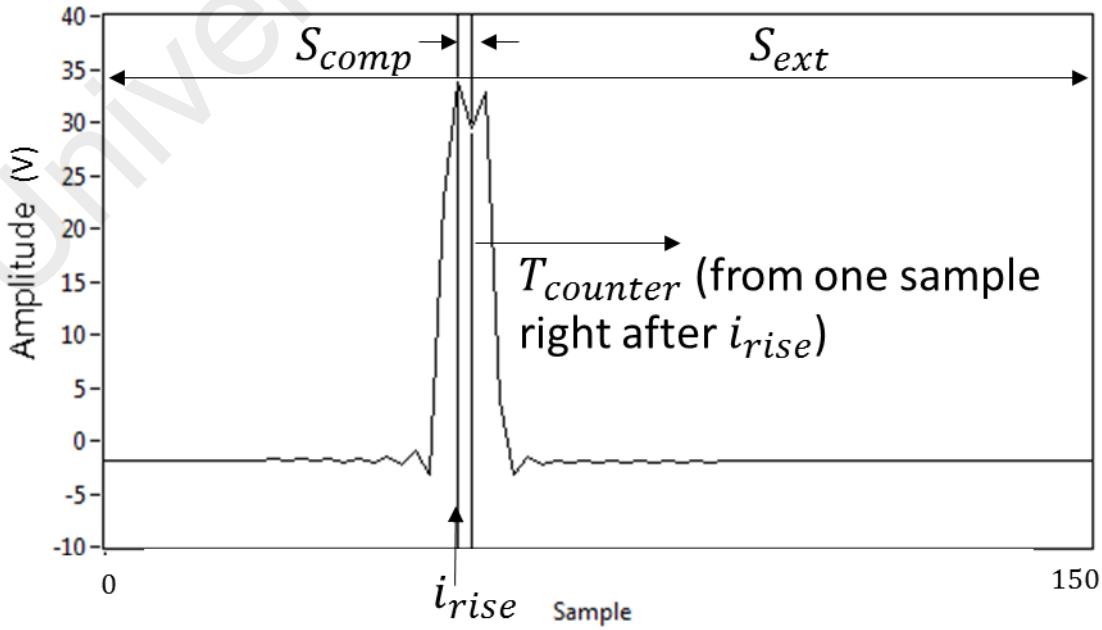

Figure 2.11: Illustration of S_{ext}, S_{comp}, i_{rise}, and $T_{counter}$ on Real Signal Measured from Tachometer

Before implementing the APCID into the real test, it is important to take into consideration time delay taken by the impact device to impart on the surface of the structure after "On" signal is sent to the device. It is determined through dummy impacts prior to the actual counted impacts and defined as $T_{offset} = t_{real} - t_{exp}$ where t_{exp} is the experimental impact time before offset adjustment and t_{real} is the real impact time observed in the response signal. Thus, the actual counter time, $T_{counter}$, forward to the controller consist of data acquisition (DAQ) system which in turns initiate an excitation signal for the impact device to impart an impact can be calculated by

$$T_{counter} = T_{\Phi} + T_{cycle} + T_{desired} - T_{lag} - T_{offset} \tag{2.20}$$

The automated impact device is designed in such a way that $T_{counter}$ is calculated from one sample right after i_{rise} maximum value of the last cycle tachometer speed component in a time block as shown in Figure 2.11. It is noted that $T_{counter}, T_{\Phi}, T_{cycle}, T_{desired}, T_{lag},$ and T_{offset} represent specific intervals of time whereas t_{real} and t_{exp} represent specific moments of time.

CHAPTER 3: RESEARCH METHODOLOGY

3.1 Introduction

The chapter begins with Section 3.2 which provides the overall research flow and scope for this study followed by Section 3.3 which has provided information on the instruments used and set-up for benchmark Experimental Modal Analysis (EMA). Next, the procedures to perform simulation study and experimental testing on the effect of phase synchronisation effect in Impact-synchronous Modal Analysis (ISMA) are presented in Section 3.4. ISMA during operation with different excitation strategies, i.e., manual impact hammer (proven concept in previously published articles) and automated impact device with non-synchronous impacts are elaborated in Section 3.5. Apart from this, the procedures for post-processing inconsistent phase selection assessment are presented in Section 3.6. The procedures and ideal input settings for Automated Phase Controlled Impact Device (APCID) in performing ISMA during operation are detailed in Section 3.7. Lastly, Section 3.8 has highlighted the experimental precautions.

3.2 Research Flow and Scope

Firstly, phase synchronisation effect on the effectiveness of ISMA during operation is investigated in simulation studies and experimental modal testing. The investigations look into two conditions, i.e., consistent and inconsistent phase condition, between response due to impact and periodic response of cyclic load. The Frequency Response Functions (FRFs) estimation obtained for these two conditions are then compared with FRFs estimation obtained during stationary condition.

Secondly, the research is based on utilising virtual instrument to control the automated impact device while performing ISMA during operation, i.e., running speed of 20 Hz and 30 Hz. Consistent impacts can be generated to be synchronised and non-synchronised with respect to the cyclic load component using this device. However, referring to the

findings from phase synchronisation assessment, the automated impact device is designed to provide non-synchronous impacts excitation. Elimination of the cyclic load component and ambient noises from the responses due to impact is then investigated in time and frequency domain. The experimental results obtained for ISMA using automated impact device with non-synchronous impacts are then compared with benchmark EMA and ISMA using manual impact hammer.

Next, a post-processing inconsistent phase selection assessment using MATLAB is proposed to further enhance the FRFs estimation. This allows selection of responses due to impact at different phase position with respect to the cyclic load component. The best FRFs estimation obtained through the phase selection assessment is then verified with the benchmark data. Subsequently, modal parameters extracted are compared with benchmark EMA and ISMA using manual impact hammer. The corresponding relationship between responses due to impact and periodic responses of cyclic load for the best FRFs estimation is thus a key factor for the following investigations.

To implement the findings from previous assessment in a real-time manner, an automated impact device is thus designed using feedforward control law, namely APCID. The device uses the electrical pulse signal from the tachometer as the initiation signal to impart impacts at a correct time/phase based on the phase difference information between signal measured from tri-axial accelerometer and tachometer. The accuracy of this device to impart impacts at desired phase location by considering offset consideration is investigated prior to implement in ISMA during operation. The FRFs estimation, as well as modal parameters obtained, are then compared with benchmark EMA and ISMA using manual impact hammer. Figure 3.1 presents the detailed research flow chart.

Figure 3.1: Research Flow Chart

3.3 Instrumentation and Set-up for Benchmark Experimental Modal Analysis

The system under testing consists of rotor shaft coupled to a motor as shown in Figure 3.2. This setup is an imitation of industrial system, particularly those in the petrochemical plant, e.g., the motor-driven metering pumps. The rotating disk aids in increasing the vibration magnitude of the system during operation as in most of the real cases, the magnitude of cyclic load component can be very high. A data acquisition (DAQ) system consisting of National Instrument NI-USB-9234 modules controlled by the DASYLab software was used. Channel 0 of NI-USB-9234 was connected to manual impact hammer whereas channel 1 to channel 3 were connected to tri-axial accelerometer. For the EMA test, Frequency Response Functions (FRFs) estimation relative to one excitation DOF, i.e., DOF 1 in vertical direction, (i.e. z-axis), were measured by impact testing and responses due to impact of 5 averages for all the DOFs were recorded. This gave a single input single output (SISO) analysis. Note that either roving hammer or roving accelerometer approach is favourable in this study but considering the experiment test using automated impact device in the later stage, roving accelerometer approach was selected. Sampling rate, SR used was 2048 samples/sec, and the vibration signal was collected for 2 seconds, so a total of 4096 samples were recorded for post-processing. Me'scope software was used to draw the three-dimensional structural model, (i.e. 20 out-of-plane DOFs/measurement points), of the test rig in coordinate points where every point was connected by straight lines as shown in Figure 3.3. Mode shape for each of the natural modes was recorded and animated through the model drawn.

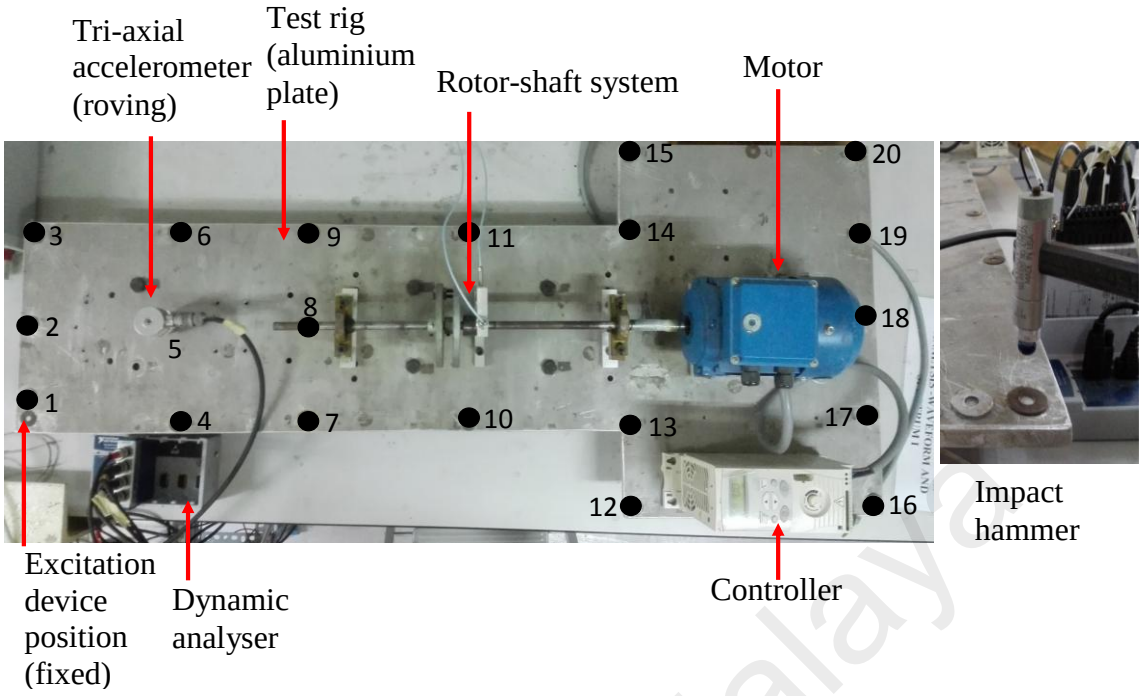

Figure 3.2: Equipment Setup with Test Rig

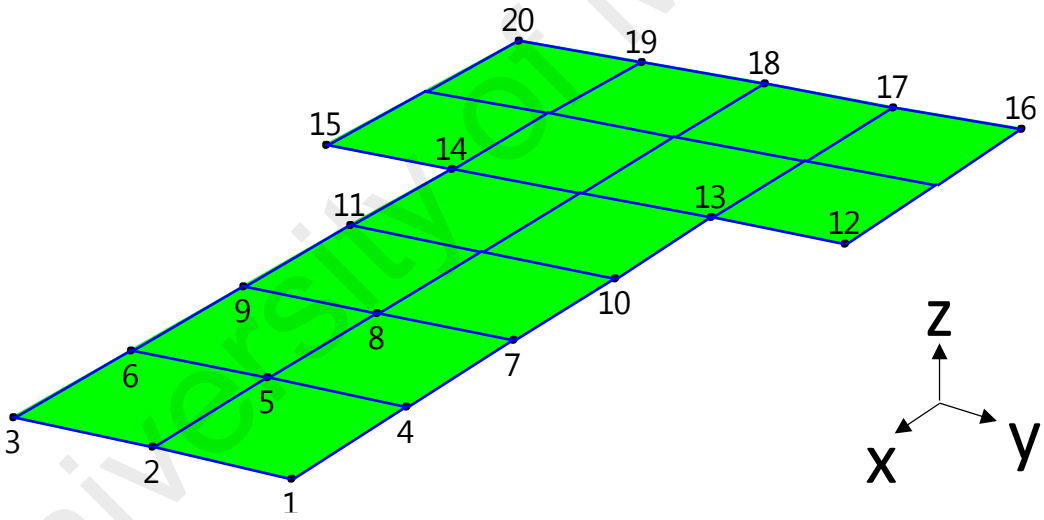

Figure 3.3: Structural Model of the Fault Simulation Rig (3D View)

3.4 The Effect of Phase Synchronisation in Impact-synchronous Modal Analysis

This section has elaborated the procedures to achieve the first objective in this research, i.e., to investigate the phase synchronisation effect in ISMA during operation, through virtual instrument simulation in Section 3.4.1 and experimental modal testing in Section 3.4.2.

3.4.1 Virtual Instrument Simulation

When performing modal testing during operation, the response due to cyclic load, i.e., a periodical signal and any ambient noise present themselves together with the responses due to impact. These unaccounted forces are filtered out in ISMA to give better results. To simulate and represent the actual scenario, this research only focuses on a periodical signal.

The phase angle of the dominant periodic responses of cyclic loads should be avoided to be consistent with every impact applied to enhance the effectiveness of ISMA. To study the effect of phase synchronisation in ISMA, virtual instrument (DASYLab) was used to simulate the required conditions, which are difficult to achieve with the existing manually operated impact hammer.

In this assessment, the responses due to consistent impacts were first designed to be consistent with the periodic responses of cyclic loads for every impact applied (Figure 3.4). Both responses contain the same frequency at 20 Hz. Meanwhile, in another simulation, consistent impacts were simulated, where the impacts applied were designed to be in the same frequency, i.e., 20 Hz, but at inconsistent phase angles with the periodic response of cyclic load (Figure 3.5). The phase angles of the response generated by each impact are not consistent with the phase angles of the response due to cyclic load. Responses due to impact and responses due to cyclic load and noise are linearly superimposed to simulate the actual scenario when performing modal testing during operation. When performing ISMA in a real practice, the unaccounted force components can be more dominant than the response due to impact. Thus, it is essential to use exponential windowing in performing the dual task as it can (1) eliminate or minimise leakage due to truncated response signal on a lightly damped structure and (2) filter out all the responses contributed by the unaccounted forces, i.e., the cyclic load component

in a time block. In the simulation, an exponential windowing function with a decay rate of 3 rad/s was applied to minimise leakage due to truncated response signal and to attenuate signals of a non-synchronous cyclic load component with respect to the impact, the harmonics, and noises to zero at the end of each time record window block as in real conditions. The effect of phase synchronisation in ISMA is studied and evaluated by comparing both the time and frequency responses of the averaged superimposed responses with the benchmarked response due to impact. Note that the reduction of frequency response magnitudes at the first and second natural peaks and the cyclic load component are defined by the percentage of improvement.

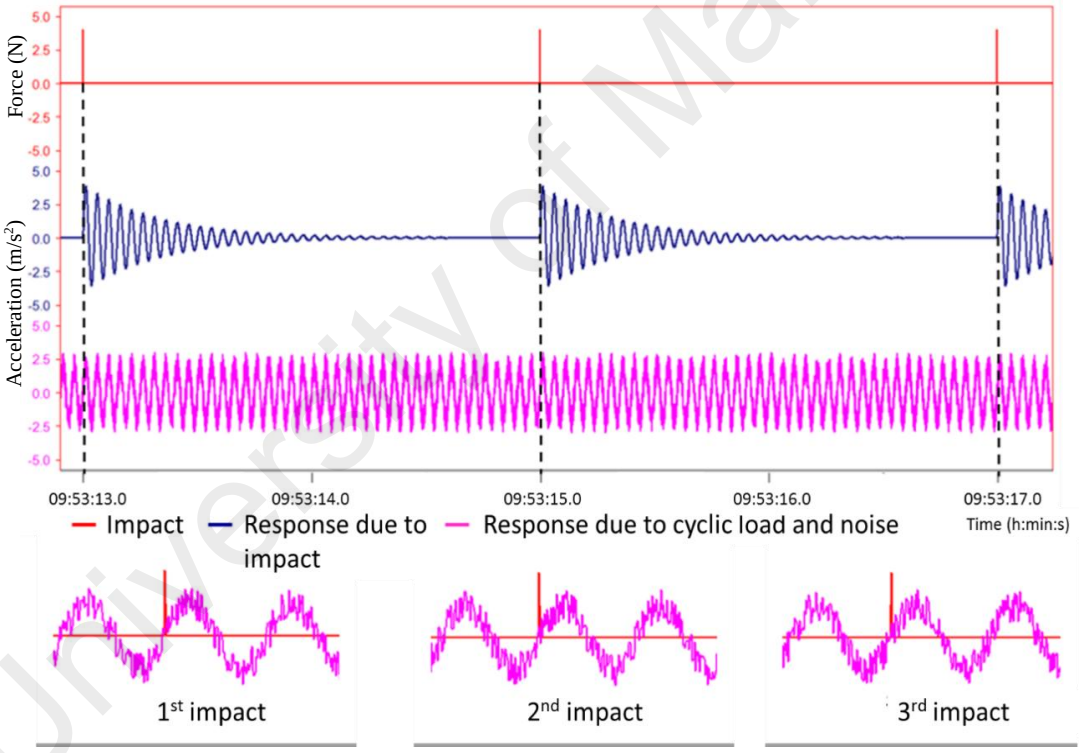

Figure 3.4: Consistent Phase with Respect to Every Impact Applied

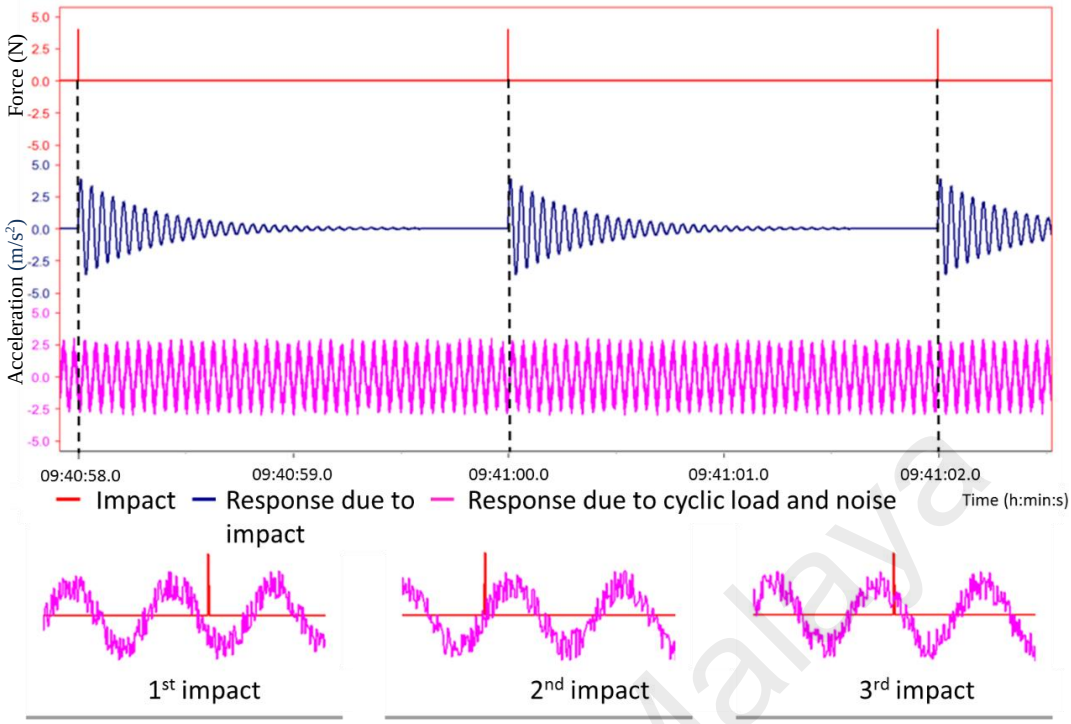

Figure 3.5: Inconsistent Phase with Respect to Every Impact Applied

3.4.2 Experimental Modal Testing

The experiment shares the same procedure that is used in Section 3.3. Four averages were taken at point 2 during static and rotating condition in order to investigate the phase synchronisation effect in ISMA during operation in experimental testing. The FRFs estimation for operation at 20 Hz was presented in four scenarios, (1) consistent phase condition for all impacts, (2) consistent phase condition for certain impacts, (3) inconsistent phase condition for all impacts (ideal case) and (4) inconsistent phase condition for all impacts. It is noted that scenarios 2 and 4 are commonly obtained when a manual impact hammer is being used. FRF estimation for a complete shutdown of the system was used as benchmark data. The estimated FRFs were then compared for both consistent and inconsistent phase conditions with benchmark data in order to evaluate the effect of phase synchronisation in modal testing during operation.

3.5 Impact-synchronous Modal Analysis with Different Excitation Strategies

This section has elaborated the procedures to achieve the second objective in this research, i.e., to validate the effectiveness of ISMA during operation using automated impact device with non-synchronous impacts. It begins with the technique in previous published article which is ISMA using manual impact hammer in Section 3.5.1 followed by the first attempt of using automated impact device in ISMA presented in Section 3.5.2.

3.5.1 Impact-synchronous Modal Analysis using Manual Impact Hammer

Same procedures as discussed in Section 3.3 were applied to ISMA using manual impact hammer. The differences here were that the test rig was operated at 20 Hz and 30 Hz instead of remained at shutdown mode whereas the number of averages were set at 20 for 20 Hz and 25 for 30 Hz, respectively. It is worth mentioning that the reason of choosing 20 Hz is because this operating frequency falls between the second and third natural mode whereas for 30 Hz, higher vibration amplitude is expected.

3.5.2 Impact-synchronous Modal Analysis using Automated Impact Device with Non-synchronous Impacts Excitation

The experiment used an automated impact device as shown in Figure 3.6 to replace the manual impact hammer in ISMA while sharing the same experiment procedures. The main body of the custom made automated impact device was a Mecalectro heavy duty linear solenoids, model 8.19.AB.83. The automated impact device was clamped firmly by using magnetic stand sitting on a C-beam type plate. This idea was developed to ensure that the impacts are more equal in force level and position, as the manual impacts may suffer from these two drawbacks. automated impact device was connected to National Instruments NI-USB-9472 via port 1 and port 10 and was supplied with 24 V_{dc}. Optimum distance between the test rig and the impact hammer tip was determined by energising

the automated impact device until the moment the impact hammer tip has just contacted the surface of the test rig in order to achieve a soft seating impact.

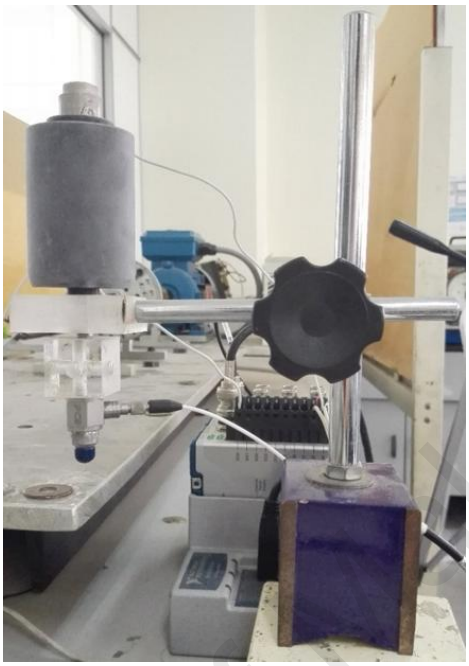

Figure 3.6: Automated Impact Device

As mentioned in (Ong and Lee, 2015), the impact contact time and impact interval of the impact device are determined by frequency of square wave (f_{square}), block size (BS), duty cycle (DC), and SR of the control signal. Note that the BS and SR used should produce a quick time response for the impact device within the data acquisition time of 2 seconds. The general setup is shown in Figure 3.7. A control signal in the form of a pulse was generated to trigger the impact device to excite the structure. As the operating frequency of the motor was set at 20 Hz, synchronisation of impacts with cyclic load component could be avoided as the impact frequency of 0.1239 Hz determined is a non-integer multiple of the cyclic load frequency as shown in Figure 3.8. It effectively creates a consistent but non-synchronous impact interval and makes the impacts not being synchronised with the cyclic load component. Time averaging of 20 blocks would diminish the cyclic load component and the desired response originated from impulse on the structure remains unchanged over time. The ideal combination of the parameters to be set into the DAQ was experimentally determined and the impact interval was

calculated as tabulated in Table 3.1. Note that 20 and 25 averages were used for 20 Hz and 30 Hz, respectively. This could differentiate the effectiveness of using the manual impact hammer and non-synchronous impacts with constant impact interval by automated impact device in FRF measurement and modal parameters extraction.

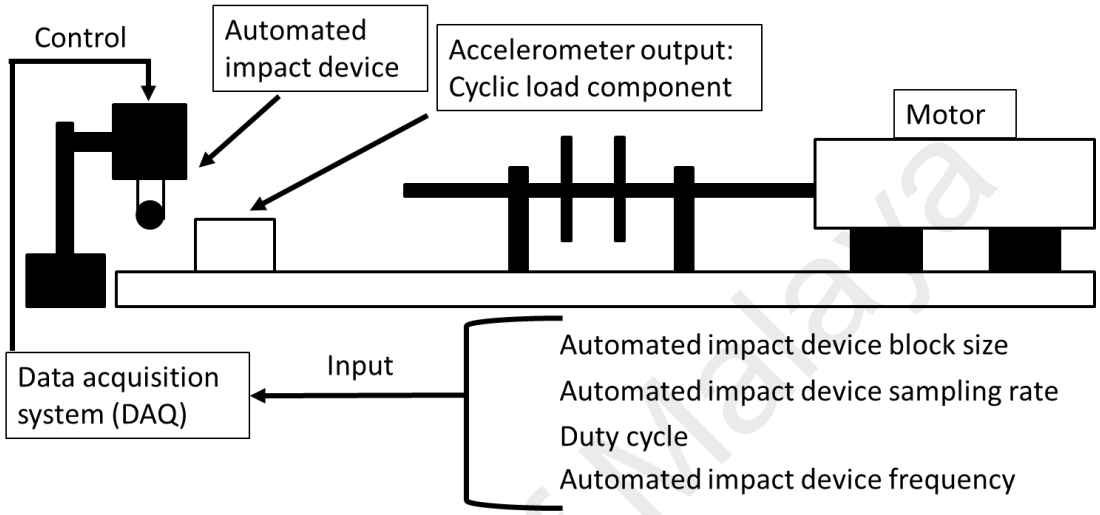

Figure 3.7: General Instrumentation Setup for Automated Impact Device with Non-synchronous Impacts

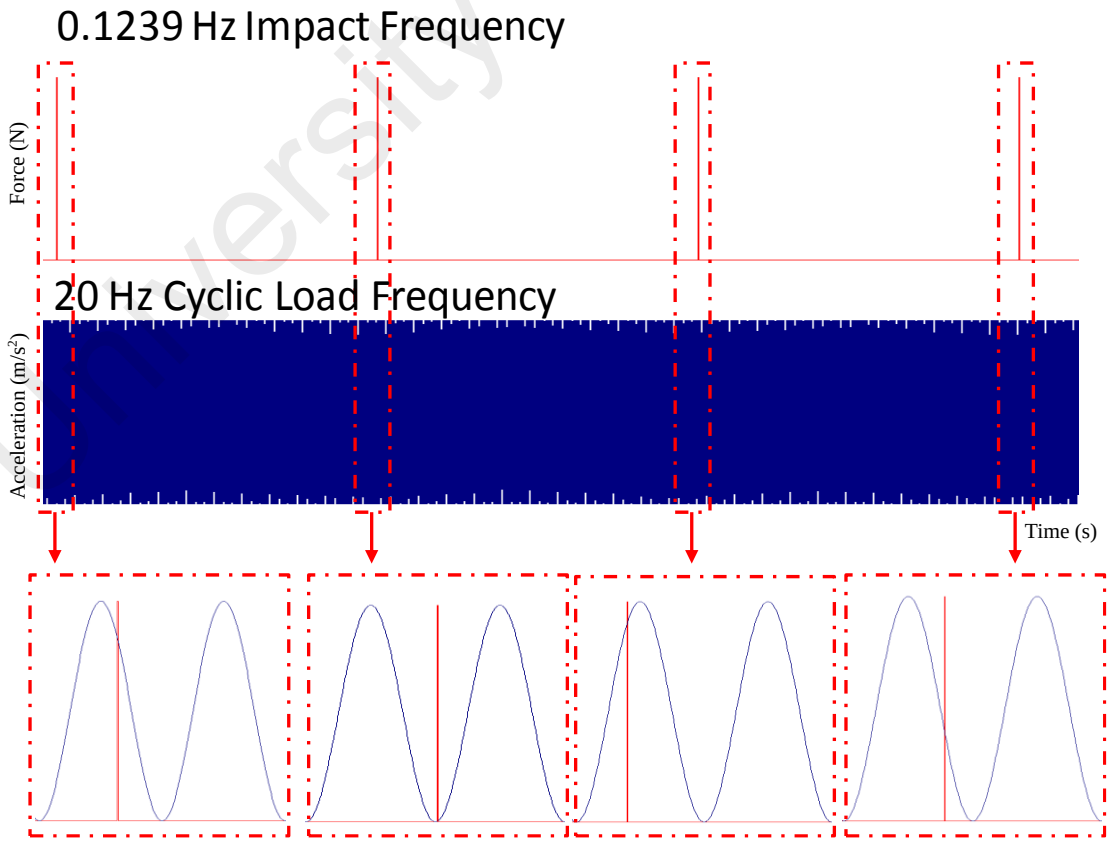

Figure 3.8: Simulation of Non-synchronous Impacts Applied Correspond to Periodic Response of Cyclic Load

Table 3.1: Summary of Input Parameters and Output Response for Automated Impact Device with Non-synchronous Impacts

Input signal to DAQ			Output response of automated impact device
Sampling Rate	(SR)	: 50,000 samples/sec	Impact interval = 0.1239 Hz
Block Size	(BS)	: 1024 samples	
Duty Cycle	(DS)	: 0.5%	
Frequency	(f_{square})	: 97.78 Hz	

3.6 Post-processing Inconsistent Phase Selection Assessment

This section has elaborated the procedures to achieve the third objective in this research, i.e., to propose a post-processing inconsistent phase selection assessment for the enhancement of ISMA during operation. In (Ong et al., 2015), it was reported that the best FRFs estimation with the most significant reduction of dominant cyclic load component was obtained when two out of phase acceleration responses/responses due to impact cancel each other out. However, this is an ideal case where it is rarely achievable when using manual impact hammer due to the lack of control on the impact timing in real-time testing. In (Brandt & Brincker, 2010), an automated optimizing FRFs estimation procedure in post-processing stage by selecting suitable force response was introduced. Initiated by this, an in-house post-processing programme was built using MATLAB 2013 utilising previous research findings which form the basic selection scheme (selection on acceleration response/response due to impact instead of force response) for the assessment in order to eliminate the harmonics; the key factor for the successful application of ISMA technique is the direct cancellation of the cyclic load component in time domain. In general, the assessment can be divided into two stages.

3.6.1 Stage 1: Define the Phase Position for All Impacts

The post-processing assessment utilised the raw data obtained from ISMA using manual impact hammer on 20 Hz and 30 Hz. The acceleration response/response due to impact captured and processed by the DASYLab in DDF-file format was first converted to MAT-

file using MATLAB. The conversion process has split up each of the acceleration responses, i.e., one particular knock point consists of 20 blocks of acceleration response to be selected. The starting position of the captured 20 acceleration responses, e.g., at measurement point 8 of 20 Hz as shown in Figure 3.9, were first defined at 100 samples phase position before the acceleration response starts. For instance, Figure 3.10 shows pre-triggered 100 samples before acceleration response starts and the zoomed in acceleration response. For that, the corresponding phase positions were determined and depicted in Figure 3.11. The same procedure was applied for all the 20 measurement points for both 20 Hz and 30 Hz.

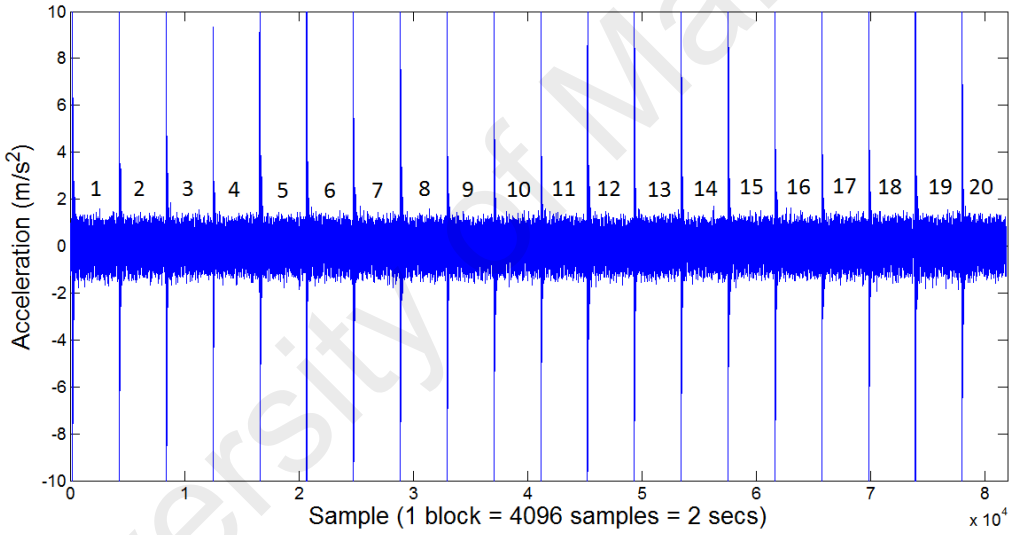

Figure 3.9: Total of 20 Acceleration Responses Acquired

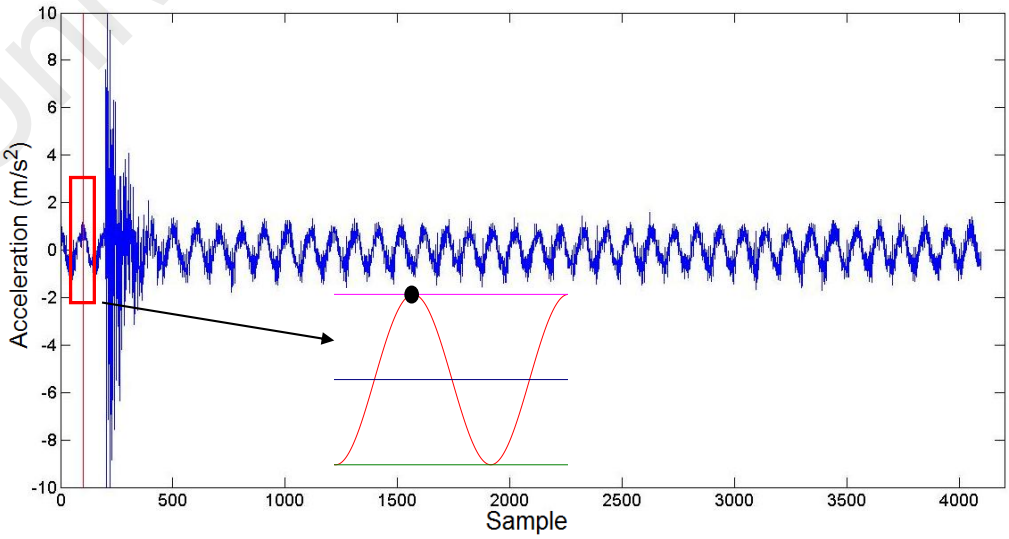

Figure 3.10: Pre-triggered 100 Samples before Acceleration Response Start and Zoomed In Acceleration Response

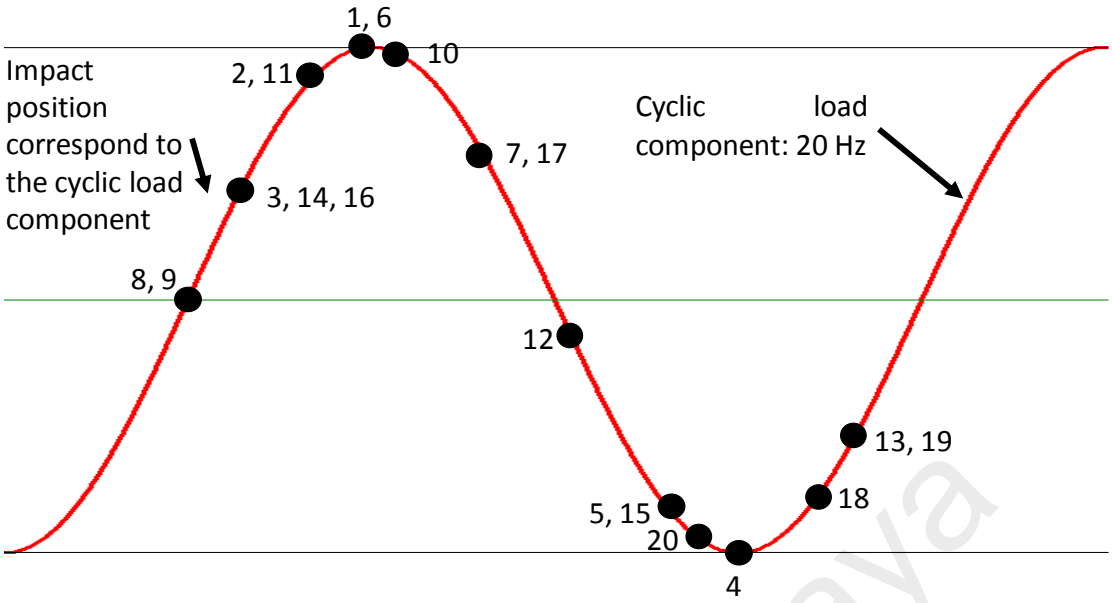

Figure 3.11: Phase Positions of 20 Impacts Corresponding to Respective Periodic Response of Cyclic Load

3.6.2 Stage 2: Selection of Impacts based on Impacts Phase Position

Synchronisation of the acceleration response with the cyclic load component could be indicated by examining the starting position of the acceleration response. If the periodic response of cyclic load is not synchronised with the acceleration response triggered by impact in the selected time blocks, these harmonic disturbances would reduce over Impact-synchronous Time Averaging (ISTA). In the case where both signatures triggered by impact are synchronised in the selected time blocks, both periodic response of cyclic load and response due to impact would average and remain over ISTA as they are treated being triggered by the impact.

For the operating frequency of 20 Hz, it is worthwhile to mention that if the cyclic load components are not dominant in the total response captured, performing ISTA on two selected impacts with 180° difference in phase angle of these two measured cyclic load responses would eliminate the harmonic disturbance at 20 Hz and random noise, with great effect, thereafter, preserving the response due to impact in just 2 averages.

For the operating frequency of 30 Hz, when the cyclic load component and its second harmonics are dominant in the total response captured, performing ISTA on two selected impacts with 90° difference in phase angle between these two measured cyclic load responses would eliminate the harmonic disturbances at 30 Hz and 60 Hz with great effect, thereafter, preserving the response due to impact in just 4 averages.

With the above mentioned information, minimum of 4 averages/impacts were manually selected from each measurement point to eliminate the periodic response of cyclic load as well as the random ambient noises during ISTA in this assessment. For instance, with the aid of Figure 3.11, it is now possible to select four averages/impacts, i.e., 4, 6, 10 and 20, in the assessment for operating frequency of 20 Hz. Subsequently, a comparison was made between the FRFs estimation generated from phase selection assessment using the acquired time signals in the post-processing stage and the full 20 averaged FRFs estimation for all measurement points. Note that the same procedure was applied to 30 Hz with 25 averages.

The procedure is more time consuming in the cases of complex geometry systems with escalated measurement points, but it is noted that the current study could find the relationship tailored between phase angle of cyclic load component with respect to impact applied for subsequent elimination of dominant cyclic load component as well as its harmonics.

3.7 Development and Implementation of Automated Phase Controlled Impact Device in Impact-synchronous Modal Analysis

This section has elaborated the procedures to achieve the fourth objective in this research which is to develop an automated impact device with inconsistent phase selection capability, i.e., APCID and to validate the effectiveness of ISMA during operation using APCID. The experiment procedures were generally the same as that of automated impact

device with non-synchronous impacts with constant impact interval with an additional tachometer connected to channel 1 of NI-USB-9234. The control and acquisition processes were done in LabVIEW 2013. Parameters that governed the control of APCID were triggering interval (T_{trig}), number of load cycles added (n_{lc}), extracted samples from the end of time block (S_{ext}), compensate sample (S_{comp}) and desired impact phase angle (Φ_p). Note that the values for phase difference time (T_Φ), lag time (T_{lag}) and time delay taken by the impact device to impart on the surface of the structure after "On" signal (T_{offset}) were different for every time block captured. The accuracy of APCID to knock at the desired impact location on the cyclic load component before and after offset adjustment was first investigated prior to perform modal testing using APCID. Responses due to impact at crest and trough of the cyclic load component were expected at the end of the investigation. During the modal testing, Φ_p between impacts was set at 180° for 20 Hz and 90° for 30 Hz. The ideal combination of the parameters to be set into the DAQ was tabulated in Table 3.2. Subsequently, 10 and 20 averages were made for 20 Hz and 30 Hz and this resulted in the direct cancellation of the harmonic disturbances leaving behind only the responses due to impact. This could differentiate the effectiveness of using the manual impact hammer and APCID with lesser number of averages in FRFs estimation and modal parameter extraction. The general setup for APCID is shown in Figure 3.12. Lastly, Table 3.3 shows the descriptions of the instrumentations used in this study.

Table 3.2: Summary of Input Parameters for APCID

Input signal to DAQ		20 Hz	30 Hz
Triggering interval	(T_{trig})	12 sec	12 sec
Number of load cycles added	(n_{lc})	11 cycles	6 cycles
Extracted samples from the end of time block	(S_{ext})	105 samples	69 samples
Compensate sample	(S_{comp})	1 sample	1 sample
Desired phase angle	(Φ_p)	0° and 180°	0°, 90°, 180° and 270°

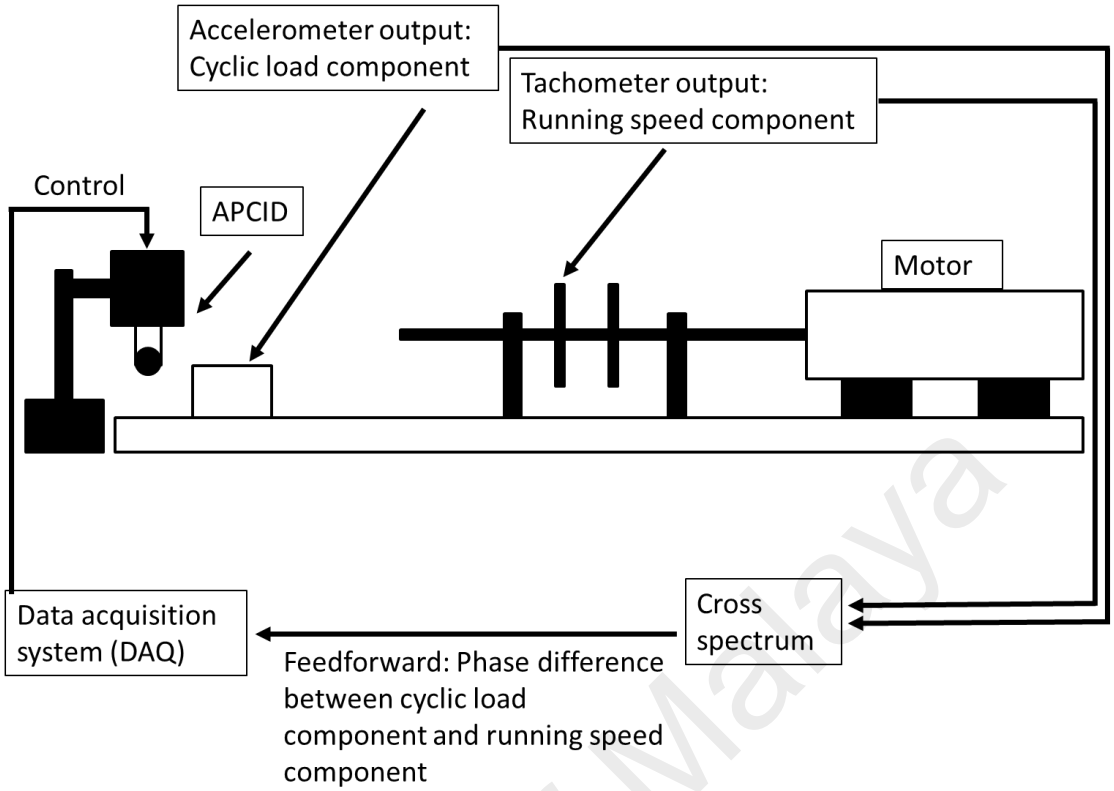

Figure 3.12: General Instrumentation Setup for APCID

Table 3.3: List of Instrumentation

Instruments	Details
UM simulation rig	Used as a test rig to perform ISTA
PCB impact hammer (Model 086C03)	Sensitivity: 2.16 mv/N Tip type: medium tip with vinyl cover Hammer mass: 0.16 kg Frequency range: 8kHz Amplitude range: ±2200 N peak Impact Period: random
Automated impact device and impact forcing sensor (Model 208C04)	Clamped with retort stand. Connected to channel 1 of National Instrument dynamic analysers Sensitivity: 1.162 mv/N Tip type: medium tip with vinyl cover a. <u>Consistent impact interval setting</u> Automated impact sampling rate: 50,000 samples/sec Automated impact block size: 1024 samples Frequency: 97.78 Hz Duty cycle: 0.5% Impact period: 8.06912 sec

Table 3.3: Continued

	b. APCID Triggering interval: 12 sec Number of load cycles added: 11 cycles for 20 Hz and 6 cycles for 30 Hz Extracted samples from the end of time block: 105 samples for 20 Hz and 69 samples for 30 Hz Compensate sample: 1 sample Desired phase angle: 0° and 180° for 20 Hz, 0°, 90°, 180° and 270° for 30 Hz
IMI tri-axial accelerometer (Model 604B31)	Sensitivity: 100 mv/g Frequency range: 0.5-5000 Hz Amplitude range: ±50 g peak
NI USB dynamic signal acquisition module (Model NI-USB 9234)	Number of channels: 4 ACD resolution: 24 bits Minimum data rate: 1650 samples/sec Maximum data rate: 51200 samples/sec
NI USB C series digital module, (Model NI-USB 9472)	Number of channels: 8 Compatible signal voltage : 6 V-30 V
NI Compact DAQ Chassis (Model NI cDAQ-9174)	Accepts up to 4 C Series I/O modules Hi-Speed USB connection to PC Input voltage range 9-30 V
DC Power Supply (Model QPX1200S)	Power: 1200W Max Current: 50A Max Voltage: 60V Supply voltage (24 V_{dc}) for automated impact device.
DASYLab v10.0	Sampling rate: 2048 samples/sec Block size: 4096 samples Channel 1: Manual impact hammer /Automated impact device Channel 2: Accelerometer (X-axis) Channel 3: Accelerometer (Y-axis) Channel 4: Accelerometer (Z-axis) In-house modal testing program Adjustment was made in Pre-setting mode.
LabVIEW 2013	Sampling rate: 2048 samples/sec Block size: 4096 samples Channel 1: APCID Channel 2: Tachometer (X-axis) Channel 3: Accelerometer (Y-axis) Channel 4: Accelerometer (Z-axis) In-house modal testing program Adjustment was made in Pre-setting mode.

Table 3.3: Continued

MATLAB 2013	To conduct post-processing inconsistent phase selection assessment.
ME'Scope v4.0	To process FRF obtained through DASYLab, MATLAB and LabVIEW. Curve fitting is done using orthopolynomial method to extract damped natural frequency, modal damping and residue mode shape.

3.8 Experimental Precautions

This research embarks on the following experimental precautions:

i. *Manual impact limit*

When the test structure is less than 1000 kg, manual impact hammer should be considered. Beyond 1000 kg, shaker driven by broadband signals, e.g. periodic chirp, pure and burst random noise, stepped-sine excitation, etc. should be used. Besides, flexibility of the test structure determines which excitation device should be used, i.e., poor coherence results due to localized non-linearity tend to happen when exciting a solid structure using manual impact hammer (Avitabile, 2017).

ii. *Cable connection*

Ensure that all cables used are functioning and the connections are tightly connected. Loss connections will result in vast amount of electrical noise being induced and may triggered unwanted measurement (Ong, 2013).

iii. *Trigger level of input excitation*

The trigger level should be set about 5% of the amplitude range. Too high may require a hard hammering on the structure and this always been the most direct evidence of unnecessary rattling comes from structure which causes non-linearity behaviour of the

structure. On the other hand, accidently trigger unwanted measurements by the analyses would be happened if the trigger level is set too low (Ong, 2013).

iv. *Windowing function*

For impulsive excitation technique, two common time domain windowing functions that have been introduced for transient signals are rectangular and exponential windows. Rectangular window is developed for fast decaying response signal and impulse. Suitable amount of exponential window will minimise the leakage effect especially when the structure is a low damped type where it takes a longer time for the structure response to decay to zero and improves the overall signal to noise ratio (Ewins, 2000).

CHAPTER 4: RESULTS AND DISCUSSIONS

4.1 Introduction

The experimental results and discussions to be described below are arranged in accordance with the objectives set in Section 1.5. The chapter begins with Section 4.2 which describes the effect of phase synchronisation effect in Impact-synchronous Modal Analysis (ISMA) during operation. Next, validation on the effectiveness of ISMA during operation through automated impact device with non-synchronous impacts, post-processing inconsistent phase selection assessment and Automated Phase Controlled Impact Device (APCID) are presented in Section 4.3, Section 4.4, and Section 4.5, respectively. It is important to note that in Section 4.3, Section 4.4, and Section 4.5, each of the excitation strategies is compared with ISMA using manual impact hammer due to the fact that the concept is proven from the previous literature and validated by benchmark Experimental Modal Analysis (EMA). In Section 4.6, a summary of comparisons between these excitation strategies are given, together with references to the most significant articles published previously.

4.2 The Effect of Phase Synchronisation in Impact-synchronous Modal Analysis during Operation

The phase synchronisation effect in simulation study for consistent and inconsistent phase condition is firstly discussed in Section 4.2.1 and Section 4.2.2. Next, four scenarios that could be happened in experimental modal testing are shown in Section 4.2.3, Section 4.2.4, Section 4.2.5, and Section 4.2.6. Note that each of the scenarios represents different phase synchronisation effect in ISMA. A summary of phase synchronisation effect in ISMA is then highlighted in Section 4.2.7.

4.2.1 Simulation of Consistent Phase Condition

In the first simulation, the phase of response due to impact is designed to be consistent with the phase of response due to cyclic load in every impact applied. Because of phase synchronisation, the unaccounted force components that contain the same frequency as the responses due to impact are dominant and could not be filtered. In this case, only the noises are eliminated after 30 averages. The linear superimposition of response due to impact and periodic response of cyclic load remain dominant as shown in Figure 4.1. When the time response is transformed to the frequency domain, the superimposed frequency response remains the same from the beginning until the end of the average where the cyclic load component is dominant and covers up the response due to impact component as shown in Figure 4.2. In this case, only the superimposed frequency response is smoothed where the noises are diminished. The dominant peak could not be diminished after 30 averages even when Impact-synchronous Time Averaging (ISTA) is utilised. From Table 4.1, frequency response amplitude improvement of less than 1% even after 30 averages shows that it is not effective in eliminating the cyclic load component when the phase is consistent with every impact applied. This quantitative assessment also shows that there is little correlation between averaged and benchmarked frequency response. In short, phase angle with respect to impact is an important parameter in ISMA.

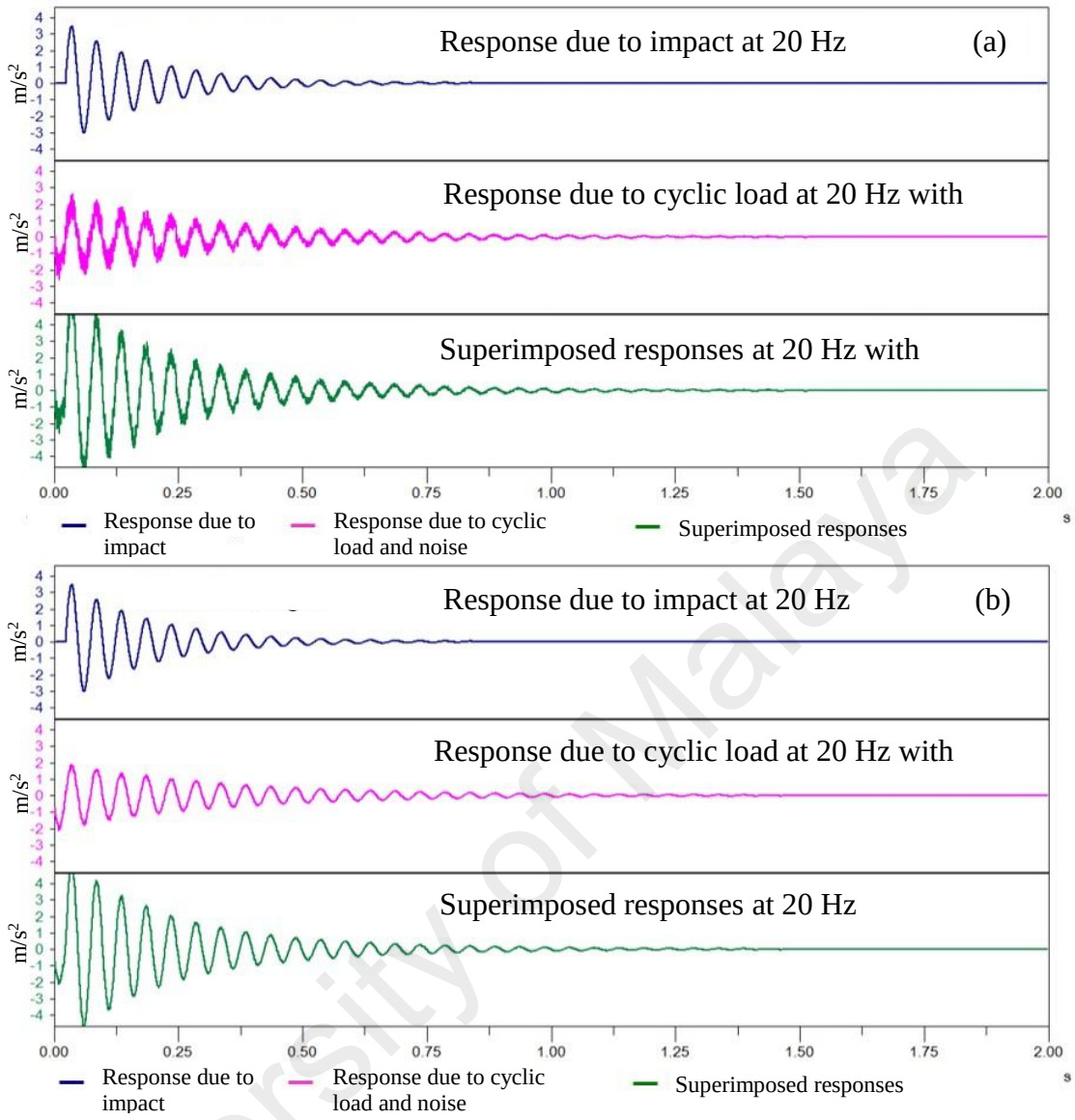

Figure 4.1: Time Responses for Consistent Phase Condition: (a) One Average, (b) 30 Averages with Less Than 1% Improvement

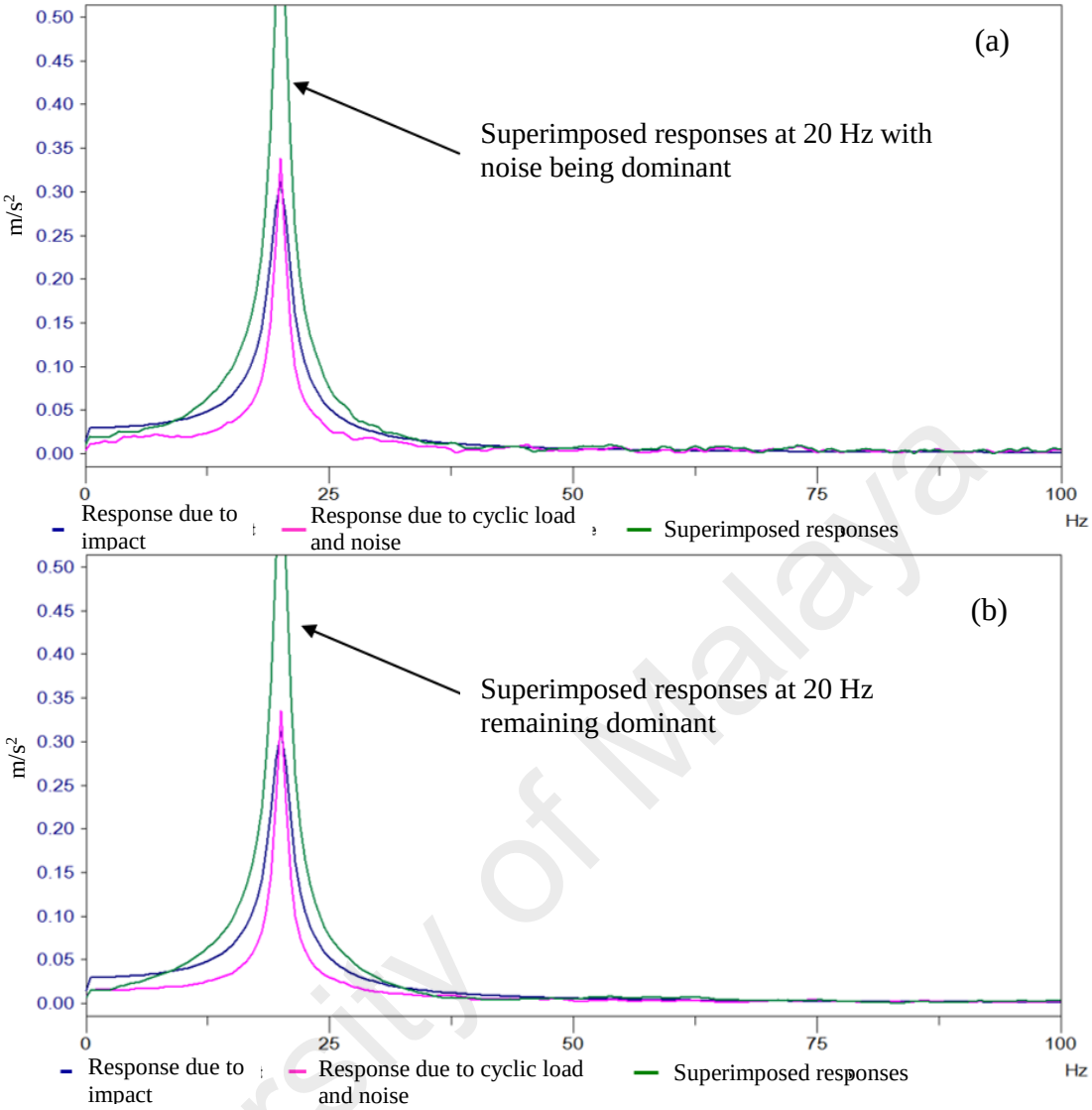

Figure 4.2: Frequency Responses for Consistent Phase Condition: (a) One Average, (b) 30 Averages with Less Than 1% Improvement

4.2.2 Simulation of Inconsistent Phase Condition

In another simulation, impacts are designed by ensuring that the phase angle of the dominant periodic responses of the cyclic loads with respect to impact is not consistent in every time record window block. Figure 4.3 (a) shows the responses generated when each time block acquisition is triggered by the impact at the beginning of average. Superimposed responses are dominant because of the dominance of the periodic response of cyclic load in the beginning when ISTA is to take place. When all of these time blocks are averaged in the time domain, the averaged time block as shown in Figure 4.3 (b)

reveals that the response due to cyclic load is filtered out maintaining the response due to impact after five averages are taken. The averaged superimposed responses are identical with the benchmarked response due to impact. Note that there is still some random ambient noise as the number of averages used is relatively small for removing all the noise. Meanwhile, in the frequency domain, Figure 4.4 shows that in the beginning of averaging, the cyclic load and noise components are dominant and they cover up the response due to the impact component. After just five averages are taken, the cyclic load and noise components are totally eliminated leaving a smooth superimposed frequency response which is identical to the benchmarked frequency response generated purely by the impact. The non-synchronous response components that contain even the same frequency as the component of the response due to impact are diminished when the phase is not consistent with respect to every impact signature. Quantitative assessment in Table 4.1 shows 98.48% of improvement, i.e., reduction in frequency response amplitude at 20 Hz, by eliminating the non-synchronous components after five averages taken. The frequency response after five averages shows very good correlation with the benchmarked result. Even if the phase angle of response due to cyclic load with every impact applied remains inconsistent until 30 averages, the improvement of frequency response amplitude remains, i.e., 98.78% and the averaged superimposed frequency response also remains identical with the benchmarked response due to impact.

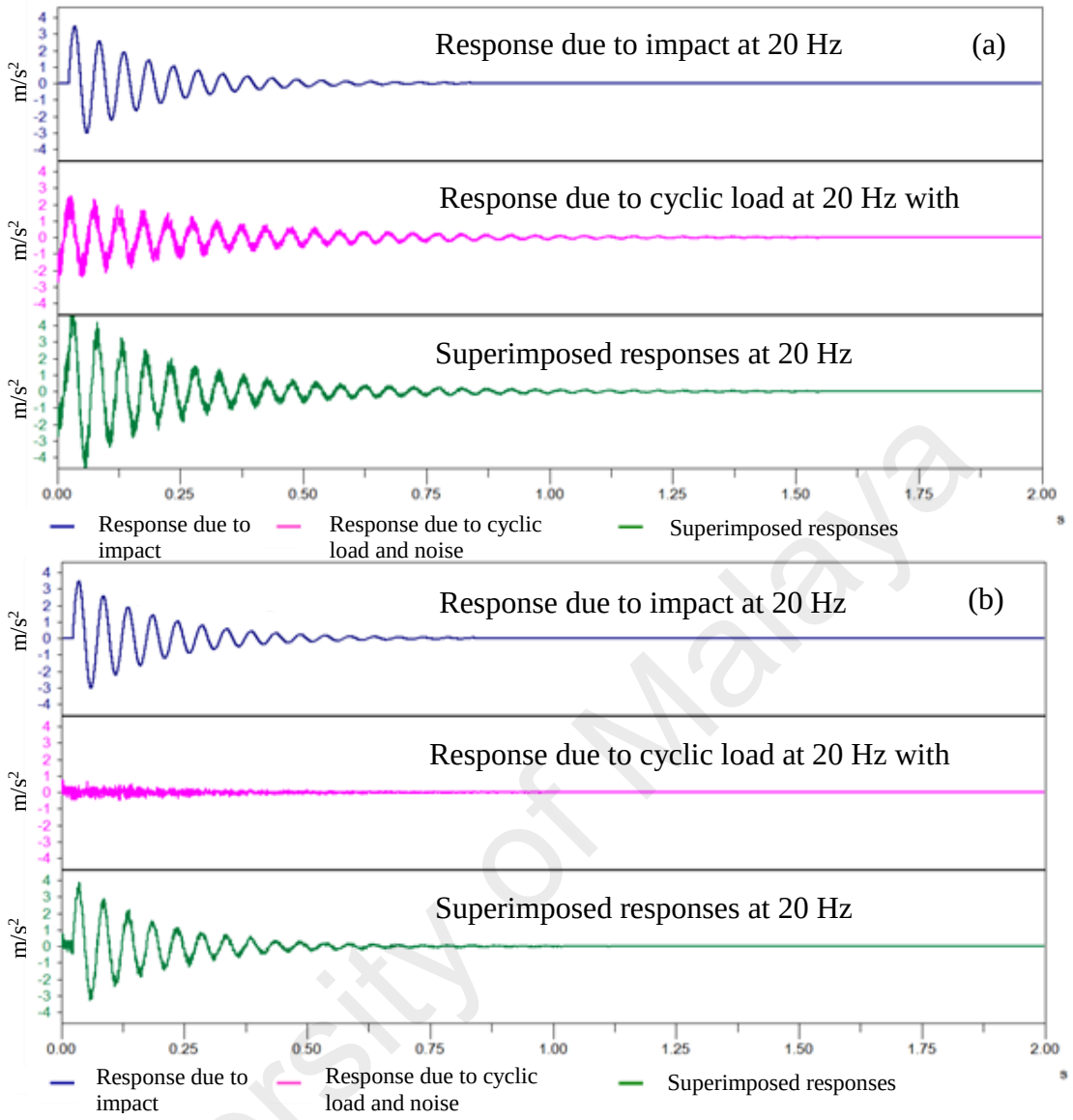

Figure 4.3: Time Responses for Inconsistent Phase Condition: (a) One Average, (b) Five Averages with 98.48% Improvement

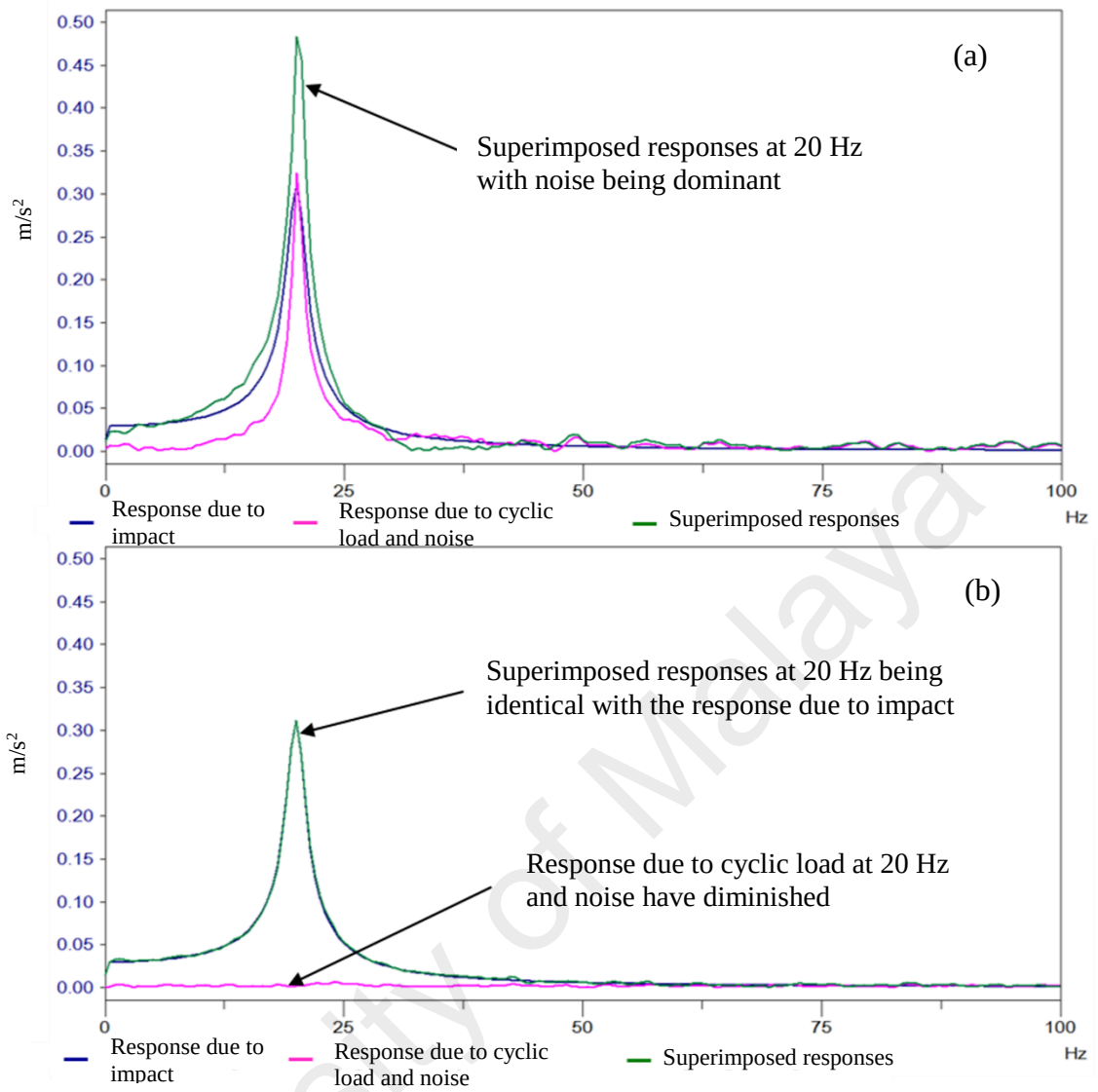

Figure 4.4: Frequency Responses for Inconsistent Phase Condition: (a) One Average, (b) Five Averages with 98.48% Improvement

Table 4.1: Closeness of Averaged Superimposed Frequency Response to the Benchmarked Frequency Response

Number of averages	Amplitude difference at 20 Hz (m/s^2)		Improvement (%)	
	Consistent phase	Inconsistent phase	Consistent phase	Inconsistent phase
1	0.33813	0.17426	-	-
5	0.33712	0.00265	0.30	98.48
30	0.33596	0.00212	0.64	98.78

4.2.3 Experimental Modal Testing for Scenario 1: Consistent Phase Condition for All Impacts

It is worth mentioning that although the possibility that a consistent phase condition occurs between the response due to impact and the response due to cyclic load is small, it is not totally impossible in modal testing using an impact hammer. Lack of knowledge and control of the impact with respect to the phase angle of the cyclic load is one of the limitations when carrying out ISMA using an impact hammer. Figure 4.5 shows four responses due to impact from modal testing for the first modal testing. It is observed that at the 100 pre-trigger samples phase position, the phases of the four responses due to impact are consistent with the phase of the response due to the cyclic load in every impact applied. In Frequency Response Function (FRF) estimation in Figure 4.6, it is observed that the cyclic load component at 20 Hz is not filtered out even when ISTA is utilised. The percentage differences for frequency response amplitude between the benchmark and consistent phase condition at first and second natural peaks are large, i.e., 66.37% and 95.29% at first and second natural peaks (Table 4.2). From Table 4.3, a frequency response amplitude improvement of less than 5% even after four averages at the first and second natural peaks and first harmonic at 20 Hz shows that it is not effective in eliminating the cyclic load component when the phase is consistent with every impact applied.

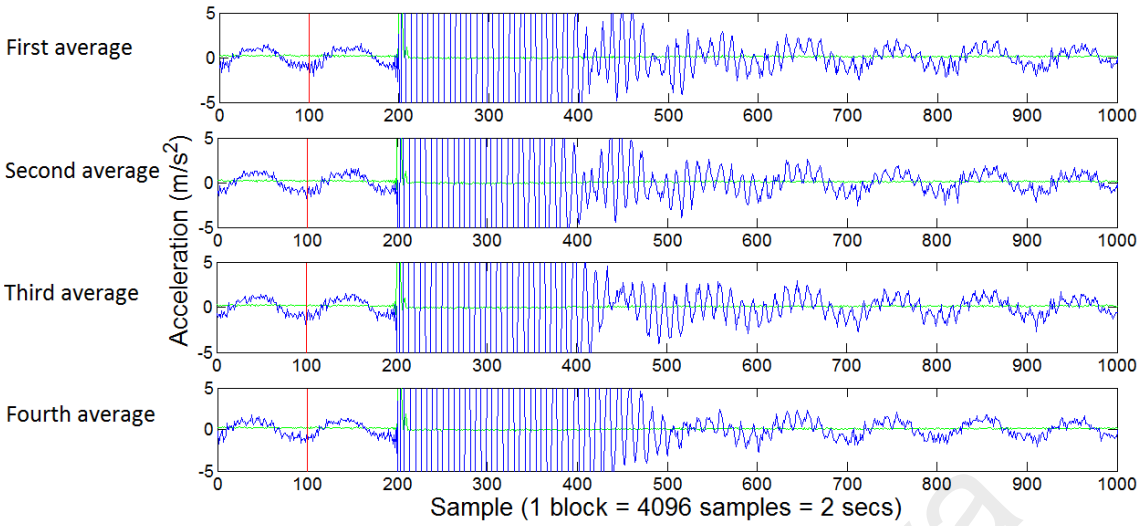

Figure 4.5: Consistent Phase Condition at 100 Pre-trigger Samples Phase Position of Responses due to Impact for Scenario 1

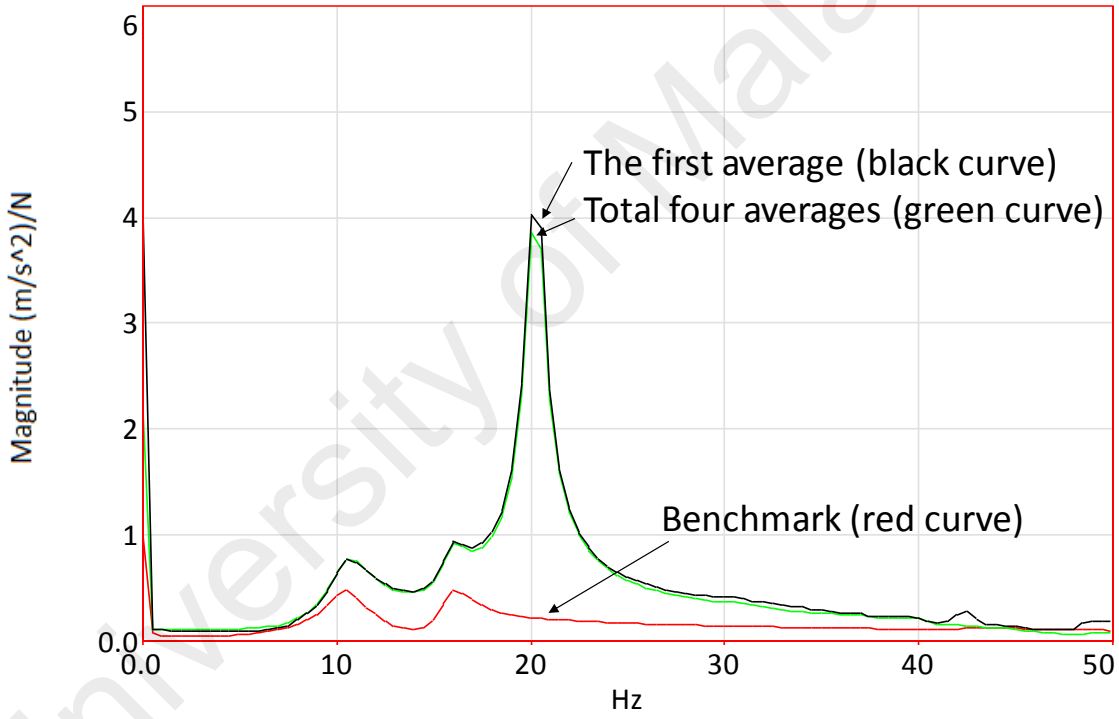

Figure 4.6: FRF Estimation for Scenario 1

4.2.4 Experimental Modal Testing for Scenario 2: Consistent Phase Condition for Certain Impacts

A more common scenario obtained when performing modal testing using a manual impact hammer on an operating system is presented in scenario 2. For scenario 2, it is observed that only the third average is synchronised with the fourth average as shown in Figure 4.7. Qualitatively, a slight decrease of frequency amplitude at 20 Hz harmonic frequency

is expected and it is observable in Figure 4.8 after performing four averages. The percentage differences for frequency response amplitude between the benchmark and consistent phase condition at the first and second natural peaks are large, i.e., 65.72% and 61.88% at first and second natural peak respectively (Table 4.2). From Table 4.3, the frequency response amplitude shows better improvement especially at 20 Hz, and recorded a value of 33.50% after four averages. The improvement in scenario 2 is due to the fact that only two averages are synchronised with the cyclic load component.

It should be noted from scenario 1 and 2 that the number of impacts which have consistent phase with the cyclic load component can significantly influence the FRF estimation. Recall that the improvement of less than 5% at harmonic frequency of 20 Hz for scenario 1 is because all the impacts are synchronised with the cyclic load component whereas scenario 2 can achieve an improvement of 33.50% because only two averages are synchronised with the cyclic load component, i.e., the third and fourth averages. Generally, during the consistent phase condition, the response from the cyclic load will dominate and disturb the natural peak which is close to it, i.e., the second natural peak, so that it leads to improper identification of the mode.

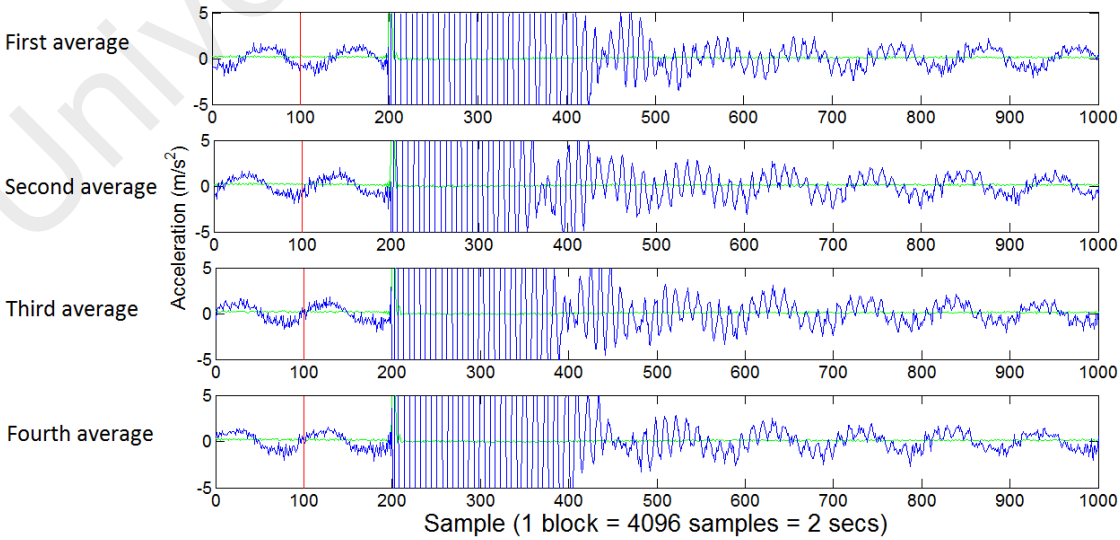

Figure 4.7: Consistent Phase Condition at 100 Pre-trigger Samples Phase Position of Responses due to Impact for Scenario 2

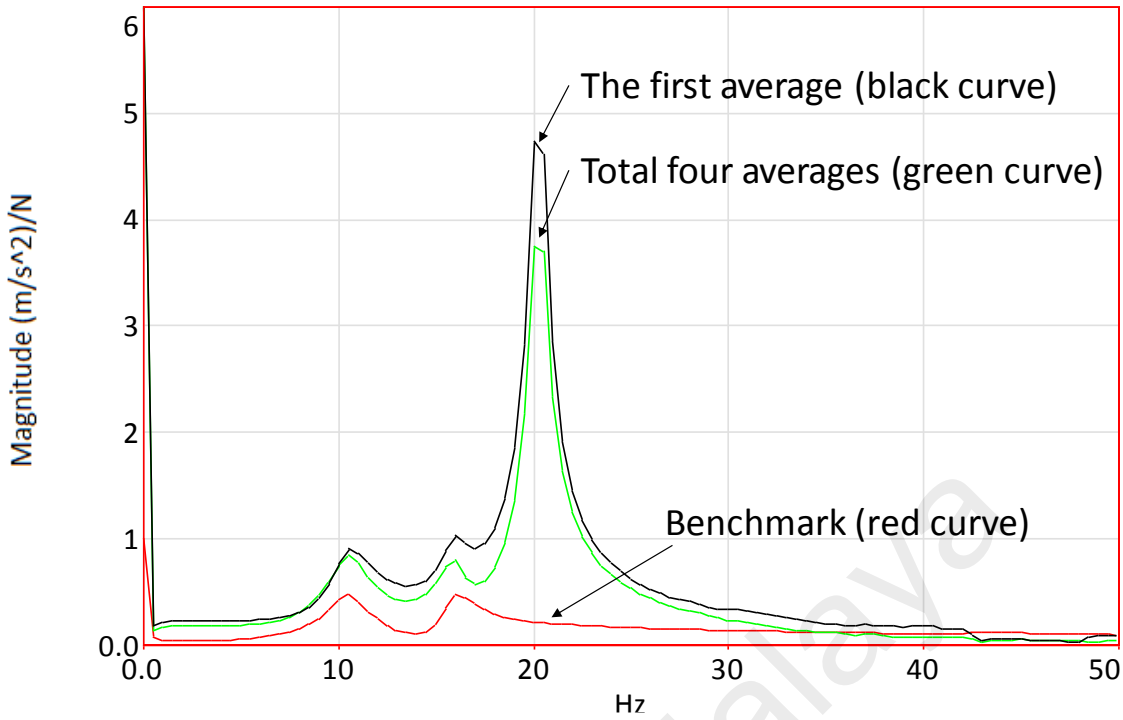

Figure 4.8: FRF Estimation for Scenario 2

Table 4.2: Frequency Response Amplitude Difference at the First and the Second Natural Peaks between Benchmark and the Consistent Phase Condition with Four Averages

Natural peak	Frequency response amplitude (m/(s^{2}N))			Percentage of difference (%)	
	Benchmark	Scenario 1	Scenario 2	Scenario 1	Scenario 2
First	0.458	0.762	0.759	66.37	65.72
Second	0.467	0.912	0.756	95.29	61.88

Table 4.3: Frequency Response Amplitude Difference at the First, the Second Natural Peaks, and 20 Hz between the First and the Total Four Averages for the Consistent Phase Condition

Frequency response amplitude (m/(s^{2}N))						
Number of averages	First natural peak		Second natural peak		20 Hz harmonic	
	Scenario 1	Scenario 2	Scenario 1	Scenario 2	Scenario 1	Scenario 2
1	0.761	0.844	0.930	0.825	4.030	4.030
4	0.762	0.759	0.912	0.756	3.830	2.680
Improvement (%)						
Number of averages	First natural peak		Second natural peak		20 Hz harmonic	
	Scenario 1	Scenario 2	Scenario 1	Scenario 2	Scenario 1	Scenario 2
1	-	-	-	-	-	-
4	-0.13	10.07	1.94	8.36	4.96	33.50

4.2.5 Experimental Modal Testing for Scenario 3: Inconsistent Phase Condition for All Impacts (Ideal Case: Cyclic Load Components Cancel Each Other Out)

Figure 4.9 shows four responses due to impact from modal testing. It is observed that at the 100 pre-trigger samples phase position, the phases of the four responses due to impact are inconsistent with the phase of the response due to cyclic load for every impact applied. In FRF estimation in Figure 4.10, it is observed that the cyclic load component at 20 Hz is filtered out when ISTA is utilised. The percentage difference for the frequency response amplitude between the benchmark and inconsistent phase condition at first and second natural peaks is comparatively small, i.e., 23.80% and 10.49% at the first and second natural peaks (Table 4.4). Quantitative assessment in Table 4.5 shows 38.97%, 54.91% and 95.22% of improvement in frequency response amplitude at first and second natural peaks and first harmonic at 20 Hz by eliminating the non-synchronous components after four averages taken. The excellent improvement in the result is due to the fact that the cyclic load components cancel each other out during ISTA for; (1) first and third average and (2) second and fourth average, leaving behind the desired response due to impact (Ong & Lee, 2015).

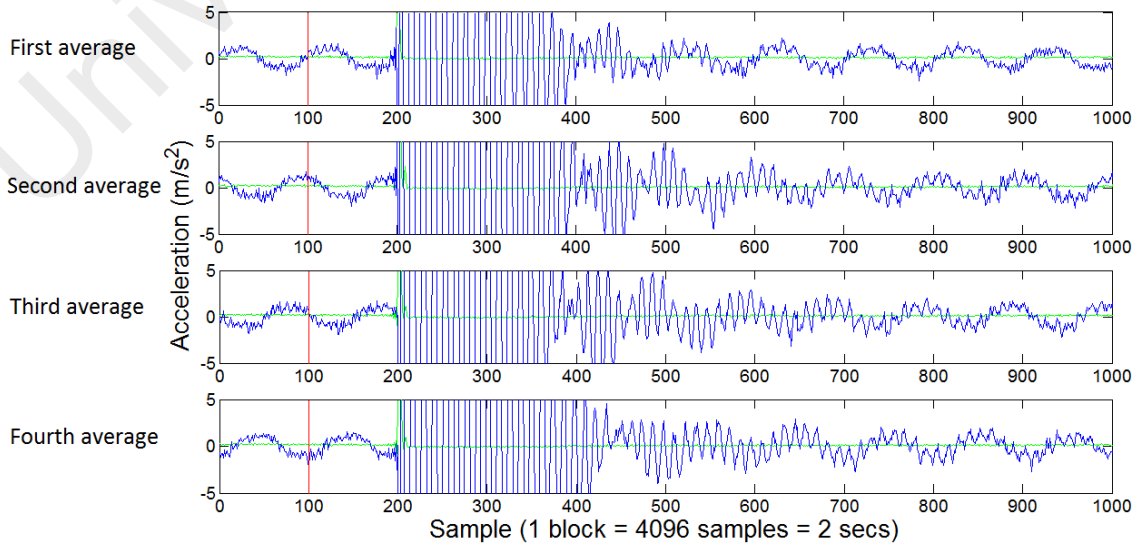

Figure 4.9: Inconsistent Phase Condition at 100 Pre-trigger Samples Phase Position of Responses due to Impact for Scenario 3

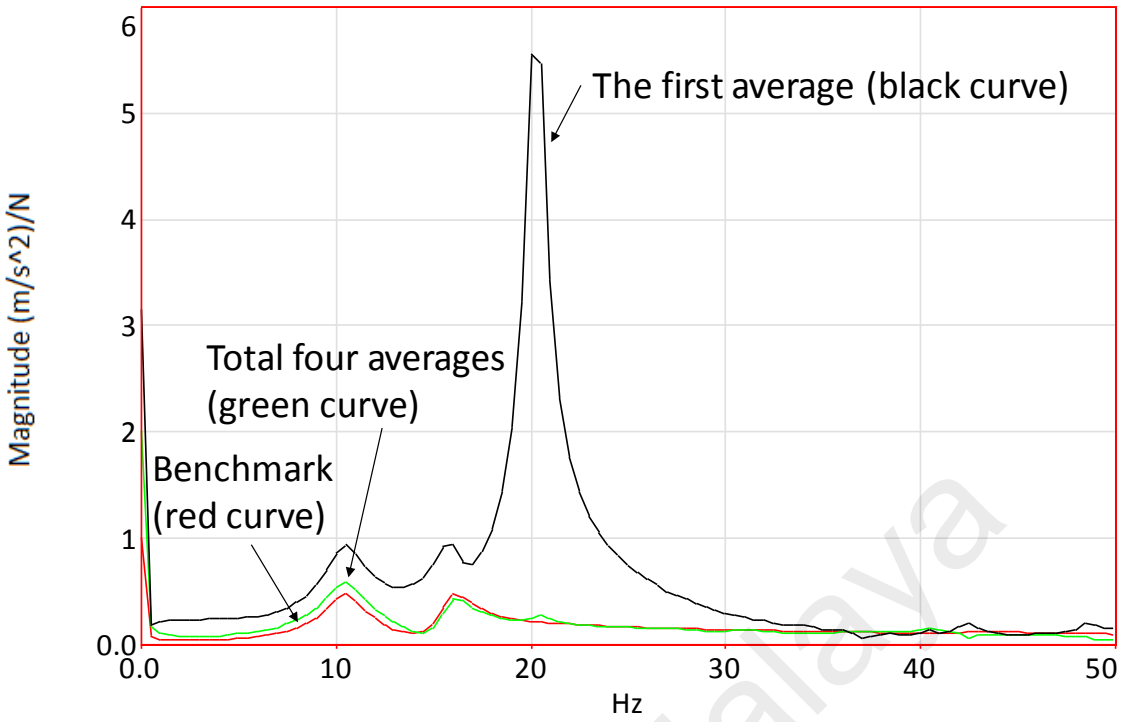

Figure 4.10: FRF Estimation for Scenario 3

4.2.6 Experimental Modal Testing for Scenario 4: Inconsistent Phase Condition for All Impacts

Scenario 3 is an ideal case, and a more relevant condition commonly achieved by a manual impact hammer, (i.e. scenario 4) is presented in this section. As shown in Figure 4.11, at the 100 pre-trigger samples phase position, the phase of the responses due to impact is inconsistent with the phase of responses due to the cyclic load component. Qualitatively, an obvious decrease of frequency amplitude at the 20 Hz harmonic frequency can be seen in Figure 4.12. It is observed that the percentage differences for frequency response amplitude between the benchmark and inconsistent phase condition at first and second natural peaks are slightly higher than in scenario 3 (Table 4.4). From Table 4.5, the frequency response amplitude also shows better improvement compared to the consistent phase condition especially at 20 Hz, and recorded a value of 74.75% after four averages. However, the cyclic load component is not totally filtered out in this case as the number of averages used is very small. It is believed that a high number of averages which satisfy the inconsistent phase condition requirement would yield a better FRF

estimation. Also, it is worth mentioning that the second natural peak experiences a higher percentage of improvement for scenarios 3 and 4 compared to the first natural peak as this mode is closer to the harmonic frequency of 20 Hz.

Recall that the percentage of improvement at a harmonic frequency of 20 Hz is higher in scenario 3 compared to scenario 4, although both scenarios satisfy the condition of inconsistent phase between response due to impact with respect to periodic response of cyclic load. However, scenario 3 presents an additional benefit in that the cyclic load components tend to cancel each other out during ISTA, leaving behind the desired response due to impact. Nevertheless, both scenarios indicate the importance of the phase synchronisation effect, i.e., inconsistent phase condition, in modal testing during operation with minimum amount of averages to eliminate the unaccounted forces components.

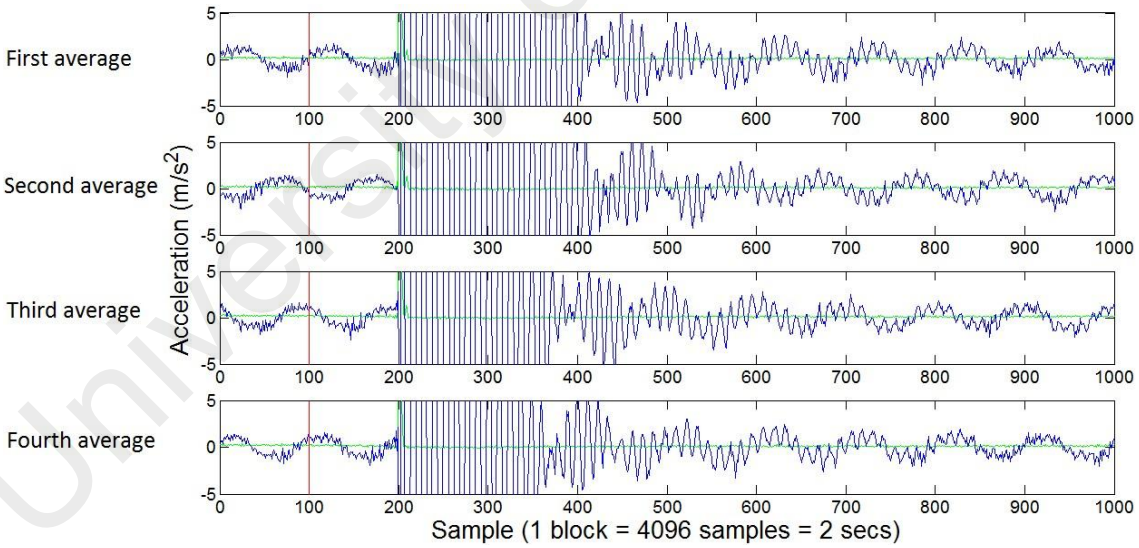

Figure 4.11: Inconsistent Phase Condition at 100 Pre-trigger Samples Phase Position of Responses due to Impact for Scenario 4

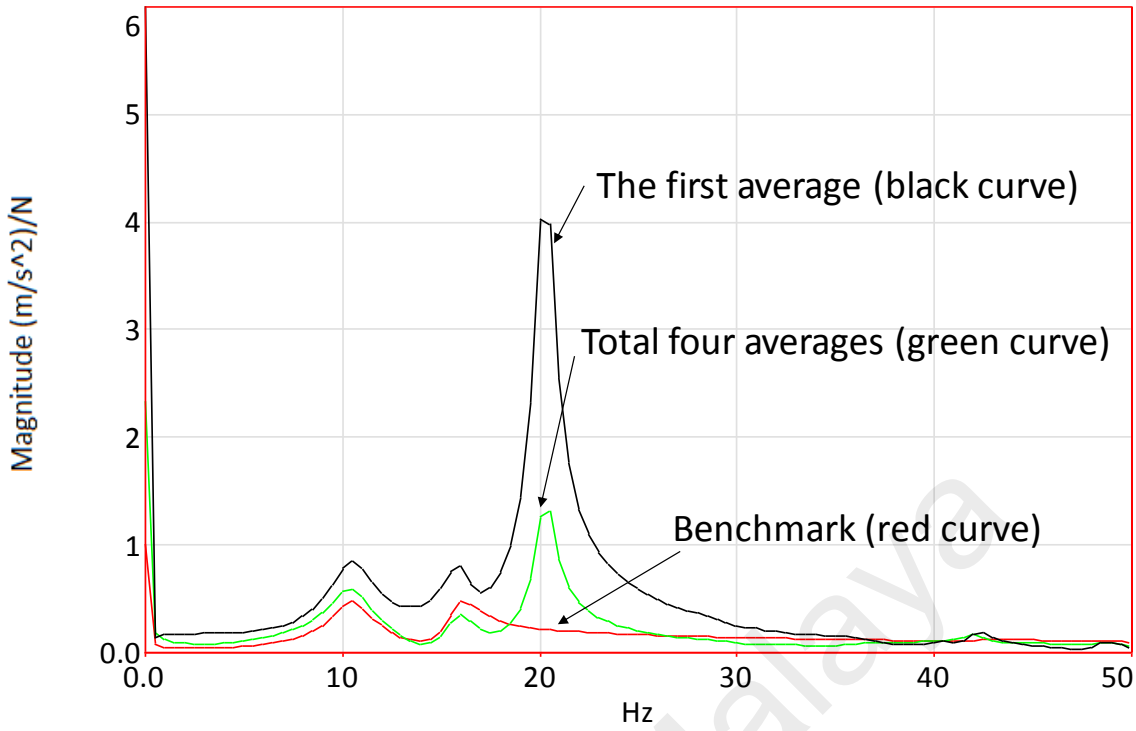

Figure 4.12: FRF Estimation for Scenario 4

Table 4.4: Frequency Response Amplitude Difference at the First and the Second Natural Peaks between the Benchmark and the Inconsistent Phase Condition with Four Averages

Natural peak	Frequency response amplitude (m/(s^{2}N))			Percentage of difference (%)	
	Benchmark	Scenario 3	Scenario 4	Scenario 3	Scenario 4
First	0.458	0.567	0.578	23.80	26.20
Second	0.467	0.418	0.336	10.49	28.05

Table 4.5: Frequency Response Amplitude Difference at the First, the Second Natural Peaks and 20 Hz between the First and the Total Four Averages for the Inconsistent Phase Condition

Frequency response amplitude (m/(s^{2}N))						
Number of averages	First natural peak		Second natural peak		20 Hz harmonic	
	Scenario 3	Scenario 4	Scenario 3	Scenario 4	Scenario 3	Scenario 4
1	0.929	0.839	0.927	0.784	5.570	4.040
4	0.567	0.578	0.418	0.336	0.266	1.300
Improvement (%)						
Number of averages	First natural peak		Second natural peak		20 Hz harmonic	
	Scenario 3	Scenario 4	Scenario 3	Scenario 4	Scenario 3	Scenario 4
1	-	-	-	-	-	-
4	38.97	28.58	54.91	49.49	95.22	74.75

4.2.7 Summary of Phase Synchronisation Effect

At the end of this stage, it is proven that to enhance the effectiveness of ISMA method, synchronisation of response due to impact with cyclic load component should be avoided. Since it is very difficult or almost impossible to achieve this when using manual impact hammer, automated impact device with non-synchronous impacts is seen to be a good solution. Thus, the effectiveness of ISMA using automated impact device with non-synchronous impacts will be discussed in the following section.

4.3 Experimental Validation on the Effectiveness of Impact-synchronous Modal Analysis during Operation using Automated Impact Device with Non-synchronous Impacts

In this section, the FRFs estimation and modal parameters using two different excitation strategies, i.e., manual impact hammer and automated impact device with non-synchronous impacts, for 20 Hz and 30 Hz are compared in Section 4.3.1, Section 4.3.2, Section 4.3.3, and Section 4.3.4. A summary of ISMA using automated impact device with non-synchronous impacts is then highlighted in Section 4.3.5.

4.3.1 Frequency Response Functions Estimation from Automated Impact Device with Non-synchronous Impacts and Manual Impact Hammer for 20 Hz

Figure 4.13 and Figure 4.14 depict the experimentally determined FRFs through modal testing during static (EMA) and operation using manual impact hammer and non-synchronous impacts by automated impact device, respectively. A better FRF estimation is the result of output response of a structure divided by the input excitation only. By comparing these estimated FRFs, the highest peak is observed at 20 Hz using manual impact hammer (0.932 m/s^2N). The cyclic load component at 20 Hz is dominant and covers up the adjacent modes and consequently seriously affects the FRFs estimation. Meanwhile, using the automated impact device with non-synchronous impacts and

constant impact interval yields lower harmonic disturbance at 20 Hz (0.516 m/s^2N) and thus the adjacent modes appear and are significantly enhanced.

The highest cyclic load component that is observed in the FRFs estimate using the manual impact hammer is possibly due to any of three reasons; (i) inconsistency in force level of input excitation; (ii) inconsistency in excitation location between the impacts, and (iii) inefficient removal of the harmonic disturbances/components when the impact instants are random. Previous research (Ong, 2013) has shown that a cyclic load component can significantly affect the quality of the estimated FRFs such that the modal parameters extraction stage becomes difficult. When the excitation is manually conducted by the user, the amount of excitation force for each impact may vary. When the input excitation force for a particular impact is too small compared to the response from the cyclic load component, the natural modes of the test structure are hardly excited. Consequently, the signatures triggered by impacts are dominated by the response from the cyclic load. Another reason is that the user may perform the excitation at locations which slightly deviate from the predefined location.

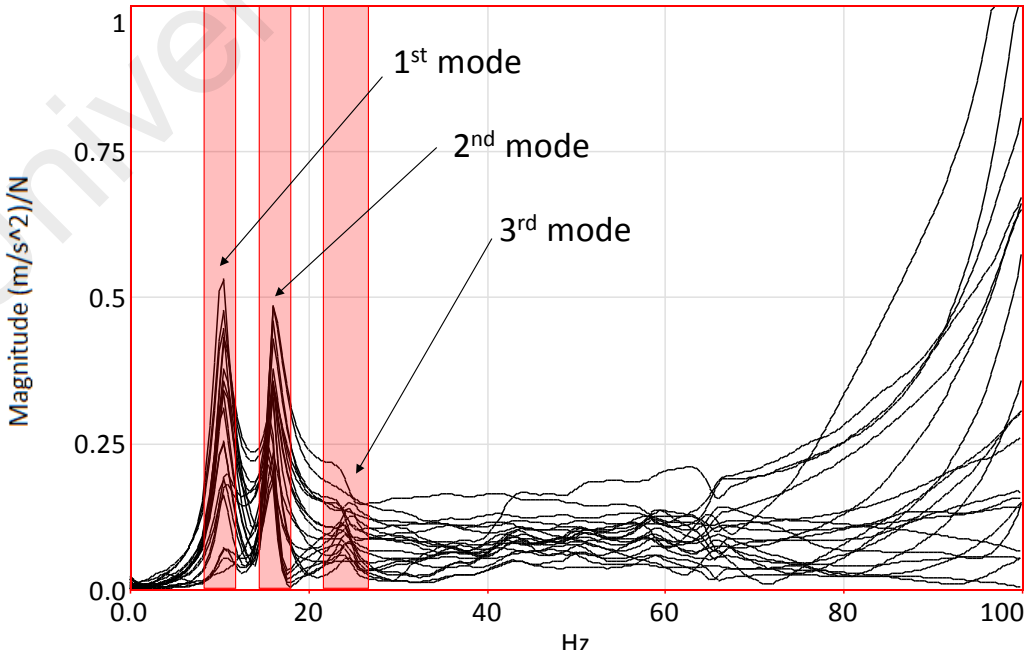

Figure 4.13: FRFs Estimation during EMA

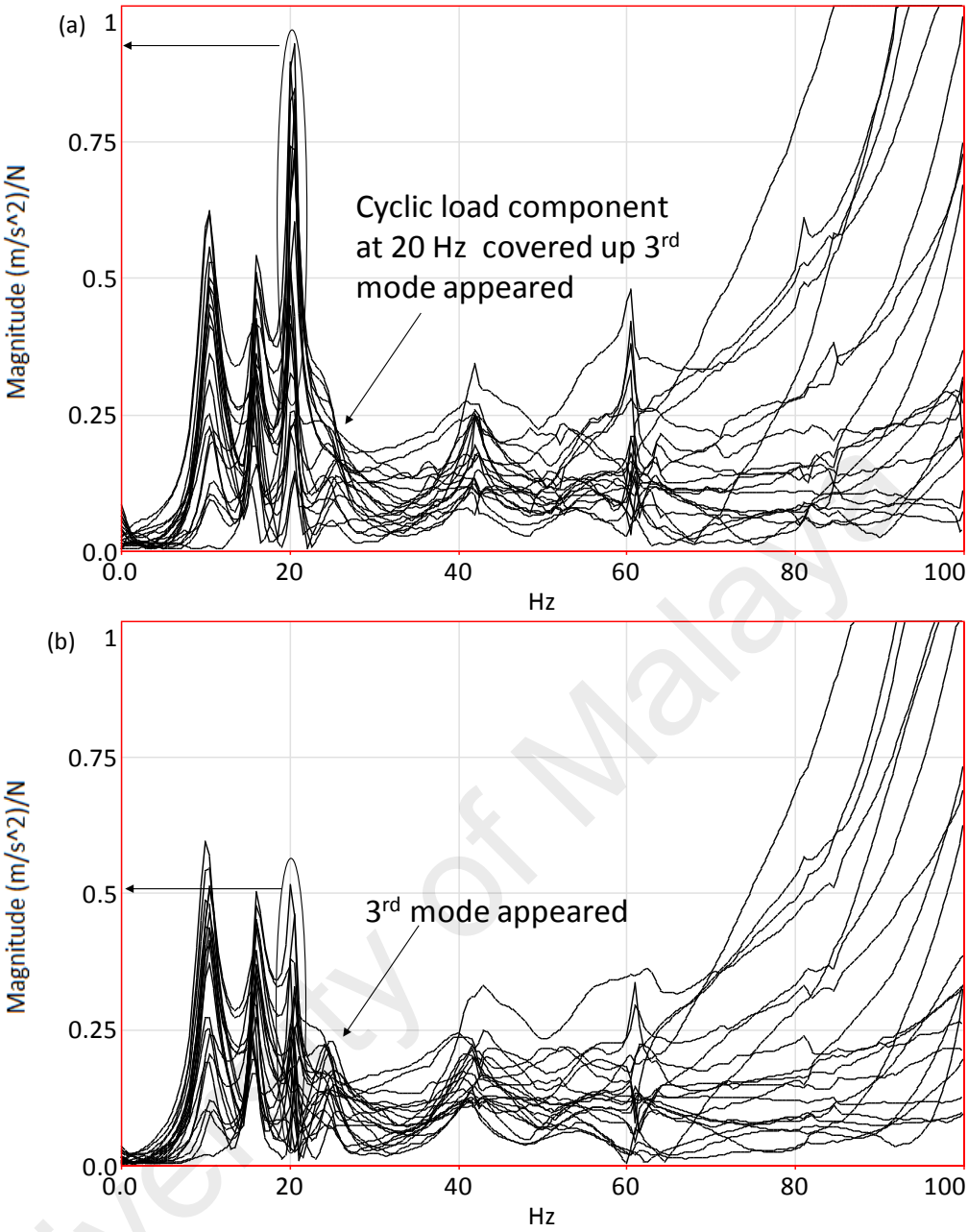

Figure 4.14: FRFs Estimation for 20 Hz: (a) Manual Impact Hammer, (b) Automated Impact Device with Non-synchronous Impacts

Replacing the manual impact hammer by an automated impact device tends to solve some of the limitations of using an impact hammer manually in the measurement. The force level of input excitation is more consistent when using an automated impact device as the input force is well controlled. This is important to ensure that each impact has force level higher than the cyclic force in order to excite all the natural modes of the test structure. Moreover, the automated impact device is clamped firmly by the retort stand, and thus it is able to consistently impart the impacts at the predefined location. An

enhancement of FRFs estimation is obtained using the automated impact device with impacts with fixed time interval, non-synchronous with the cyclic load. A significant decrease of the cyclic load component at 20 Hz by 45% compared to using a manual impact hammer is observed. Thus, a better FRFs estimation is generated using automated impact device with non-synchronous impacts.

4.3.2 Frequency Response Functions Estimation from Automated Impact Device with Non-synchronous Impacts and Manual Impact Hammer for 30 Hz

At running speed of 30 Hz, as expected, the vibration amplitude is further increased compared to 20 Hz. Note that in this case, two dominant peaks are observed in the FRFs estimation. These peaks are originated from the cyclic load component at 30 Hz and its second harmonic at 60 Hz. By comparing FRFs estimation in Figure 4.15, higher dominant peaks with magnitude of 2 m/s^2N at 30 Hz and 0.561 m/s^2N at 60 Hz are observed for the case of ISMA using manual impact hammer, respectively. By using automated impact device with non-synchronous impacts, these harmonic peaks are thus reduced by 31.5% at 30 Hz and 17.11% at 60 Hz. The harmonic disturbances at 30 Hz and 60 Hz are identified as 1.37 m/s^2N and 0.465 m/s^2N, respectively.

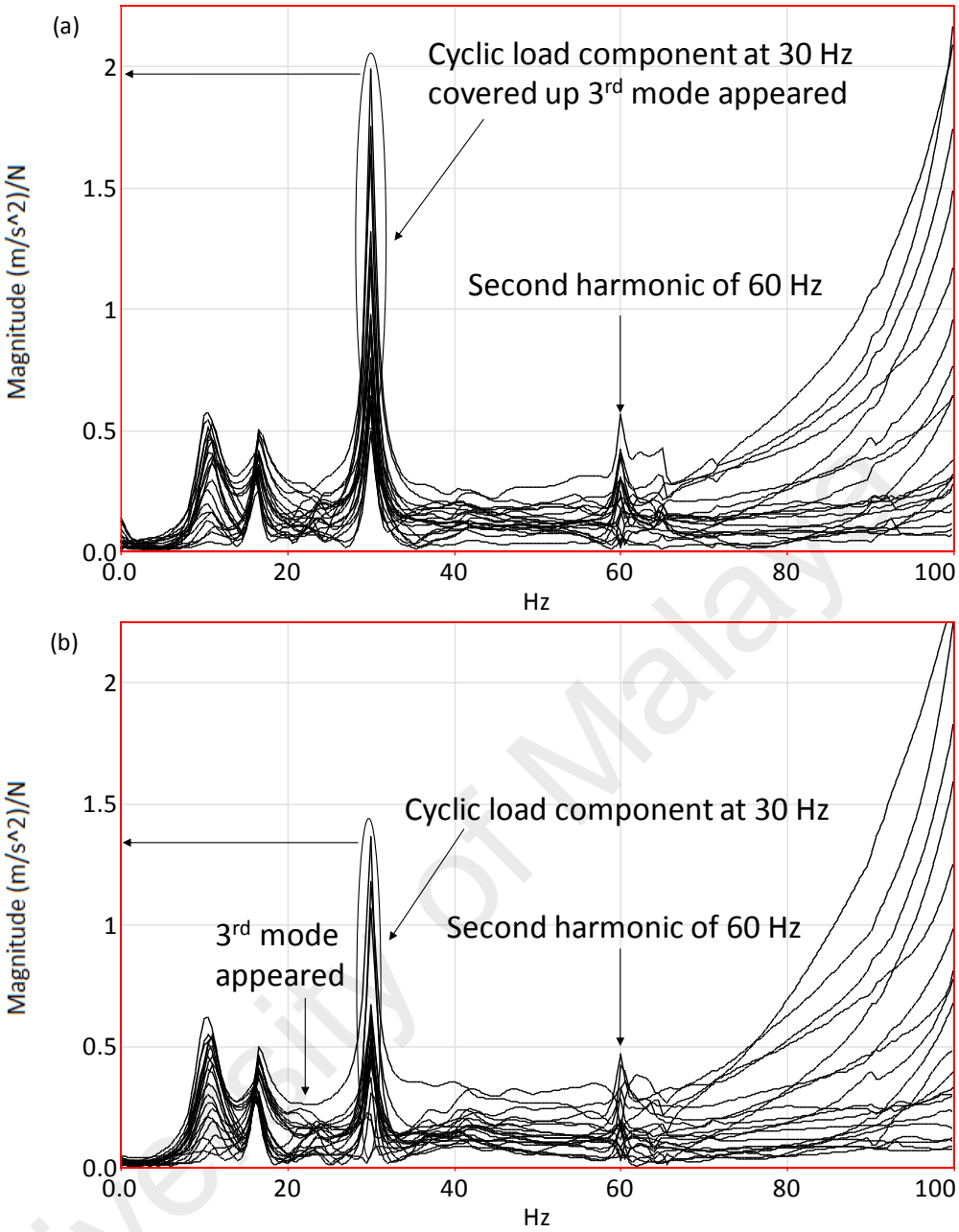

Figure 4.15: FRFs Estimation for 30 Hz: (a) Manual Impact Hammer, (b) Automated Impact Device with Non-synchronous Impacts

4.3.3 Modal Extraction Data from Automated Impact Device with Non-synchronous Impacts and Manual Impact Hammer for 20 Hz

Next, estimated FRFs described in Section 4.3.1 are used to obtain the modal parameters. The EMA results obtained are used as a benchmark to compare and validate the effectiveness of using the different excitation strategies, and results are tabulated in Table 4.6 and Table 4.7. As can be seen in Table 4.7, only the first two natural modes are excited by manual impact hammer and are estimated at 10.5 Hz and 15.9 Hz. The third natural

mode is covered up by the cyclic load component at 20 Hz. On the other hand, the automated impact device with non-synchronous impacts resulted in good elimination of the harmonic at 20 Hz, resulting in estimates of the first three modes of 10.4 Hz, 15.8 Hz, and 24.4 Hz. All the natural frequencies determined are very close to the benchmark EMA, with deviation less than 2%. Also, a higher percentage difference in damping ratio is observed for excitation using manual impact hammer for the first two natural modes. The percentage difference between the benchmark and automated impact device with non-synchronous impacts in damping ratio estimates for the third natural mode is 12.54%. The fact that the harmonic at 20 Hz is not totally eliminated could cause the error in the damping ratio estimates, although the errors are small, indicating a good suppression of the harmonic. In addition to that, the deviation of damping ratio estimates for first natural mode is probably due to a slight difference in boundary condition for the system during static and operational modal testing.

Modal assurance criterion (MAC) values between the benchmark EMA data and ISMA data using manual impact hammer and automated impact device are summarised in Table 4.6. The first and second natural modes are far from the cyclic load frequency at 20 Hz where it has little effect on the modal extraction and this, in turn, yields a stable and high MAC value when only 20 averages were taken in all three experiments. The third natural mode could be estimated when the automated impact device with non-synchronous impacts is used. The correlation of the mode shape with the benchmark EMA is high with a MAC value of 0.90. From Figure 4.16 and Figure 4.17, it can be observed that all excitation strategies shows identical mode shapes as EMA which are pitching for mode 1 and heaving for mode 2. Also, the successful extraction of the third natural mode by using automated impact device with non-synchronous impacts showing a rolling mode shape in Figure 4.18.

Table 4.6: Summary of Natural Frequencies and Mode Shapes Comparison between Modal Parameter Extraction Based on FRFs from a Benchmark (BM) Measurement without the Harmonic and ISMA using (A) Manual Impact Hammer and (B) Automated Impact Device with Non-synchronous Impacts for 20 Hz

	Natural frequency (Hz)			Percentage of difference (%)		MAC	
Mode	BM	A	B	BM vs. A	BM vs. B	BM vs. A	BM vs. B
1	10.4	10.5	10.4	0.96	0	0.922	0.925
2	15.9	15.9	15.8	0	0.63	0.892	0.893
3	24.0	N/A	24.4	N/A	1.67	N/A	0.902

Table 4.7: Summary of Damping Ratios from Modal Parameter Extraction Based on FRFs from a Benchmark (BM) Measurement without the Harmonic and using the ISMA with (A) Manual Impact Hammer and (B) Automated Impact Device with Non-synchronous Impacts for 20 Hz

	Damping ratio			Percentage of difference (%)	
Mode	BM	A	B	BM vs. A	BM vs. B
1	0.0832	0.0949	0.0933	14.06	12.14
2	0.0448	0.0436	0.0440	2.68	1.79
3	0.0566	N/A	0.0495	N/A	12.54

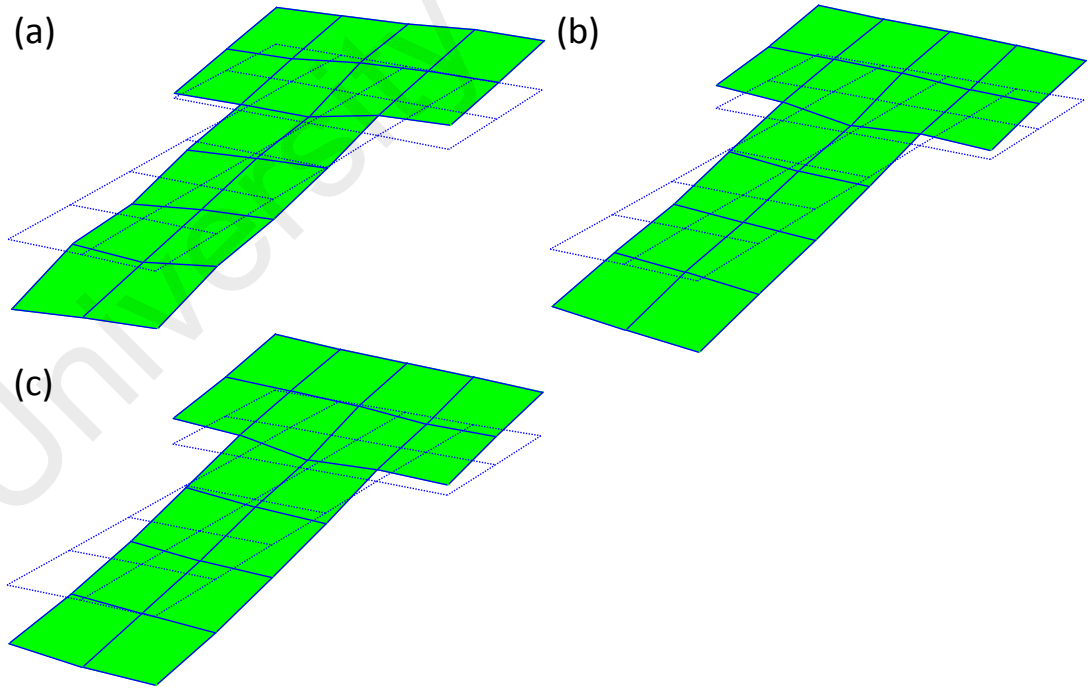

Figure 4.16: First Mode Shape (Pitching) for 20 Hz: (a) EMA, (b) Manual Impact Hammer, (c) Automated Impact Device with Non-synchronous Impacts

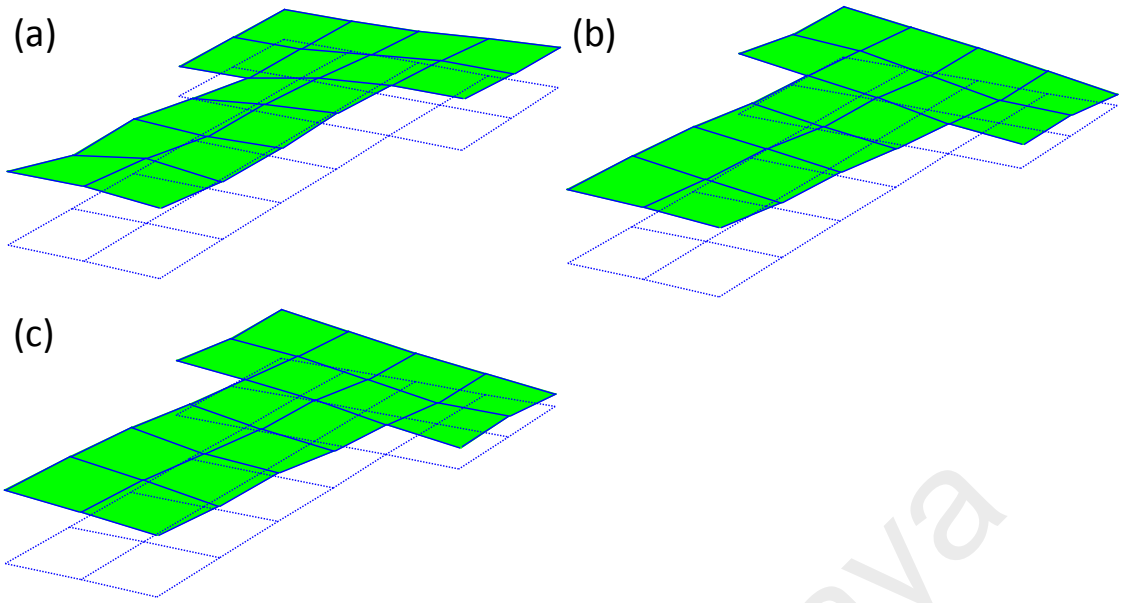

Figure 4.17: Second Mode Shape (Heaving) for 20 Hz: (a) EMA, (b) Manual Impact Hammer, (c) Automated Impact Device with Non-synchronous Impacts

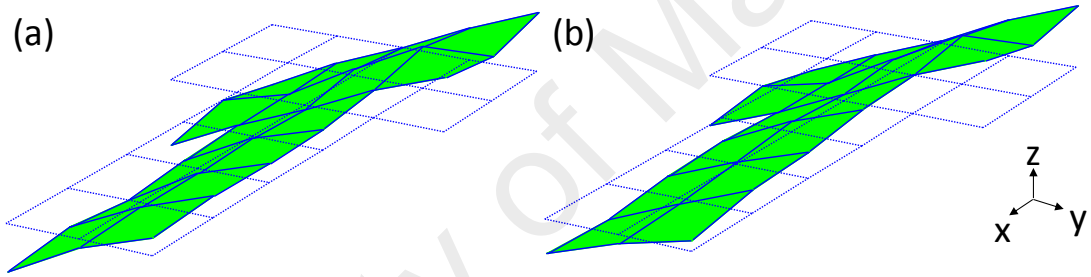

Figure 4.18: Third Mode Shape (Rolling) for 20 Hz: (a) EMA, (b) Automated Impact Device with Non-synchronous Impacts

4.3.4 Modal Extraction Data from Automated Impact Device with Non-synchronous Impacts and Manual Impact Hammer for 30 Hz

Modal parameters for the system obtained at this running speed and MAC values are again tabulated in Table 4.8 and Table 4.9. With manual impact hammer, the estimated frequencies are 10.6 Hz and 16.3 Hz. The corresponding damping ratios are 0.0971 and 0.0405, respectively. On one hand, this results should not be surprising, i.e., third natural mode is not identified. The reason for this is that the increasing vibration amplitude at 30 Hz has actually covered up the appearance of third natural mode, as can be seen from Figure 4.15 (a). Similarly, the estimated frequencies from the automated impact device with non-synchronous impacts are 10.5 Hz, 16.3 Hz, and 23.4 Hz, and the corresponding damping ratios are 0.0923, 0.0423, and 0.0668. Comparison of natural frequencies shows

that the ones identified from both excitation methods are close to the benchmark EMA, with deviation less than 3%. It has also shown some difficulties in analysing satisfactorily damping ratios with more than 10% deviation, particularly on first and third natural mode. Since first natural mode is far away from the cyclic load component of 30 Hz, the large deviation is probably due to a slight change in boundary condition in two different test conditions (static and operating condition). For the third natural mode, it is believed that the harmonic disturbances are not totally removed could be an additional reason for the large deviation. Lastly, when comparing MAC values, slight additional improvements are observed for ISMA using automated impact device with non-synchronous impacts since all mode shapes are well correlated with the benchmark EMA. The mode shapes corresponding to each natural mode are shown in Figure 4.19, Figure 4.20 and Figure 4.21.

Table 4.8: Summary of Natural Frequencies and Mode Shapes Comparison between Modal Parameter Extraction Based on FRFs from a Benchmark (BM) Measurement without the Harmonic and ISMA using (A) Manual Impact Hammer and (B) Automated Impact Device with Non-synchronous Impacts for 30 Hz

	Natural frequency (Hz)			Percentage of difference (%)		MAC	
Mode	BM	A	B	BM vs. A	BM vs. B	BM vs. A	BM vs. B
1	10.4	10.6	10.5	1.92	0.96	0.916	0.908
2	15.9	16.3	16.3	2.52	2.52	0.945	0.947
3	24.0	N/A	23.4	N/A	2.5	N/A	0.922

Table 4.9: Summary of Damping Ratios from Modal Parameter Extraction Based on FRFs from a Benchmark (BM) Measurement without the Harmonic and using the ISMA with (A) Manual Impact Hammer and (B) Automated Impact Device with Non-synchronous Impacts for 30 Hz

	Damping ratio			Percentage of difference (%)	
Mode	BM	A	B	BM vs. A	BM vs. B
1	0.0832	0.0971	0.0923	16.71	10.94
2	0.0448	0.0405	0.0423	9.60	5.58
3	0.0566	N/A	0.0668	N/A	18.02

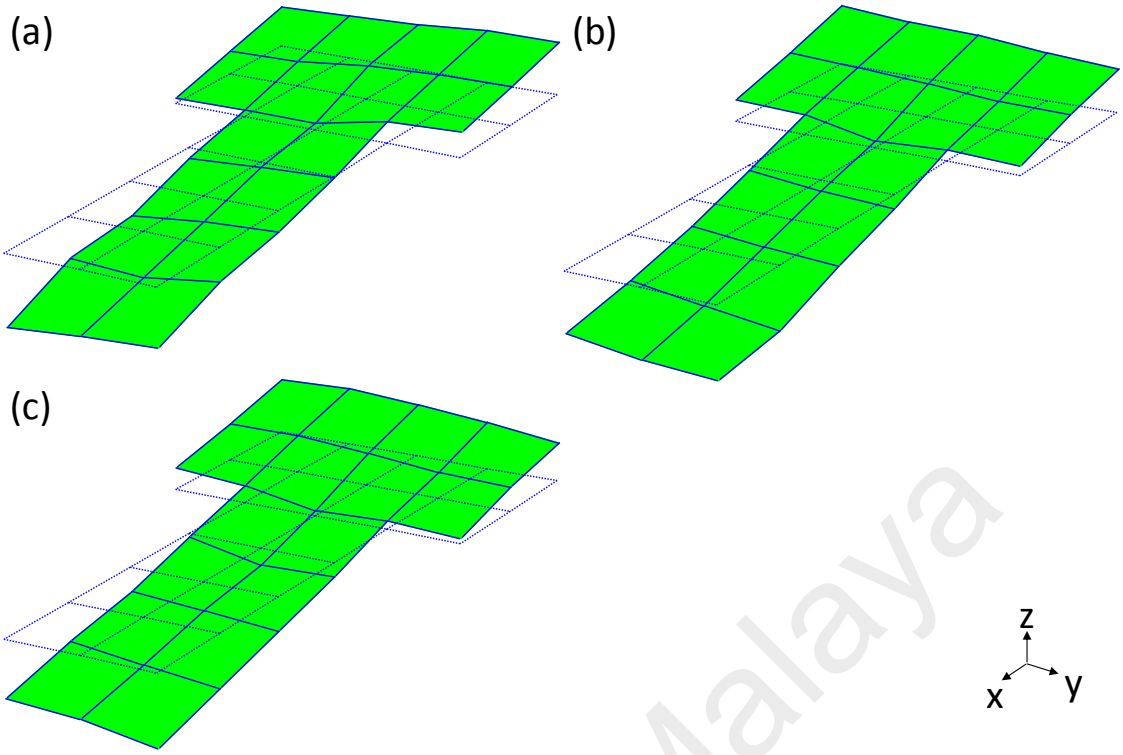

Figure 4.19: First Mode Shape (Pitching) for 30 Hz: (a) EMA, (b) Manual Impact Hammer, (c) Automated Impact Device with Non-synchronous Impacts

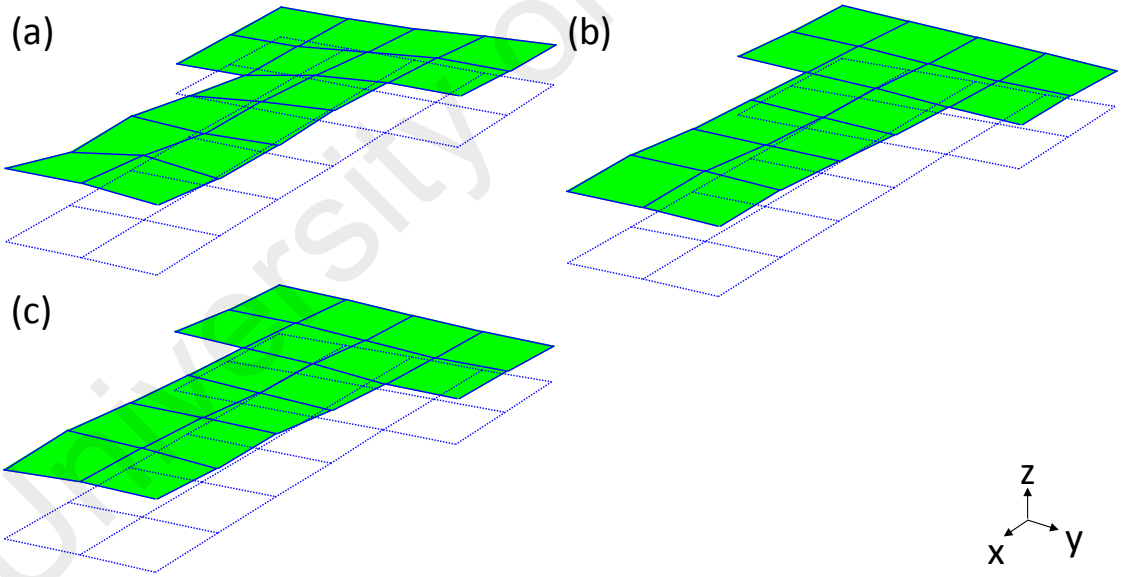

Figure 4.20: Second Mode Shape (Heaving) for 30 Hz: (a) EMA, (b) Manual Impact Hammer, (c) Automated Impact Device with Non-synchronous Impacts

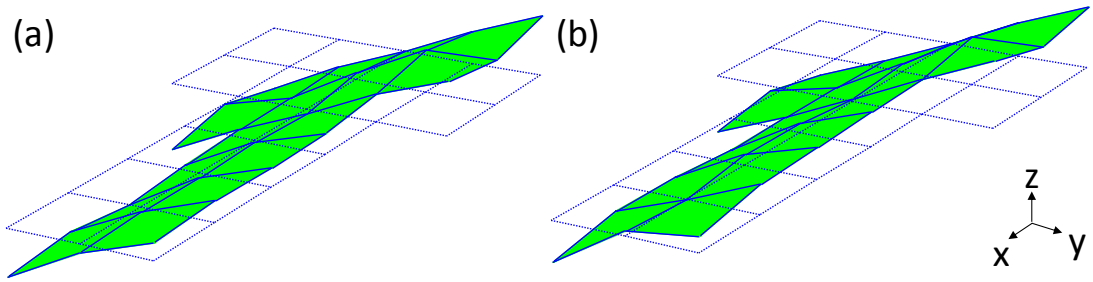

Figure 4.21: Third Mode Shape (Rolling) for 30 Hz: (a) EMA, (b) Automated Impact Device with Non-synchronous Impacts

4.3.5 Summary of Impact-synchronous Modal Analysis using Automated Impact Device with Non-synchronous Impacts

This is the first attempt of using automated impact device with non-synchronous impacts in ISMA during operation. The efficiency of this device is evidenced by the reduction of harmonic disturbances and the subsequent appearance of third natural mode. For comparison of modal parameters, in overall, good agreements are also observed between benchmark EMA. Although the harmonic peaks have been reduced by using this device, the harmonic peaks are still remained observable in the FRFs estimation. Thus, to further enhance ISMA method, a more-thorough investigation on the relationship tailored between phase angle of cyclic load component with respect to impact applied are required. This is done through a post-processing inconsistent phase selection assessment and the results obtained will be discussed in the following section.

4.4 Post-processing Inconsistent Phase Selection Assessment

At the beginning of the section, two cases are discussed. The first scenario in Section 4.4.1 concerning the removal single dominant cyclic load component while the second scenario in Section 4.4.2 concerning the removal of dominant cyclic load component and its harmonic. Next, FRFs estimation and modal parameters using manual impact hammer and inconsistent phase selection assessment for 20 Hz and 30 Hz are compared in Section 4.4.3, Section 4.4.4, Section 4.4.5, and Section 4.4.6. A summary for this assessment is then highlighted in Section 4.4.7.

4.4.1 Inconsistent Phase Selection Assessment for Scenario 1: Presence of Cyclic Load Component (20 Hz)

Figure 4.22 shows the 100 pre-trigger samples phase position plotted for 20 acceleration responses. In the inconsistent phase selection assessment, 4 out of 20 acceleration response, i.e., acceleration response 4, 6, 10, 20 are manually selected in ISMA as the phase angle of dominant periodic response of cyclic load with respect to impact is not consistent in these 4 impacts. By referring to the phase position at 100 pre-trigger samples in Figure 4.23, the selection procedure is made based on 180° difference in phase angle of these four measured cyclic load responses (Ong et al., 2015). In doing so, the harmonic disturbances are cancelling each other out during the ISTA process. From the qualitative point of view, the FRF estimation in Figure 4.24 shows a good reduction of harmonic disturbance at 20 Hz. The results are said to be in accord with the results report in (Ong et al., 2015).

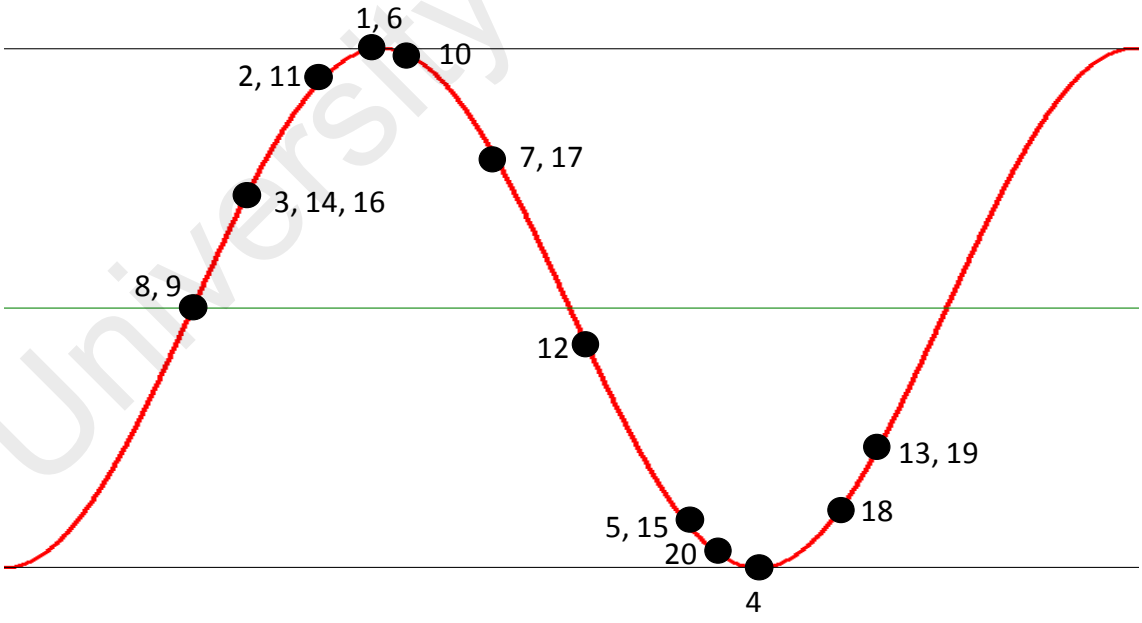

Figure 4.22: 100 Pre-trigger Samples Phase Position of 20 Acceleration Responses

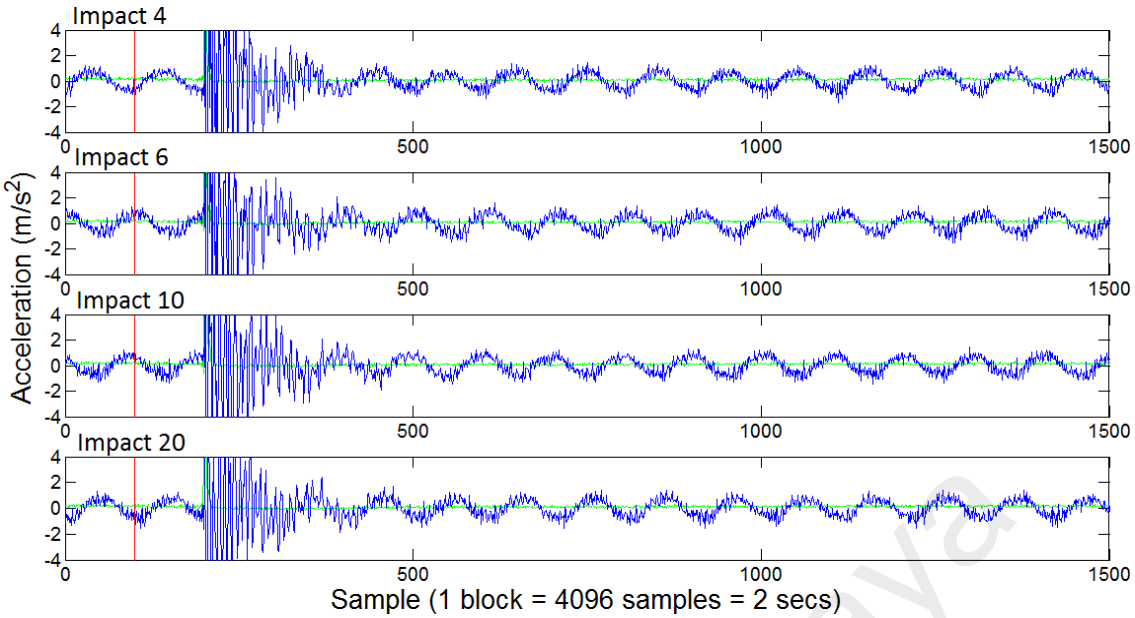

Figure 4.23: Phase Position of Selected Impacts, i.e., 4, 6, 10, 20

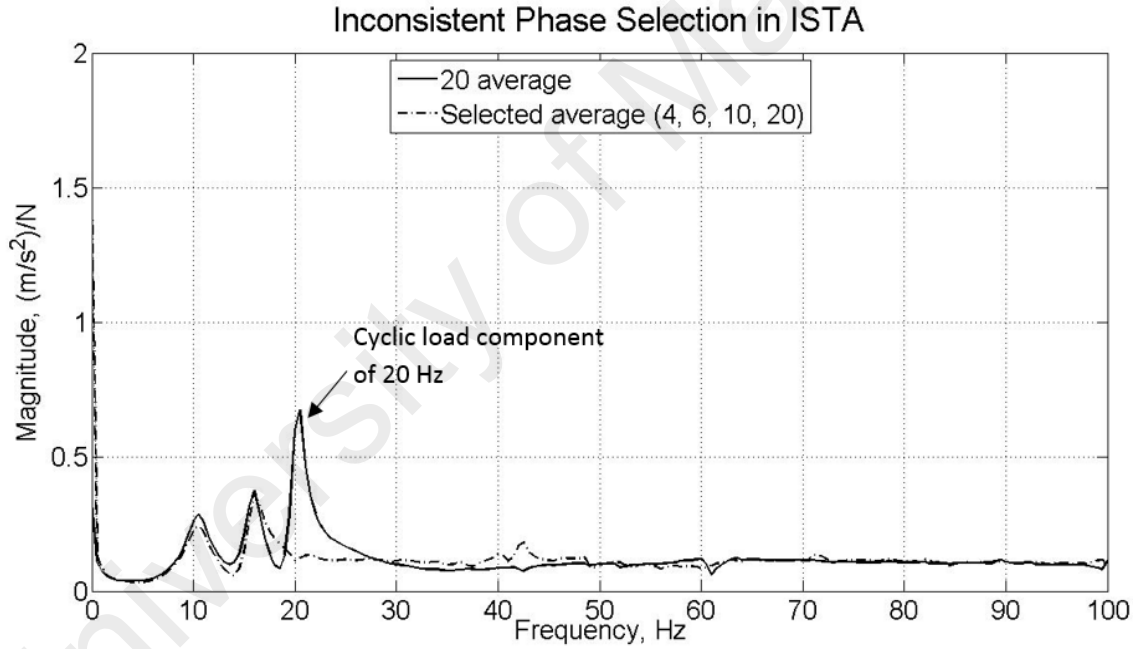

Figure 4.24: FRF Estimation using Impacts 4, 6, 10, and 20

4.4.2 Inconsistent Phase Selection Assessment for Scenario 2: Presence of Cyclic Load Component (30 Hz) and its Second Harmonic (60 Hz)

The idea on how to select acceleration responses in inconsistent phase selection assessment with severe harmonic peak at 30 Hz and multiple of that frequency (60 Hz) has been investigated in this section. Acceleration responses, i.e., 8, 18, 19, 20, are considered in ISTA. From Figure 4.25, it is observed that at a phase position of 100 pre-trigger samples, the phase of the periodic response of cyclic load (2 pairs of data where

the selected impacts in each pair are 180° difference) is inconsistent (out of phase) with the phase of responses due to impact. Almost in parallel with the investigation on 20 Hz, the periodic responses of cyclic load of 30 Hz tend to cancel each other out during ISTA and leads to a successful suppression of the harmonic disturbance at 30 Hz. As depicted in the FRF estimation in Figure 4.26, it can be seen that the harmonic disturbance at 30 Hz is almost entirely removed while the response due to impact is preserved after performing ISTA with the manually selected 4 impacts. It is clear that no sharp peak can be detected in this figure with fewer number of averages while for the full 25 averages FRFs estimation, the harmonic disturbance at 30 Hz remains dominant.

However, it is seen that its second harmonic at 60 Hz experiences an increase in peak. Figure 4.27 shows the impacts position of the 4 manually selected impacts corresponding to the periodic responses of cyclic load and its second harmonic. It is seen that the phase of the periodic response of its second harmonic is consistent (in phase) with the phase of responses due to impact and thus the preserving the second harmonic remains over ISTA. In field testing, it would be a serious consequence as the analyst could be erroneously assumed the harmonics to be natural modes.

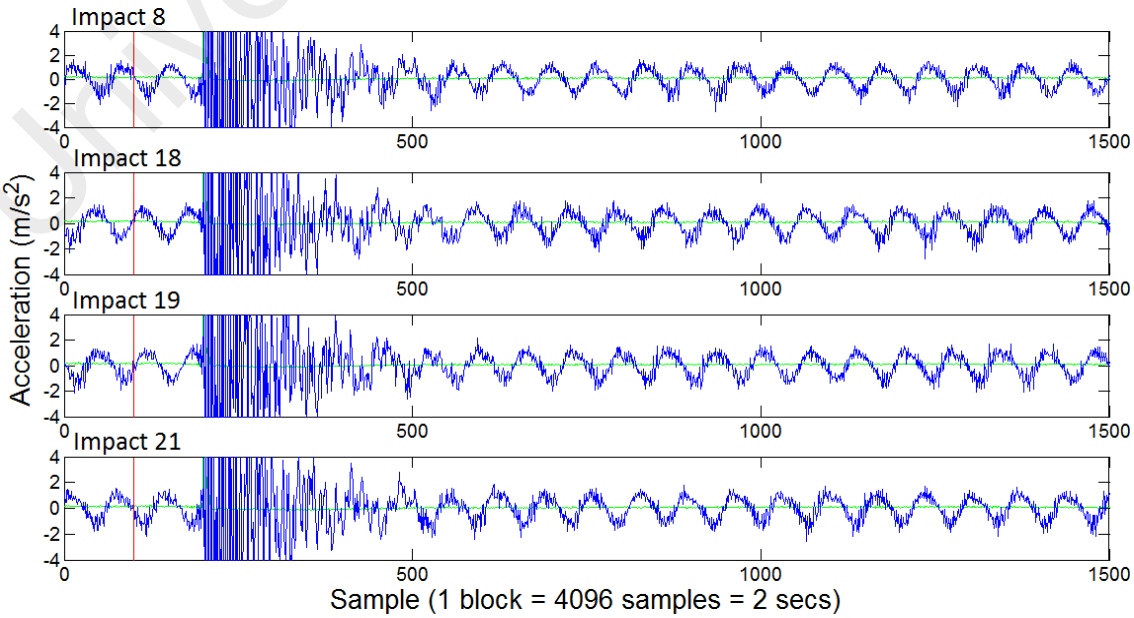

Figure 4.25: Phase Position of Selected Impacts, i.e., 8, 18, 19, and 21

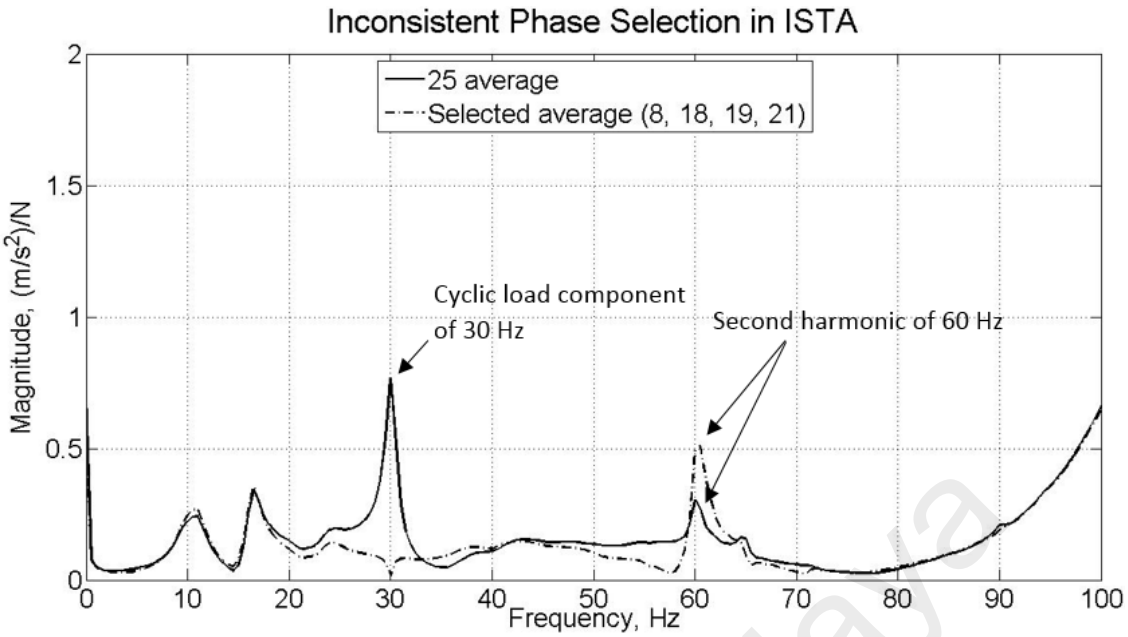

Figure 4.26: FRF Estimation using Impacts 8, 18, 19 and 21

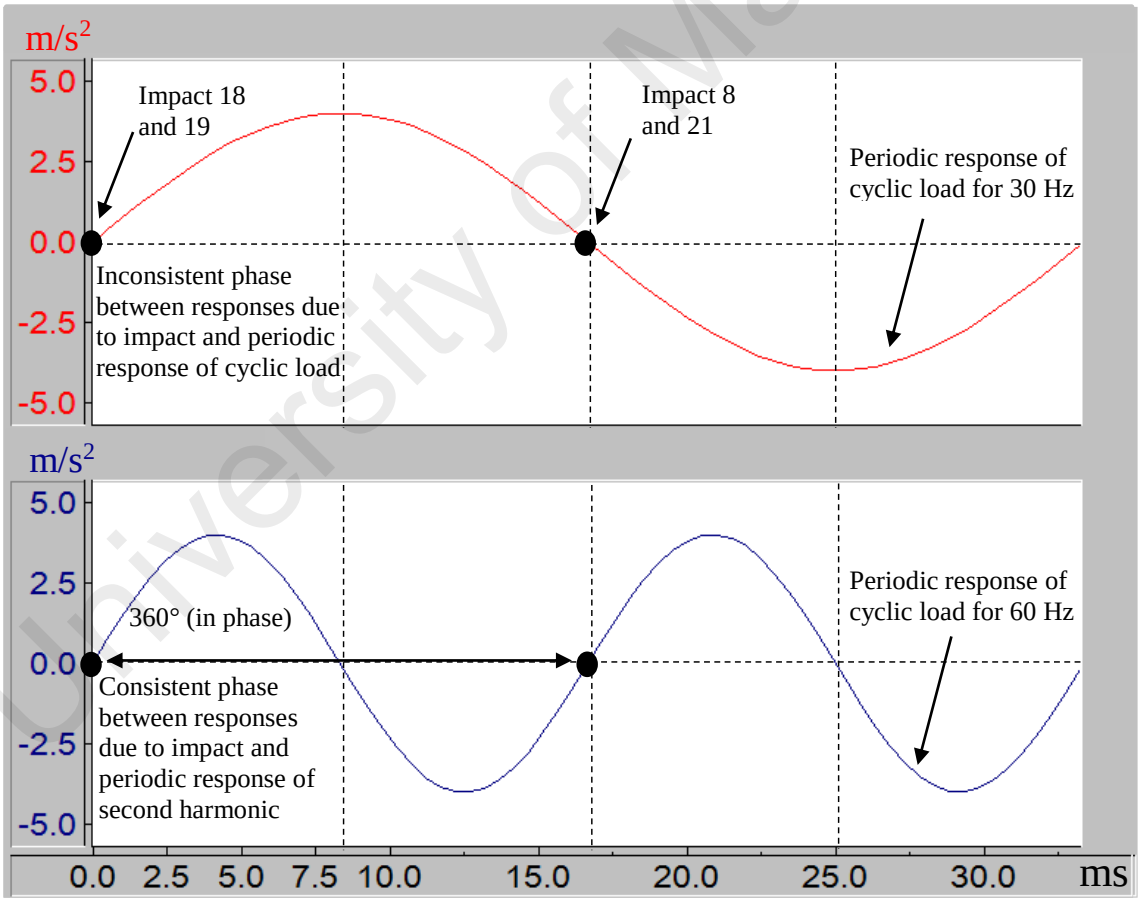

Figure 4.27: Position of Impacts 8, 18, 19 and 21 Corresponding to the Periodic Response of Cyclic Load and Second Harmonic

To further investigate the effect of phase synchronisation between acceleration response and periodic response of cyclic load on FRF estimation, another 4 impacts out of 25 impacts, i.e., impacts 7, 18, 20, 21 are selected. The results in Figure 4.28 show that at a phase position of 100 pre-trigger samples, the phase of the periodic response of cyclic load (2 pairs of data where each subsequent selected impacts is 90° difference) is inconsistent (out of phase) with the phase of acceleration responses. From Figure 4.29, it is observed that the dominant cyclic load component and its second harmonic diminish after performing ISTA, remains over is the response due to impact. Figure 4.30 shows the impacts position of the 4 manually selected impacts corresponding to the periodic responses of cyclic load and its second harmonic. It is observed that the phase of the periodic response of cyclic load is inconsistent (out of phase) with the phase of acceleration responses, i.e., (1) impacts 7 and 20 and (2) impacts 18 and 21. Moreover, it is seen that the phase of the periodic response of its second harmonic is also inconsistent (out of phase) with the phase of acceleration responses, i.e., (1) impacts 7 and 18 and (2) impacts 20 and 21. Table 4.10 summarises the criteria for removing periodic response of cyclic load during modal testing.

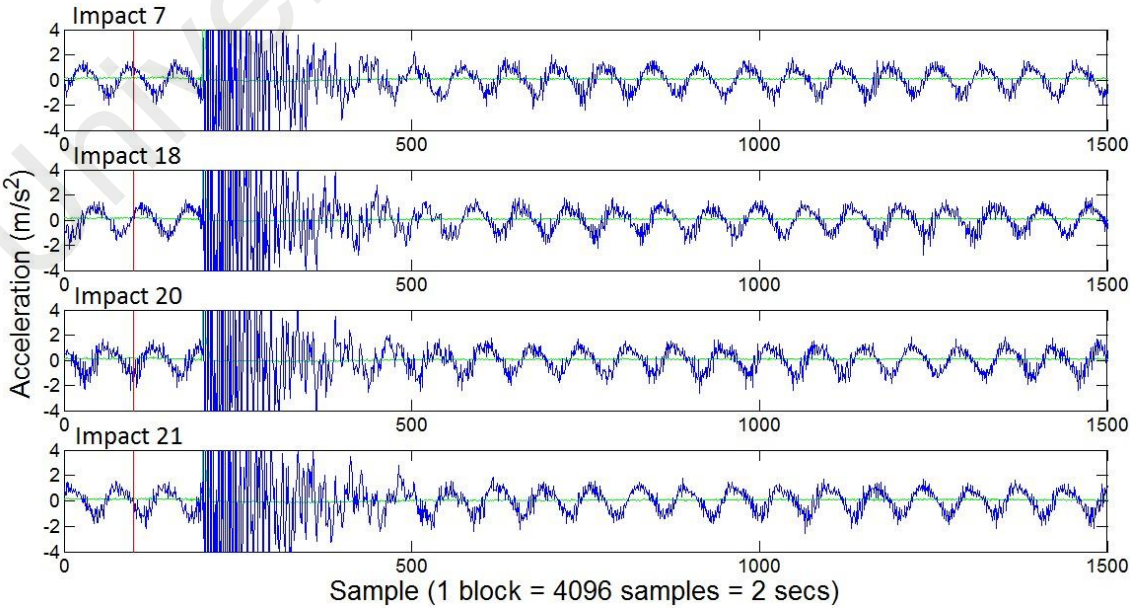

Figure 4.28: Phase Position of Selected Impacts, i.e., 7, 18, 20, 21

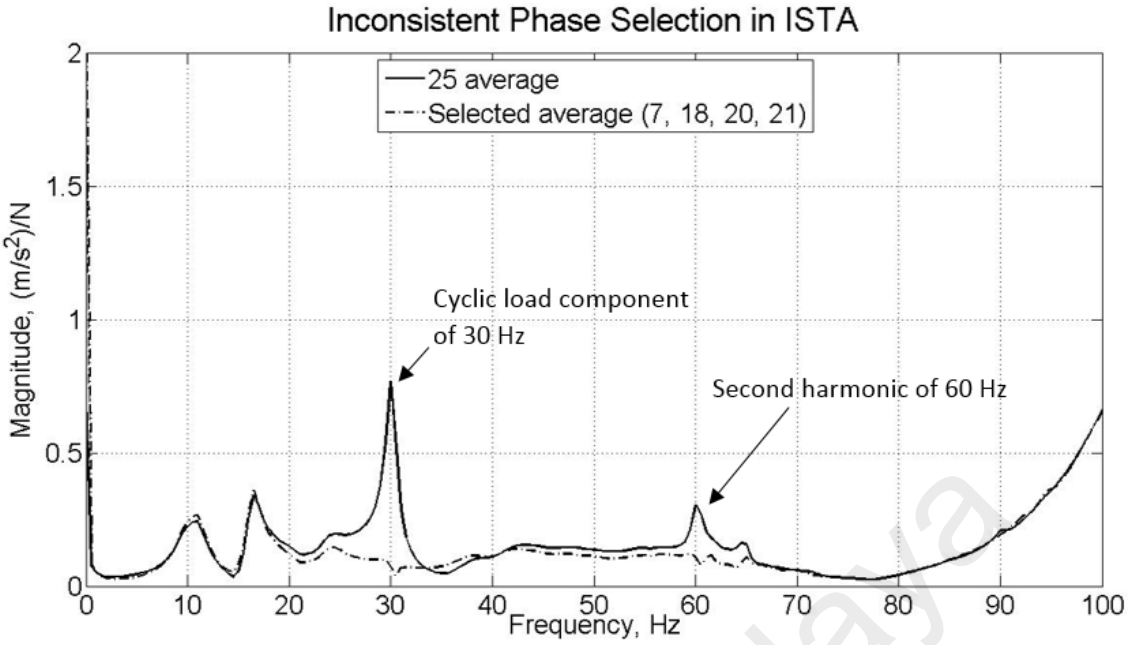

Figure 4.29: FRF Estimation using Impacts 7, 18, 20 and 21

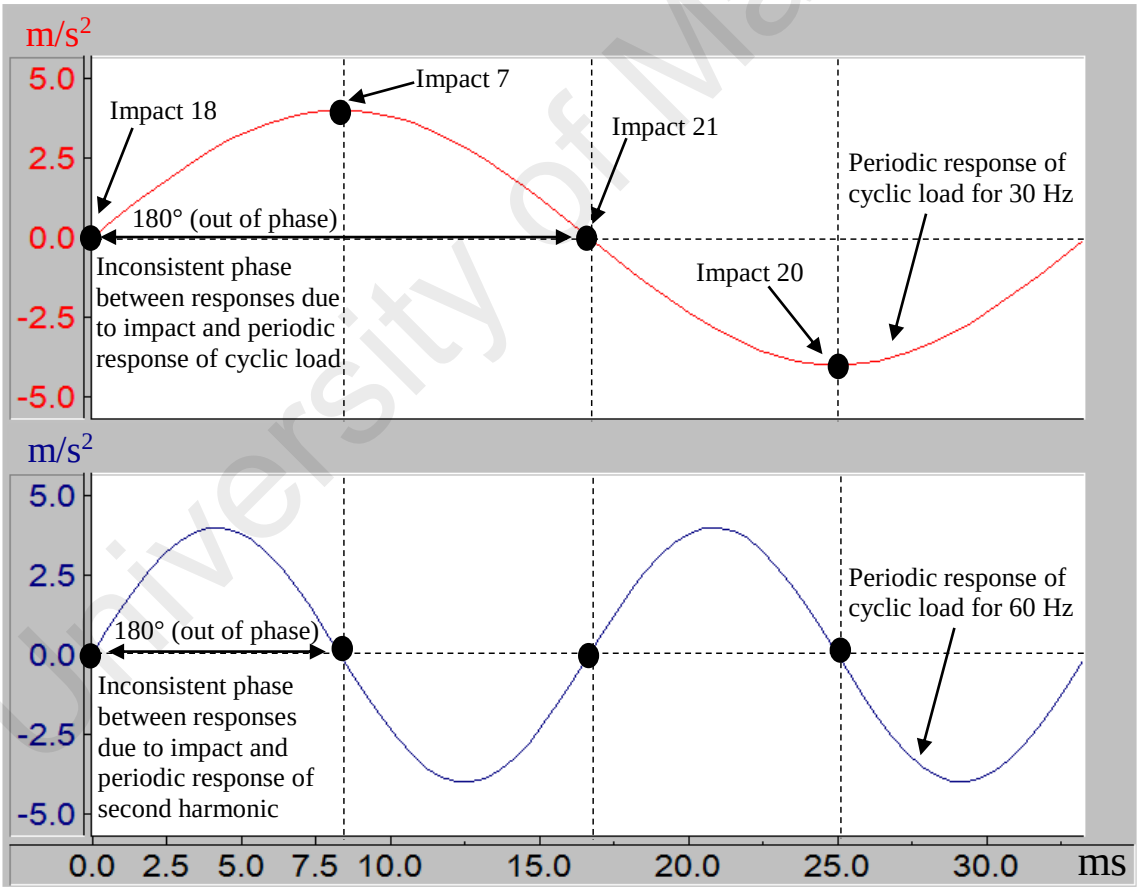

Figure 4.30: Position of Impacts 7, 18, 20 and 21 Corresponding to the Periodic Response of Cyclic Load and Second Harmonic

Table 4.10: Summary of the Criteria for Removing Periodic Responses of Cyclic Load during Operational Modal Testing

Periodic response	Different in phase due to periodic response of cyclic load with respect to impacts (°)	Number of average (n= 1, 2, 3…)
Cyclic load component	180	2n
Cyclic load component + 2nd harmonic	90	4n
Cyclic load component + 2nd and 3rd harmonics	90	4n
Cyclic load component + 2nd, 3rd and 4th harmonics	45	8n
Cyclic load component + 2nd, 3rd, 4th and 5th harmonics	45	8n
Cyclic load component + 2nd, 3rd, 4th, 5th and 6th harmonics	45	8n

4.4.3 Frequency Response Functions Estimation from Inconsistent Phase Selection Assessment and Manual Impact Hammer for 20 Hz

The FRFs estimation between full 20 averages from manual impact hammer and inconsistent phase selection are experimentally measured and presented in Figure 4.31. Excellent harmonic disturbances suppression often leads to an improved and easy to interpret FRFs estimation. Note that in conventional manual impact hammer, the acceleration response due to excitation force is uncontrollable and random. Some of the acceleration responses tend to synchronise with the cyclic load component. Although ISTA is utilised, the remaining response is still comprised of the cyclic load component and the acceleration response. On the other hand, with the inconsistent phase selection assessment, the harmonic disturbance at 20 Hz is successfully eliminated and generates a better FRFs estimation. This is evidenced by the percent reduction of 72.96% of harmonic disturbance at 20 Hz from 0.932 m/s^2N to 0.252 m/s^2N.

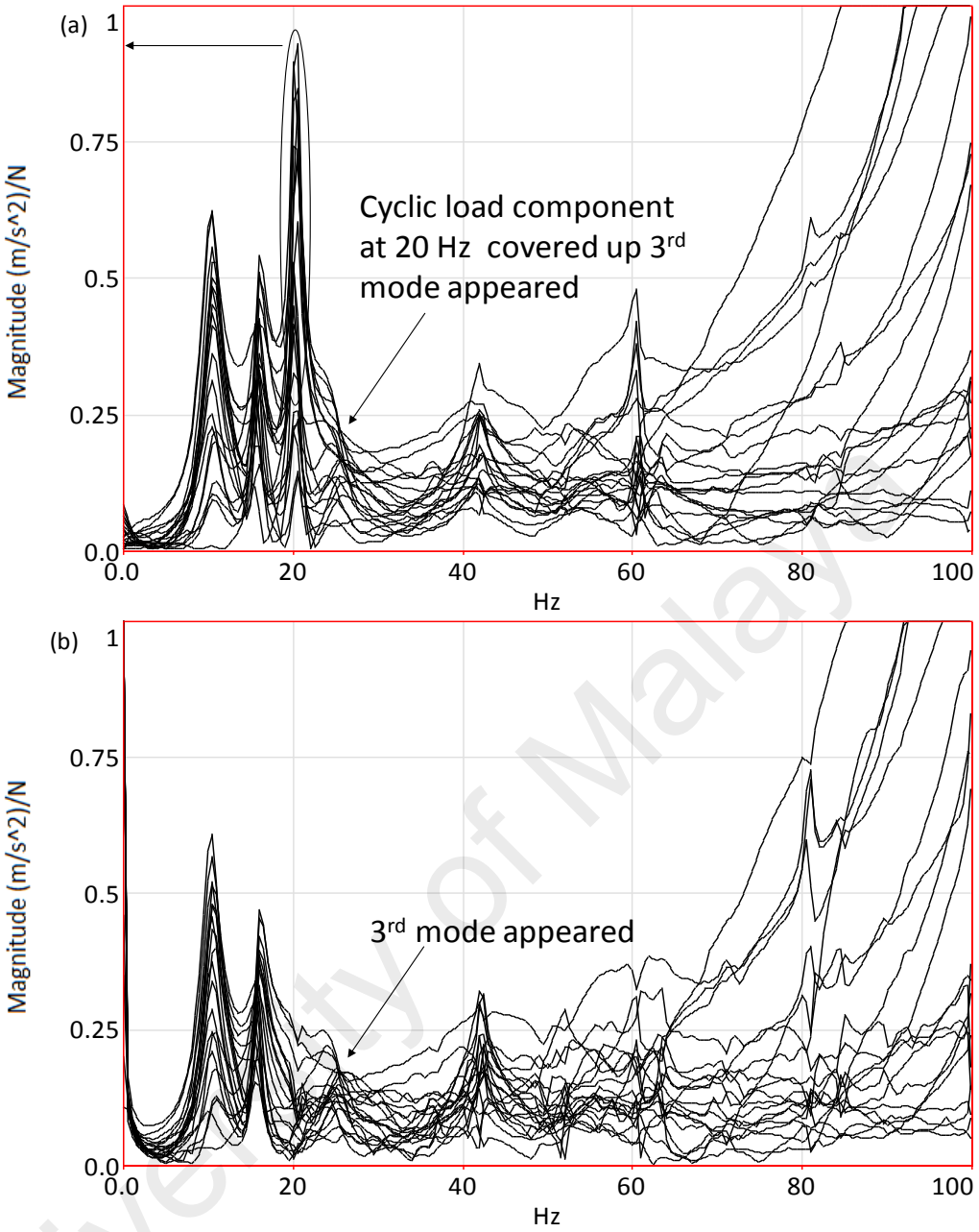

Figure 4.31: FRFs Estimation for 20 Hz: (a) Manual Impact Hammer, (b) Inconsistent Phase Selection Assessment

4.4.4 Frequency Response Functions Estimation from Inconsistent Phase Selection Assessment and Manual Impact Hammer for 30 Hz

Figure 4.32 shows the FRFs estimation between full 25 averages from manual impact hammer and inconsistent phase selection. Note that in this case, two dominant peaks are observed in the FRFs estimation. These peaks are originated from the cyclic load component at 30 Hz and its second harmonic at 60 Hz. Applying the knowledge in Section 4.4.2, with minimal 4 number of averages/impacts, the harmonic disturbances at 30 Hz

and 60 Hz are eliminated and the responses due to impact are preserved. This is proven in the FRFs estimation for inconsistent phase selection where the peak contributed by the cyclic load component and its second harmonic have significantly reduced from 2 m/s^{2}N to 0.355 m/s^{2}N at 30 Hz and from 0.561 m/s^{2}N to 0.268 m/s^{2}N at 60 Hz. The percentage of reduction is thus determined as 82.25% for 30 Hz and 52.23% for 60 Hz.

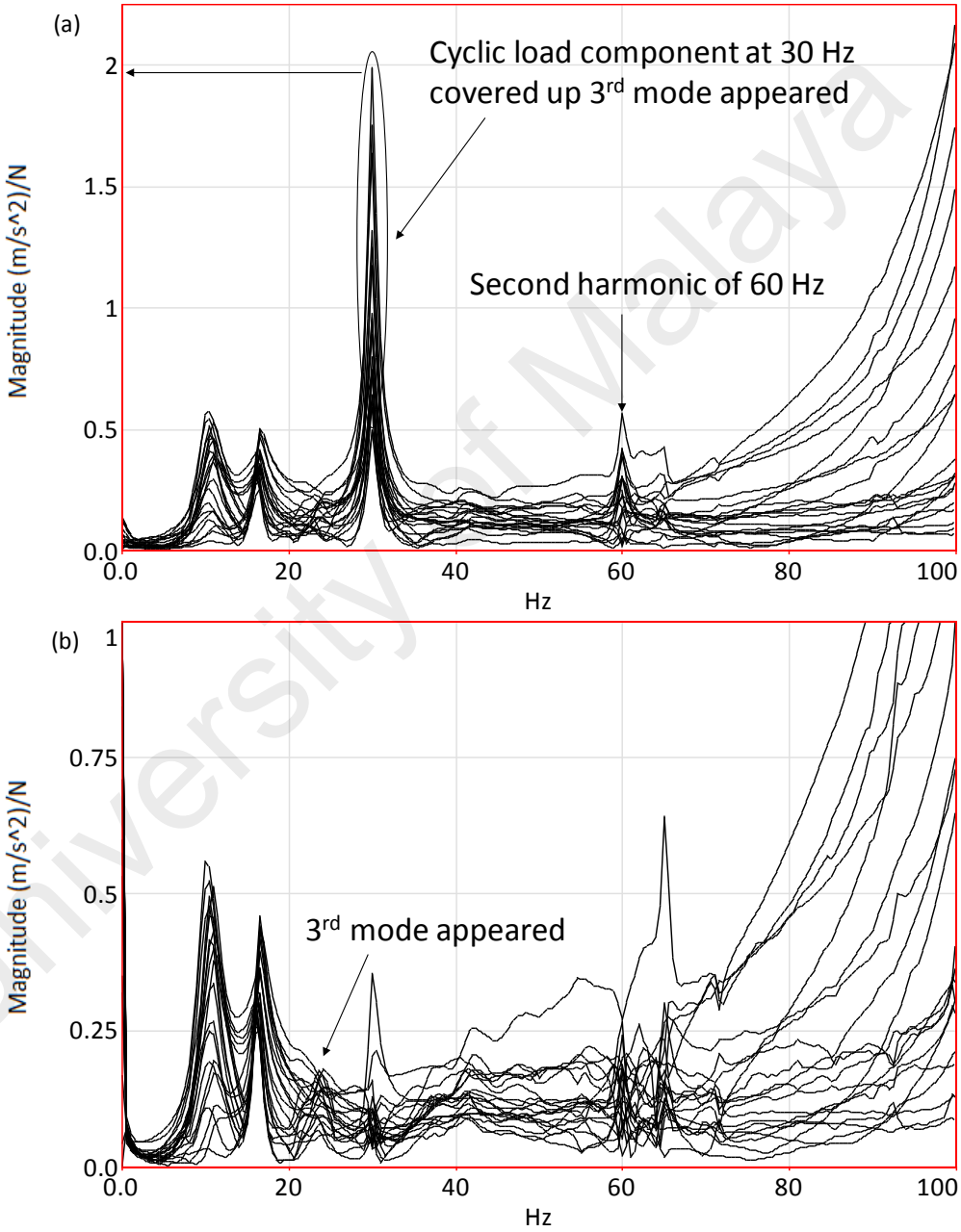

Figure 4.32: FRFs Estimation for 30 Hz: (a) Manual Impact Hammer, (b) Inconsistent Phase Selection Assessment

4.4.5 Modal Extraction Data from Inconsistent Phase Selection Assessment and Manual Impact Hammer for 20 Hz

From Table 4.11, first and second natural frequencies for full 20 averages are 10.5 Hz and 15.9 Hz respectively. Meanwhile, the first, second and third natural modes for 4 selected impacts in inconsistent phase selection are identified with a value of 10.5 Hz, 15.8 Hz, and 24.7 Hz. On the contrary, the third natural mode for manual impact hammer (20 averages) is not extracted as it has been covered up. This is due to the dominancy of the harmonic disturbance has shielded the response of the structure due to the excitation force and thus, covered up that particular mode. It is shown that the percentage difference is so small for all natural modes and thus good correlation is achieved in term of natural frequency. Again, a higher percentage of difference for damping ratios is observed for the first and third natural mode in Table 4.12. Slight change of boundary condition during static and operational modal testing is believed to be the reason for this deviation for the first natural mode. Besides, the closeness of the third natural mode to the cyclic load component at 20 Hz could be the reason for this deviation in damping ratio.

A well-known MAC is used to quantitatively compare the mode shape between the benchmark EMA and experimental data. The results are tabulated in Table 4.11. The MAC values obtained for first and second natural mode for full 20 averages are 0.922 and 0.892. Besides, for inconsistent phase selection assessment, the MAC values obtained for the first three modes are 0.925, 0.893, and 0.876 accordingly. In general, for inconsistent phase selection assessment, increments in MAC values are observed and these results indicate that the mode shapes are in accord with the benchmark data. However, the closeness of the natural frequency to the excitation frequency has affected the accuracy of modal extraction quantitatively. The first natural mode is far while the second and the third natural mode are close to the excitation frequency of 20 Hz which causes a contamination on modal parameter extraction. Thus, this explains the high MAC value

for first natural mode and a slightly lower value for second and third natural mode. Mode shapes for all identified natural mode are shown in Figure 4.33, Figure 4.34 and Figure 4.35.

Table 4.11: Summary of Natural Frequencies and Mode Shapes Comparison between Modal Parameter Extraction Based on FRFs from a Benchmark (BM) Measurement without the Harmonic and ISMA using (A) Manual Impact Hammer and (B) Inconsistent Phase Selection Assessment for 20 Hz

	Natural frequency (Hz)			Percentage of difference (%)		MAC	
Mode	BM	A	B	BM vs. A	BM vs. B	BM vs. A	BM vs. B
1	10.4	10.5	10.5	0.96	0.96	0.922	0.925
2	15.9	15.9	15.8	0	0.63	0.892	0.893
3	24.0	N/A	24.7	N/A	2.92	N/A	0.876

Table 4.12: Summary of Damping Ratios from Modal Parameter Extraction Based on FRFs from a Benchmark (BM) Measurement without the Harmonic and using the ISMA with (A) Manual Impact Hammer and (B) Inconsistent Phase Selection Assessment for 20 Hz

	Damping ratio			Percentage of difference (%)	
Mode	BM	A	B	BM vs. A	BM vs. B
1	0.0832	0.0949	0.0950	14.06	14.18
2	0.0448	0.0436	0.0435	2.68	2.90
3	0.0566	N/A	0.0645	N/A	13.96

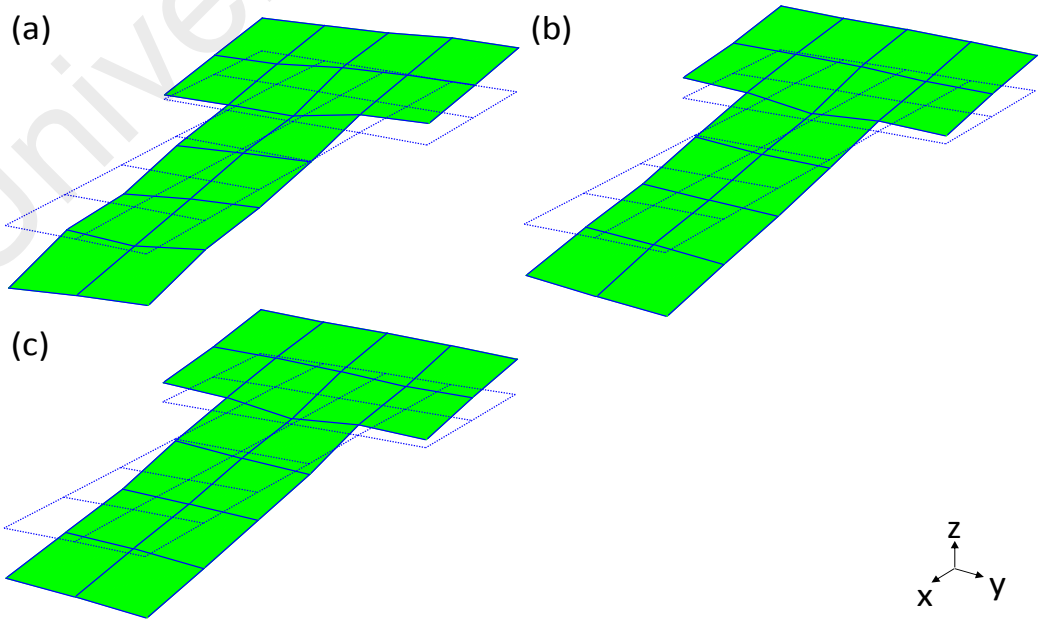

Figure 4.33: First Mode Shape (Pitching) for 20 Hz: (a) EMA, (b) Manual Impact Hammer, (c) Inconsistent Phase Selection Assessment

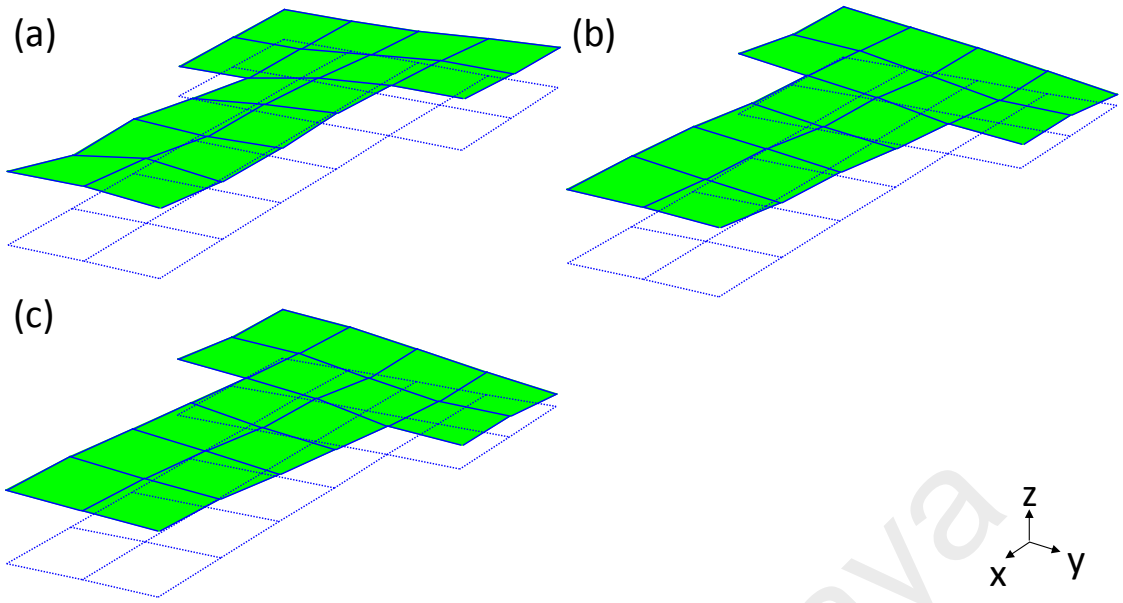

Figure 4.34: Second Mode Shape (Heaving) for 20 Hz: (a) EMA, (b) Manual Impact Hammer, (c) Inconsistent Phase Selection Assessment

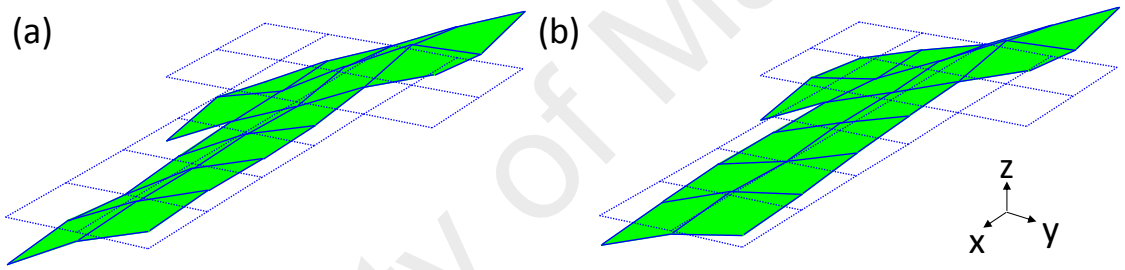

Figure 4.35: Third Mode Shape (Rolling) for 20 Hz: (a) EMA, (b) Inconsistent Phase Selection Assessment

4.4.6 Modal Extraction Data from Inconsistent Phase Selection Assessment and Manual Impact Hammer for 30 Hz

From Table 4.13, first two natural modes have been identified as 10.6 Hz, 16.3 Hz for both full 25 averages and 4 selected impacts in inconsistent phase selection assessment. By eliminating the periodic response of cyclic load and thus obtained a better FRFs estimation, the third natural mode is successfully extracted for inconsistent phase selection. The third natural mode recorded at 23.5 Hz with a high MAC value of 0.880. For inconsistent phase selection assessment, a slight decrement in MAC values is observed for the first natural mode. This is well explained by the number of averages taken in the phase selection assessment are comparably small (4 averages) in order to

completely eliminate the random ambient noise. In general, the results indicate that the mode shapes are in accord with the benchmark data. Figure 4.36, Figure 4.37 and Figure 4.38 have depicted the corresponding mode shape obtained using EMA, ISMA using manual impact hammer and inconsistent phase selection assessment. When comparing damping ratio in Table 4.14, a similar case is observed for first natural mode as in 20 Hz. Remark that the measurements were performed under two different condition, i.e., static and operational condition. This might well be the reason for the deviation in first natural mode. Apart from this, the cyclic load component at 30 Hz is not totally eliminated could be the reason for the deviation in third natural mode.

Table 4.13: Summary of Natural Frequencies and Mode Shapes Comparison between Modal Parameter Extraction Based on FRFs from a Benchmark (BM) Measurement without the Harmonic and ISMA using (A) Manual Impact Hammer and (B) Inconsistent Phase Selection Assessment for 30 Hz

	Natural frequency (Hz)			Percentage of difference (%)		MAC	
Mode	BM	A	B	BM vs. A	BM vs. B	BM vs. A	BM vs. B
1	10.4	10.6	10.6	1.92	1.92	0.916	0.915
2	15.9	16.3	16.3	2.52	2.52	0.945	0.945
3	24.0	N/A	23.5	N/A	2.08	N/A	0.880

Table 4.14: Summary of Damping Ratios from Modal Parameter Extraction Based on FRFs from a Benchmark (BM) Measurement without the Harmonic and ISMA using (A) Manual Impact Hammer and (B) Inconsistent Phase Selection Assessment for 30 Hz

	Damping ratio			Percentage of difference (%)	
Mode	BM	A	B	BM vs. A	BM vs. B
1	0.0832	0.0971	0.0970	16.71	16.59
2	0.0448	0.0405	0.0404	9.60	9.82
3	0.0566	N/A	0.0680	N/A	20.14

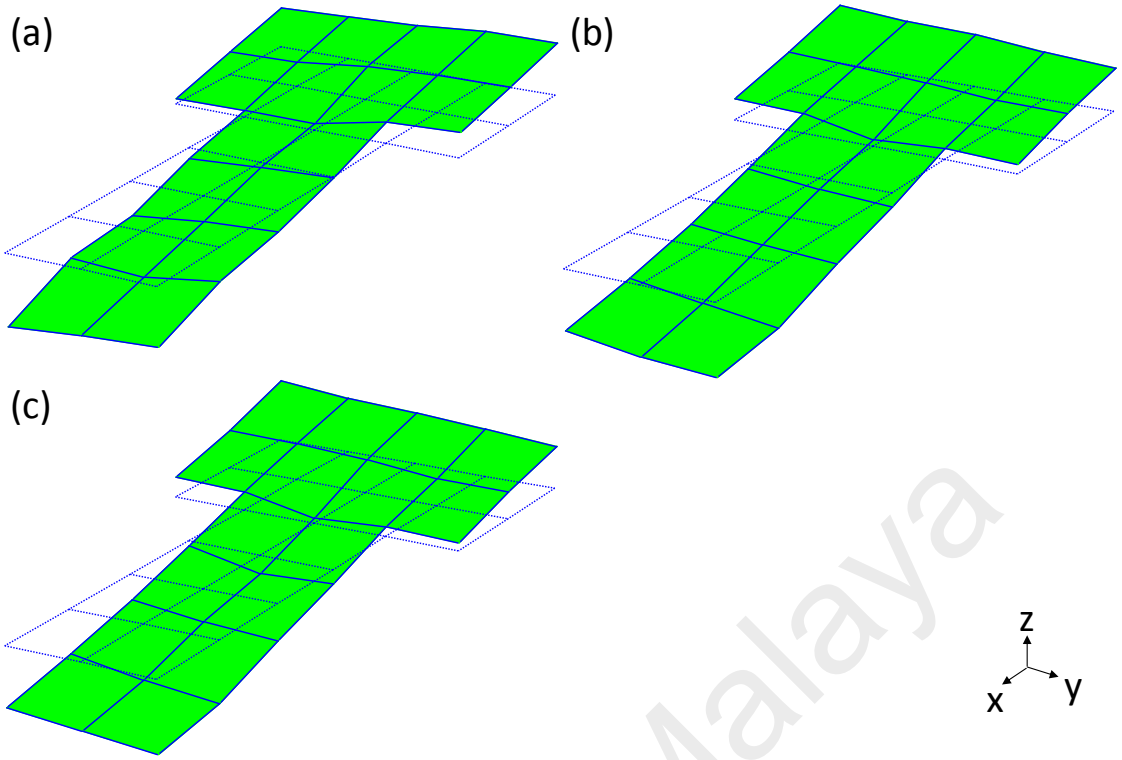

Figure 4.36: First Mode Shape (Pitching) for 30 Hz: (a) EMA, (b) Manual Impact Hammer, (c) Inconsistent Phase Selection Assessment

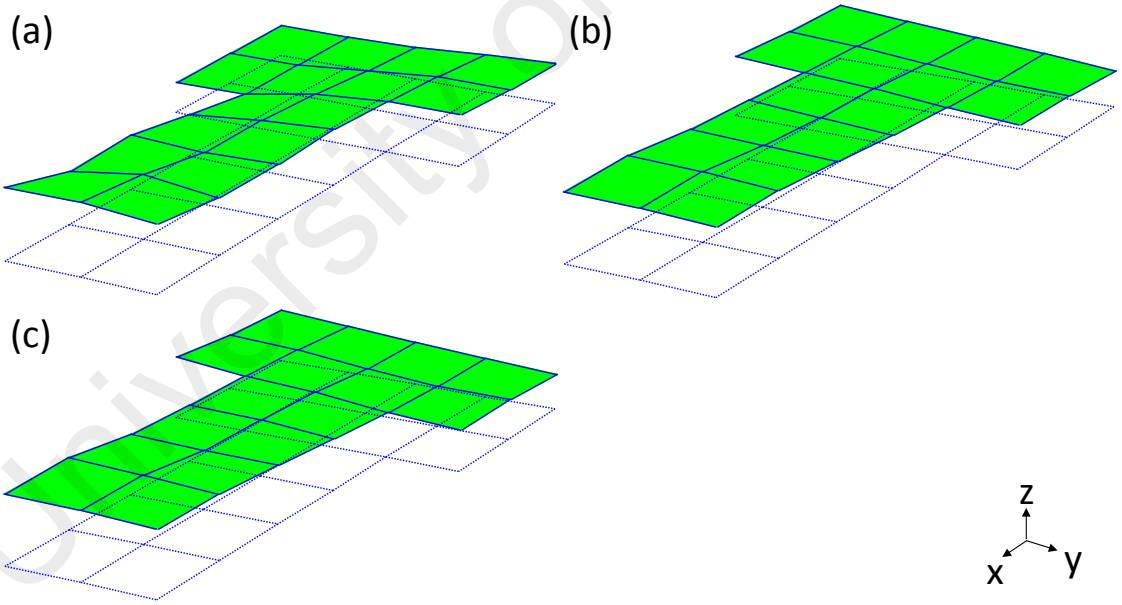

Figure 4.37: Second Mode Shape (Heaving) for 30 Hz: (a) EMA, (b) Manual Impact Hammer, (c) Inconsistent Phase Selection Assessment

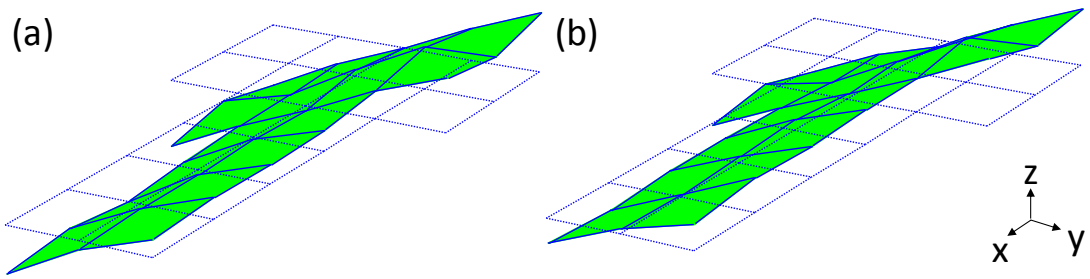

Figure 4.38: Third Mode Shape (Rolling) for 30 Hz: (a) EMA, (b) Inconsistent Phase Selection Assessment

4.4.7 Summary of Post-processing Inconsistent Phase Selection Assessment

The assessment has revealed several advantages of inconsistent phase selection assessment; (1) a better FRFs estimation with high SNR showed by the appearance of the third natural mode for running speed of 20 Hz and 30 Hz; (2) a percentage reduction of 72.96% cyclic load component at the maximum peak of 20 Hz, 82.25% at the maximum peak of 30 Hz and 52.23% at its second harmonic, 60 Hz; (3) minimal number of averages/impacts applied has relatively fasten the modal testing procedure; (4) improved and higher MAC values for the case of 20 Hz and 30 Hz and (5) overall good agreement with the benchmark data. In fact, this assessment can actually serve as an offline tool to process the raw vibration signal obtained during operation, as the selection criteria are well defined in Table 4.10. Besides, an additional benefit is to have the entire recording as one, long time series. This allows for efficient signal processing, for example, highpass filtering to remove rigid body vibrations, which can sometimes cause leakage effects when the system is slowly oscillating on free-free supporting soft springs and removal of line frequency in motor. Furthermore, the following section will uncover a refined picture of how the findings from this assessment are tailored with ISMA method as it is a formulation of guidelines for the design and deployment of an automated impact device with phase selection capability in modal testing during operation, i.e., APCID.

4.5 Experimental Validation on Effectiveness of Impact-synchronous Modal Analysis during Operation using Automated Phase Control Impact Device

Firstly, the ability of the APCID to knock at desired phase location on the periodic response of cyclic load before and after considering offset adjustment is presented in Section 4.5.1. Next, FRFs estimation and modal parameters using manual impact hammer and APCID for 20 Hz and 30 Hz are compared in Section 4.5.2, Section 4.5.3, Section 4.5.4, and Section 4.5.5. A summary of ISMA using APCID is then highlighted in Section 4.5.6.

4.5.1 Offset Consideration for Automated Phase Control Impact Device

Figure 4.39, Figure 4.40, Figure 4.41 and Figure 4.42 depict four out of six responses due to impact before offset adjustment. The time intervals for actual counter time ($T_{counter}$), phase difference time (T_{Φ}), time interval of load cycles (T_{cycle}), time interval of desired impact ($T_{desired}$), lag time (T_{lag}), and time delay taken by the impact device to impart on the surface of structure after "On" signal (T_{offset}) are indicated in the figures. Ideally, the accuracy of APCID is proven if and only if the impact location, i.e., process output (L_{real}) equals to set-point (L_{exp}) from the qualitative point of view. Besides, for ease of investigating the accuracy, it is more convenient to quantitatively compare the results of impact time, i.e., experimental impact time before offset adjustment (t_{exp}) and real impact time observed in the response signal (t_{real}). In other words, comparison between L_{exp} and L_{real} can be represented by the difference between t_{exp} and t_{real}, respectively. For example, a value near 0 indicates that L_{exp} and L_{real} are consistent.

As seen, L_{exp} and L_{real} are not at the same position where the response due to impacts tend to happen at L_{real} instead of L_{exp}. Also, it is noted that t_{exp} is not equivalent to t_{real} in this context when T_{offset} is not taken into consideration when computing $T_{counter}$. Therefore, an averaged offset time, T_{offset} of 0.085928 s is calculated through 6 dummy

impacts prior to the actual counted impacts as tabulated in Table 4.15. This time delay is suspected to be caused by the time travel of the tip of APCID from resting position to surface of structure.

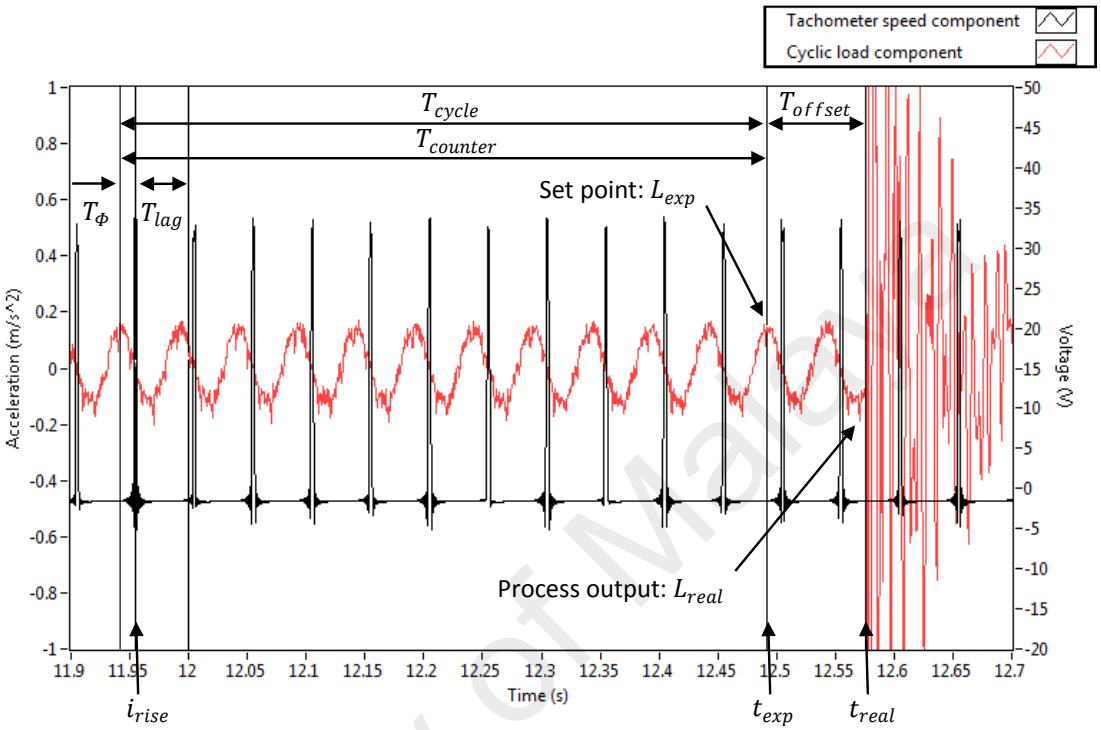

Figure 4.39: First Response due to Impact at Crest before Offset Adjustment

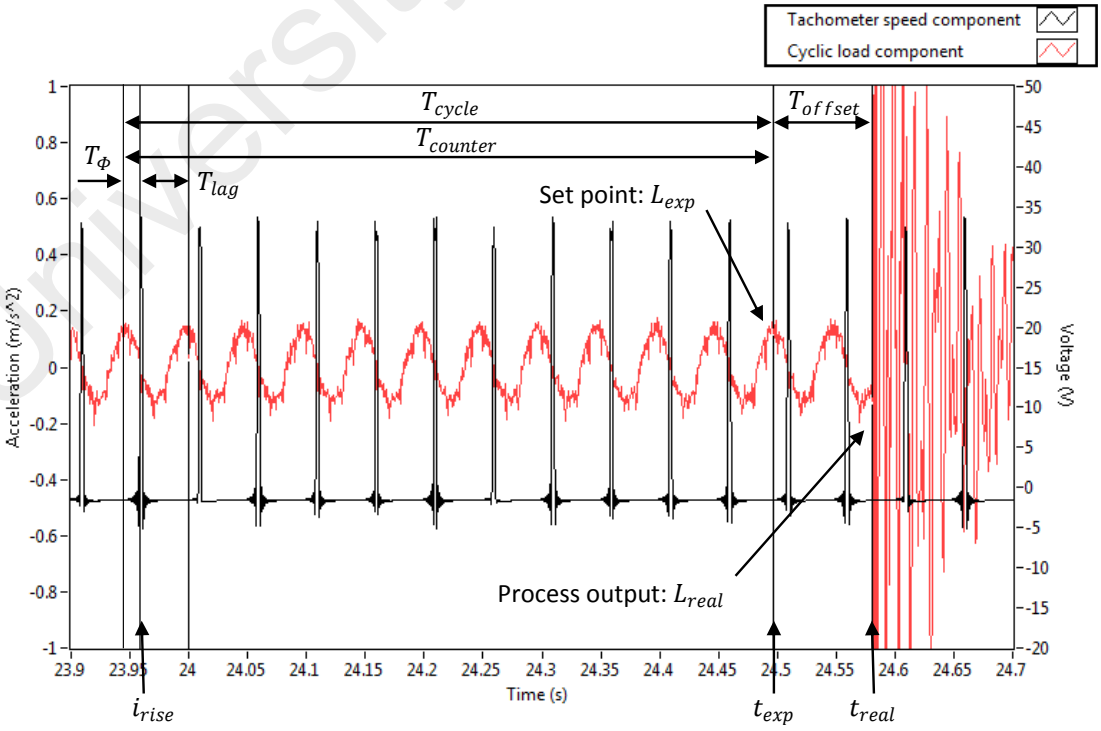

Figure 4.40: Second Response due to Impact at Crest before Offset Adjustment

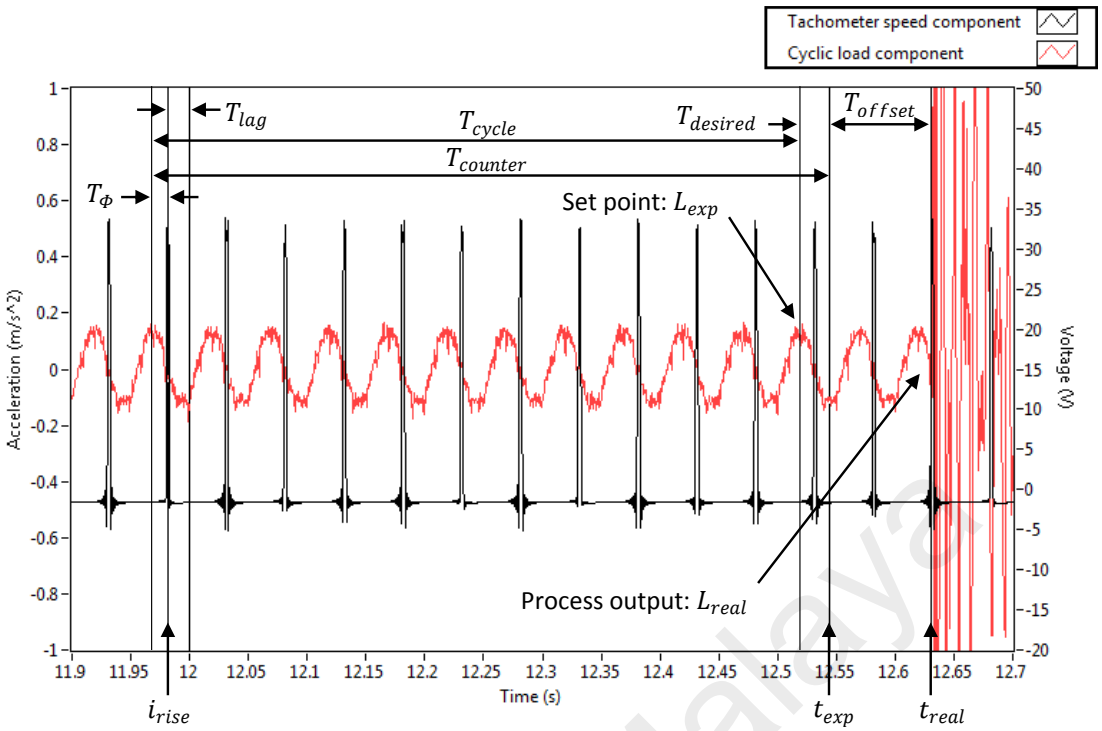

Figure 4.41: First Response due to Impact at Trough before Offset Adjustment

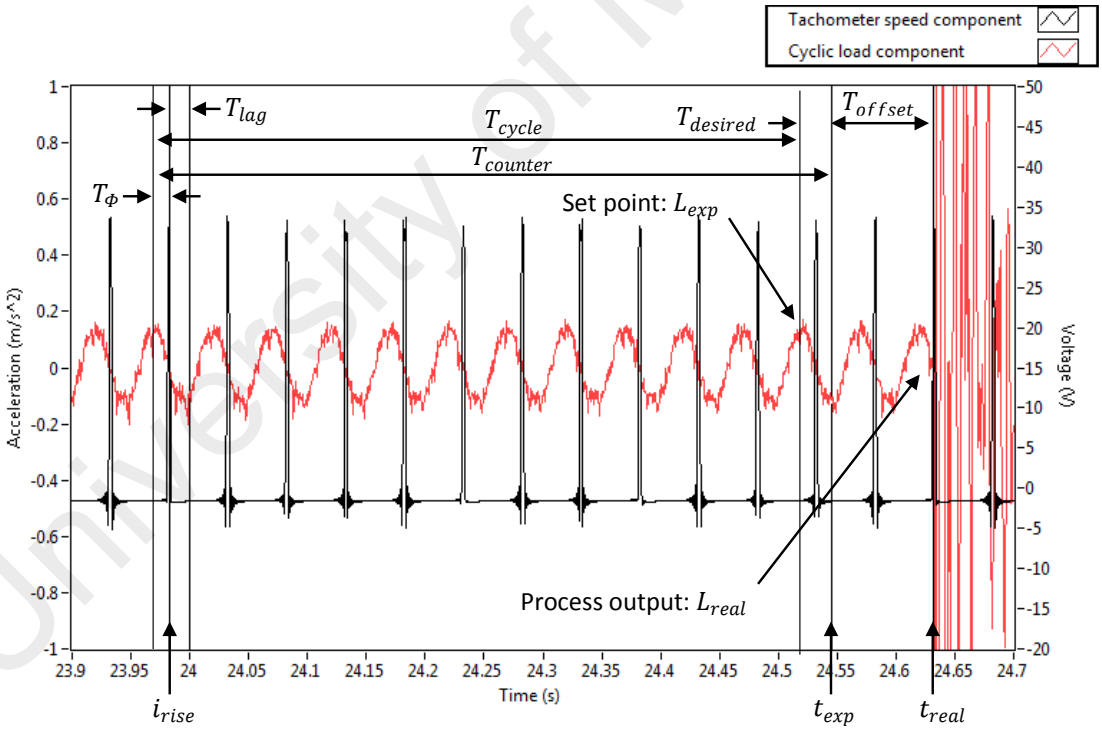

Figure 4.42: Second Response due to Impact at Trough before Offset Adjustment

Table 4.15: Responses due to Impact Summary before Offset Adjustment

Impact	t_{exp} (s)	t_{real} (s)	$T_{offset} = t_{real} - t_{exp}$ (s)
1	12.492147	12.575195	0.083048
2	24.496612	24.580566	0.083954
3	36.498765	36.584473	0.085708
4	12.543946	12.631836	0.087890
5	24.544711	24.631348	0.086637
6	36.543506	36.631836	0.088330
		Averaged	0.085928

Figure 4.43, Figure 4.44, Figure 4.45 and Figure 4.46 show four out of six responses due to impact after offset adjustment. The latter has shown improvement where responses due to impact are as expected to occur at the crest and trough of the cyclic load component shown by L_{real} and L_{exp}. It is worth noticing that the results have been greatly improved where t_{real} are almost equal to t_{exp} as shown in Table 4.16 and this has suggested that the L_{real} is very close to the set-point, L_{exp}. Thus, offset adjustment plays an important role for the impact device to impart at desired impact location on the cyclic load component. Examples of responses due to impact corresponding to the desired phase angle taken from a series of time recorded signal for 20 Hz and 30 Hz are shown in Figure 4.47 and Figure 4.48.

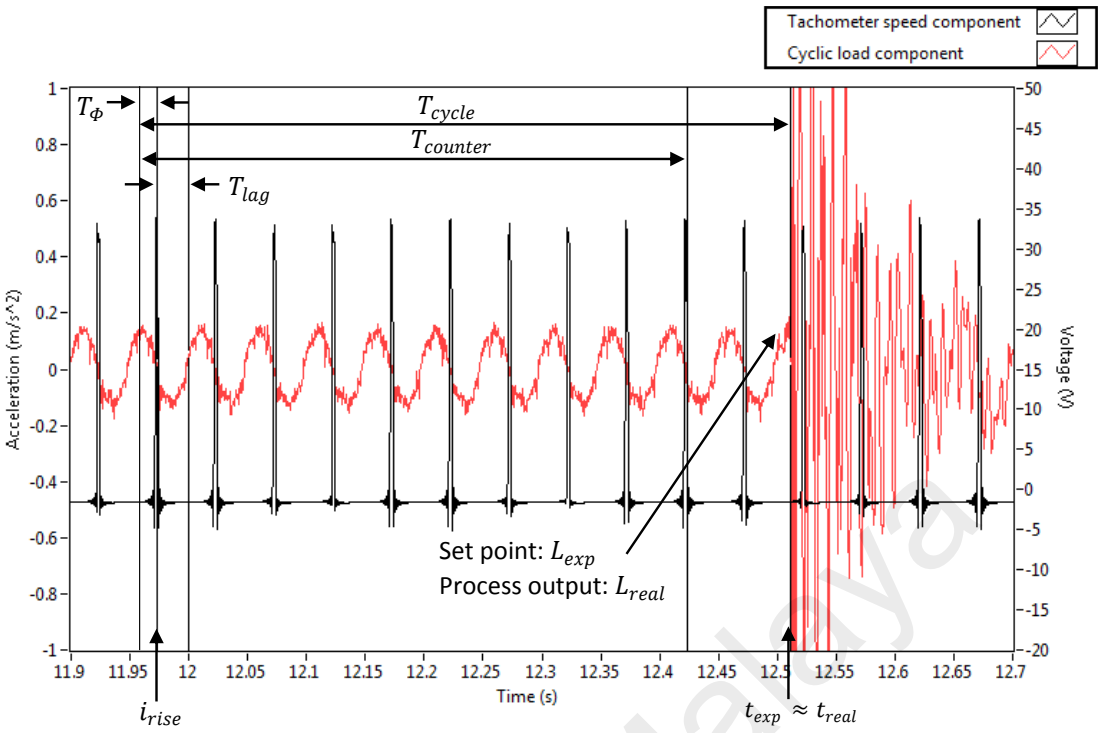

Figure 4.43: First Response due to Impact at Crest after Offset Adjustment

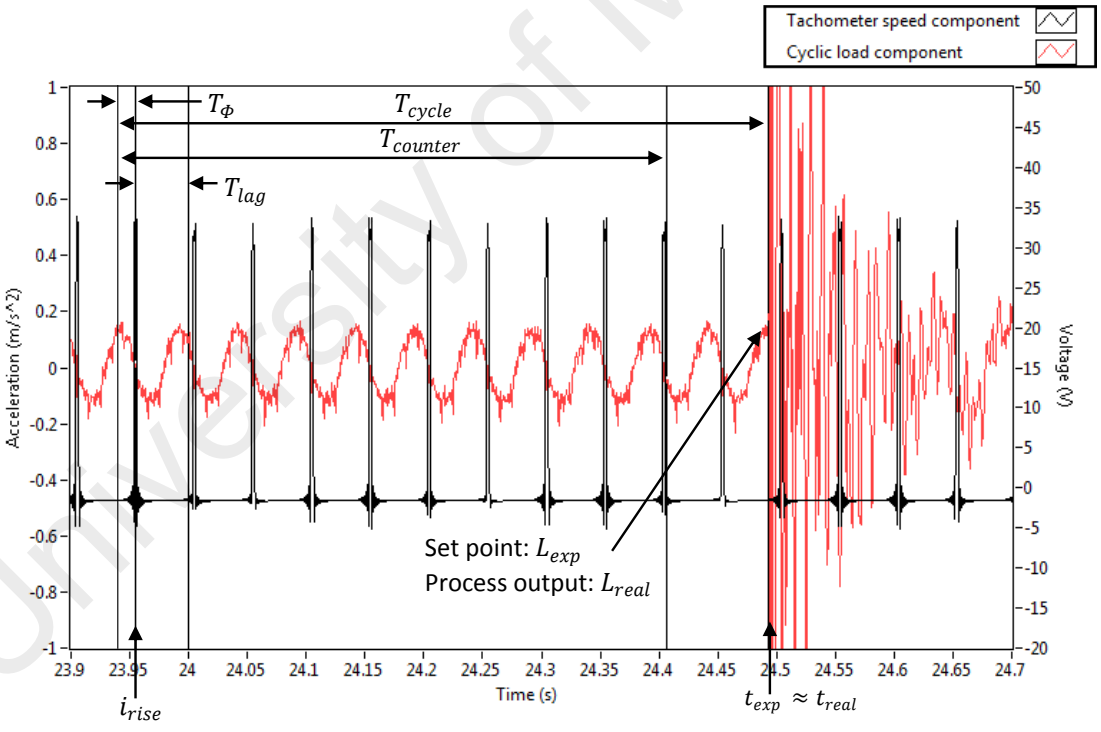

Figure 4.44: Second Response due to Impact at Crest after Offset Adjustment

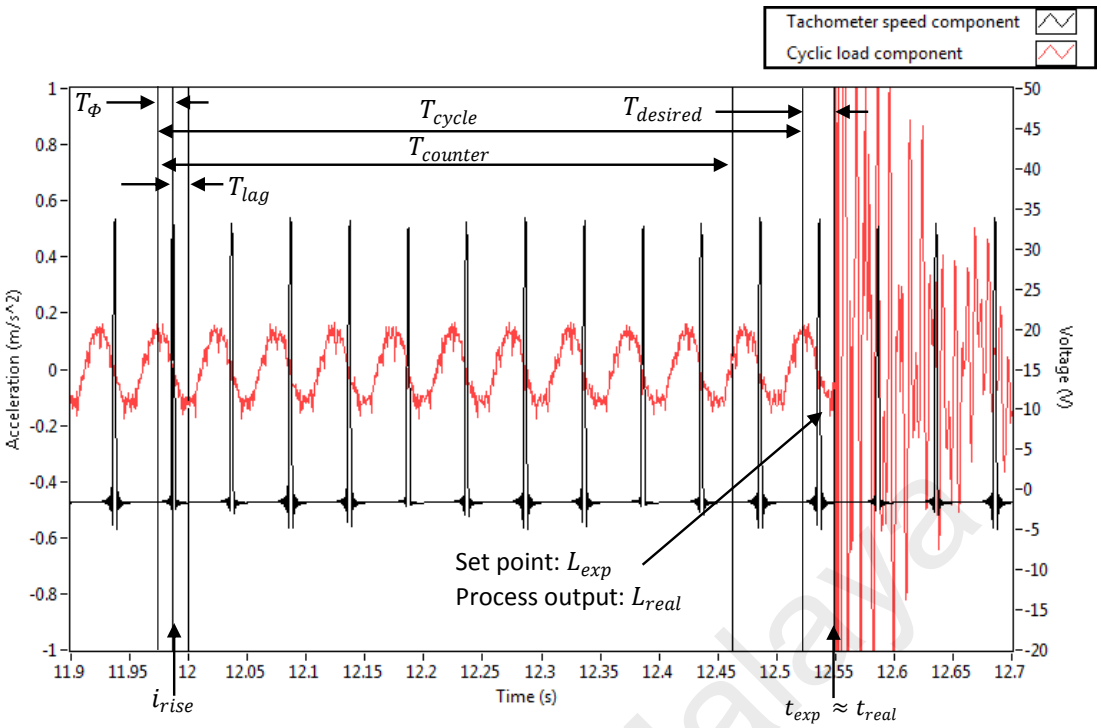

Figure 4.45: First Response due to Impact at Trough after Offset Adjustment

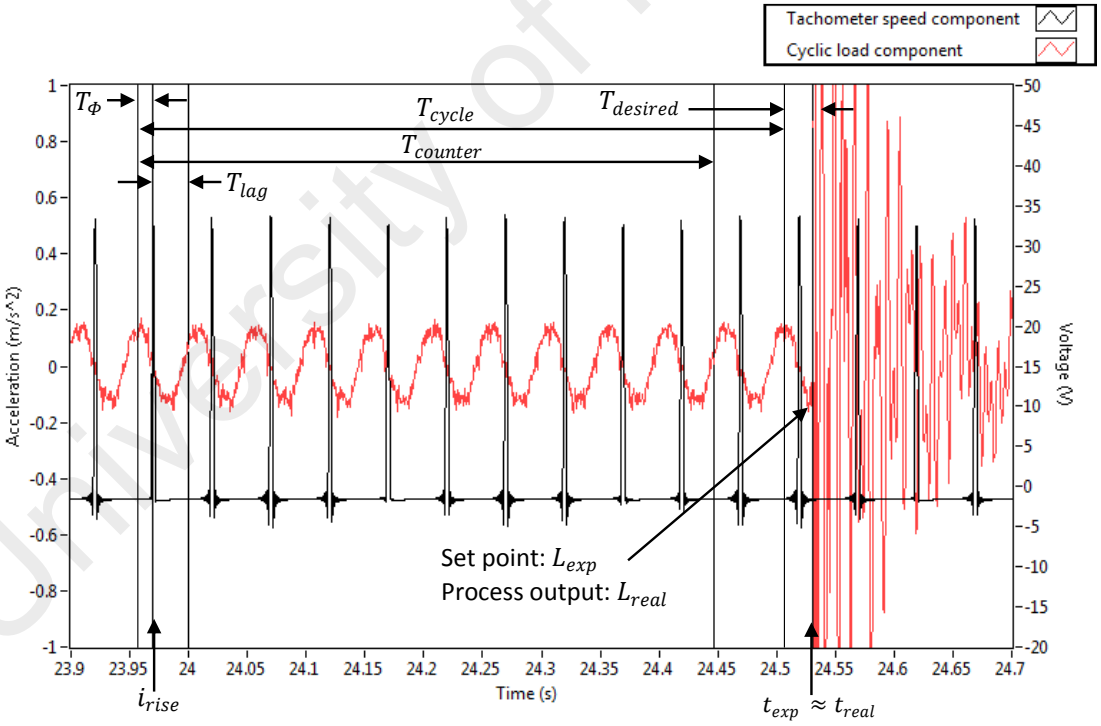

Figure 4.46: Second Response due to Impact at Trough after Offset Adjustment

Table 4.16: Responses due to Impact Summary after Offset Adjustment

Impact	t_{exp} (s)	t_{real} (s)	$t_{real} - t_{\exp}$ (s)
1	12.509141	12.510742	0.001601
2	24.491389	24.493164	0.001775
3	36.522669	36.524902	0.002233
4	12.547776	12.549316	0.001540
5	24.531599	24.530273	-0.001326
6	36.512740	36.512695	-0.000045

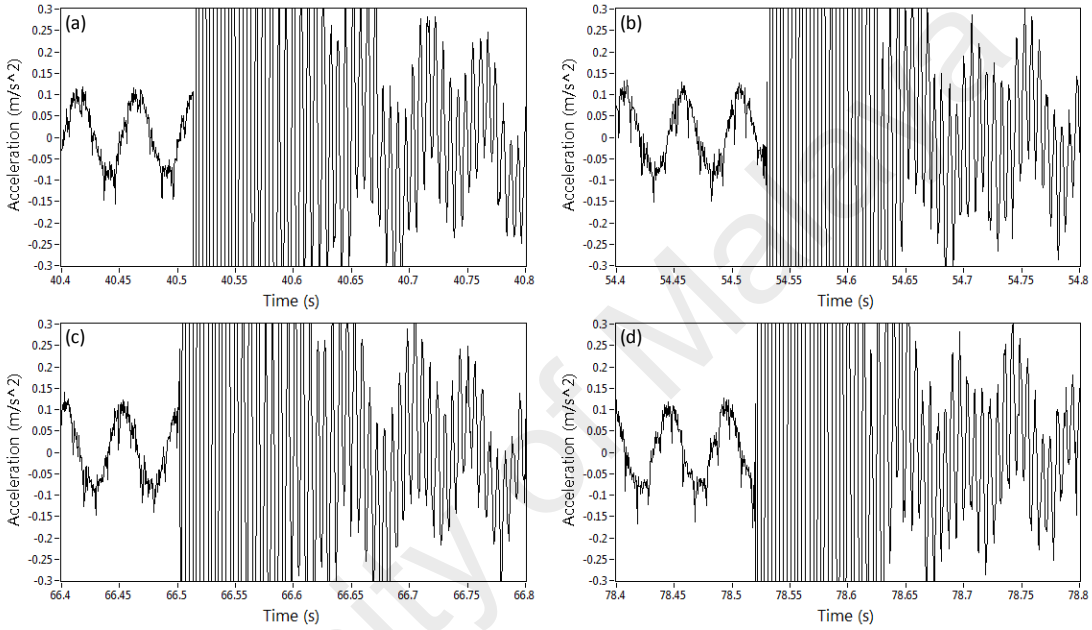

Figure 4.47: Starting Position of Responses due to Impact when using APCID for 20 Hz: (a) 0°, (b) 180°, (c) 0°, (d) 180°

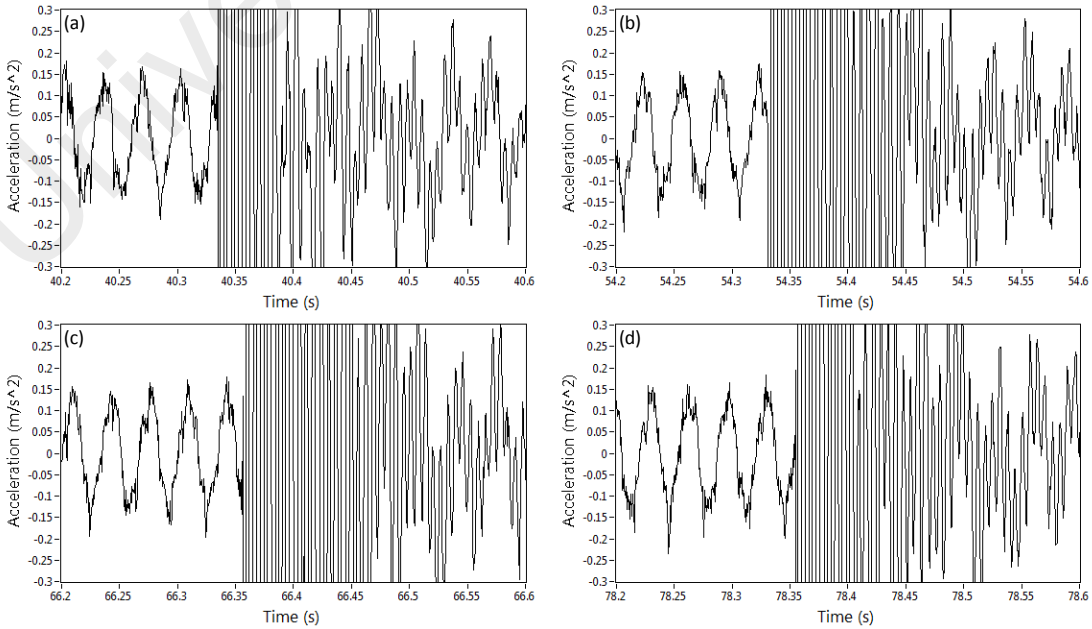

Figure 4.48: Starting Position of Responses due to Impact when using APCID for 30 Hz: (a) 0°, (b) 90°, (c) 180°, (d) 270°

4.5.2 Frequency Response Functions Estimation from Automated Phase Controlled Impact Device and Manual Impact Hammer for 20 Hz

A more common scenario obtained when performing modal testing using a manual impact hammer on an operating system is presented in Figure 4.49 (a). A better FRFs estimation should be free of measurement noise and leakage error. However, a highest peak originated from the cyclic load component is observed at 20 Hz with a value of 0.932 m/s^2N. The peak is dominant and covers up the adjacent mode subsequently a poor FRFs estimation is obtained. Recall that the presence of the dominant cyclic load component in the FRFs estimation using the manual impact hammer is possibly due to any of three reasons; (i) inconsistency in input force levels; (ii) inconsistency in excitation location between the impacts, and (iii) inefficient removal of the harmonic disturbances/components when the impact instants are random. For modal testing using manual impact hammer, the input force levels may vary between impacts. Problem can be developed over time when the uncontrollable impact force levels are much lower than the cyclic force originated from the cyclic load component. Thus, sufficient amount of impact force is very important to dominate the total response generated by impacts and to filter out the harmonic disturbances. Besides, the user may perform the excitation at locations which slightly deviate from the predefined location. Moreover, it is worth mentioning that although the possibility that a synchronisation occurs between the response due to impact and the response due to cyclic load is small, it is not totally impossible in modal testing using an impact hammer.

Using APCID as the excitation device tends to overcome some of the limitations faced by using manual impact hammer in modal testing. The excitation has a consistent impact force level which stays relatively constant as the input force is well controlled by supplying constant voltage on the APCID and setting the same optimum distance between impact tip and operating structure. This will assure each impact has force level higher

than the cyclic force in order to excite the natural mode of the system. Besides, the APCID is isolated and clamped firmly by the retort stand in the horizontal position, and thus it is able to consistently impart the impacts at the predefined location in z-axis. Figure 4.49 (b) shows the FRFs estimation using APCID. It can be noted that the dominant cyclic load component has been significantly reduced during ISTA with 10 averages compared to using a manual impact hammer. The highest peak recorded a value of 0.248 m/s^2N. The reduction is considerably successful and the percentage of reduction is high, 73.39%. APCID utilises the phase angle information from responses due to cyclic load component and imparts 10 impacts at a phase difference of 180° on the operating system. This produces five pairs of responses at the crest and trough of the cyclic load component. Since the total responses captured are at a phase difference of 180° between each impact, the signature responses due to impact are preserved while the harmonic disturbances are cancelling each other out during ISTA. Thus, the adjacent modes appear and are enhanced significantly. It is worth mentioning that the modal testing using APCID only requires half amount of averages compared to using manual impact hammer and the reduction of dominant response from cyclic load component is significant. This is, in fact, more effective and time-saving in enhancing ISMA if the information of phase angles with respect to impact is known and utilised.

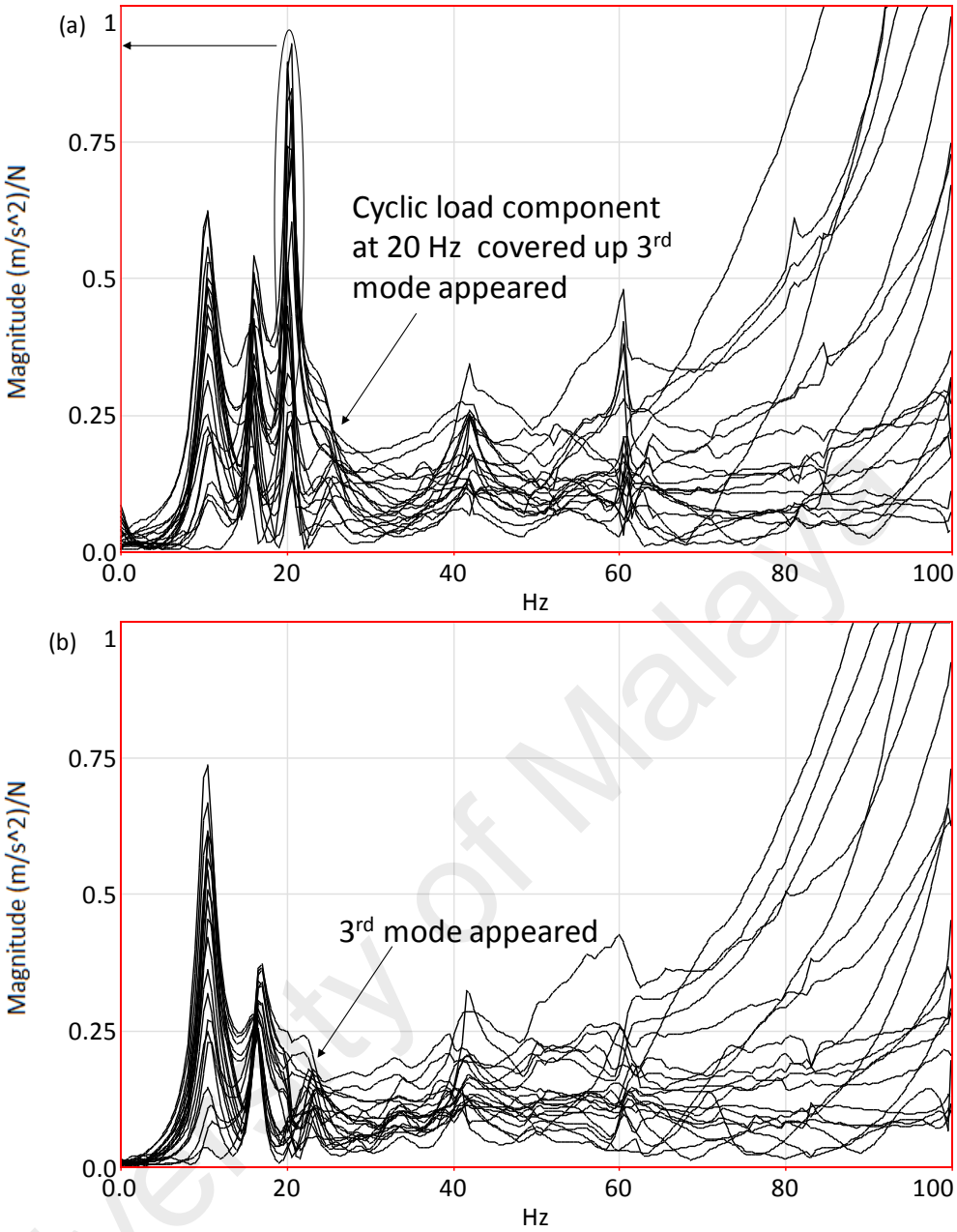

Figure 4.49: FRFs Estimation for 20 Hz: (a) Manual Impact Hammer, (b) APCID

4.5.3 Frequency Response Functions Estimation from Automated Phase Controlled Impact Device and Manual Impact Hammer for 30 Hz

Figure 4.50 (a) shows the FRFs estimation for ISMA using manual impact hammer. At 30 Hz, the vibration increases because of higher rotational or imbalance force. As can be seen, there are two dominant peaks originated from the cyclic load component at 30 Hz and its second harmonic at 60 Hz. The magnitude of peaks at 30 Hz and 60 Hz are identified as 2 m/s^{2}N and 0.561 m/s^{2}N. The reasons for this phenomenon are as discussed in Section 4.5.2, i.e., inconsistency in input force levels, inconsistency in excitation

location between the impacts, and inefficient removal of the harmonic disturbances/components when the impact instants are random. In order to eliminate the harmonic disturbances, the device is set to impart each impact at a phase difference of 90°. This is proven in Figure 4.50 (b) where the peak contributed by the cyclic load component and its second harmonic are significantly removed. The magnitude of peaks is reduced to 0.167 m/s^{2}N and 0.254 m/s^{2}N. The percentage of reduction is determined as 91.65% and 54.72%. Also, successful elimination of harmonic disturbances has led to the appearance of third natural mode.

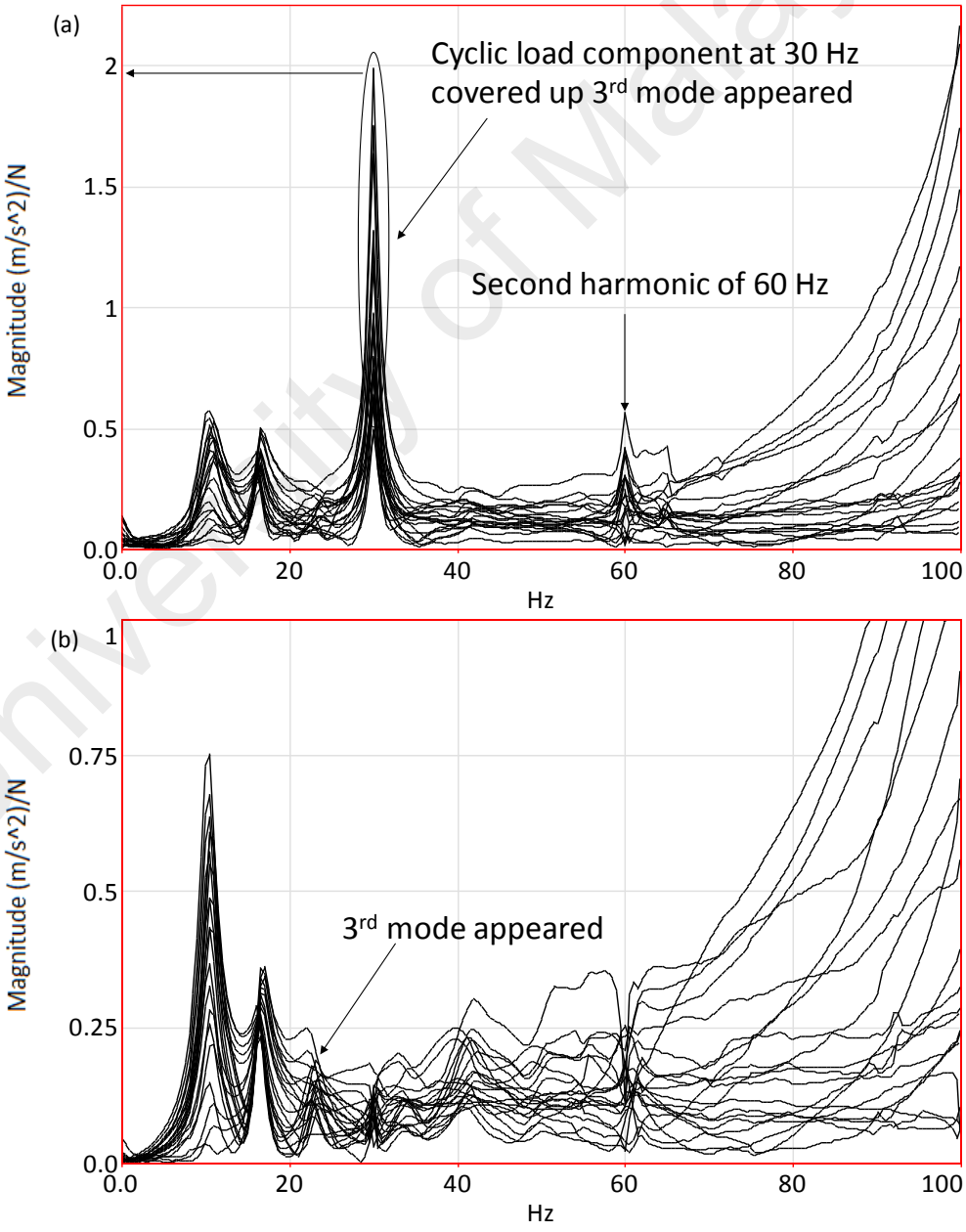

Figure 4.50: FRFs Estimation for 30 Hz: (a) Manual Impact Hammer, (b) APCID

4.5.4 Modal Extraction Data from Automated Phase Controlled Impact Device and Manual Impact Hammer for 20 Hz

Next, modal parameters are extracted from the FRFs estimation described in Section 4.5.2. An experimental benchmark data is obtained during stationary condition and used for the comparison and validation of the effectiveness of using the different excitation strategies, and results are tabulated in Table 4.17. As can be seen, the first two natural modes are excited by both manual impact hammer and the APCID. For the case of using manual impact hammer, the first two modes are estimated at 10.5 Hz and 15.9 Hz, respectively. However, the less sensitive third natural mode is covered up by the dominant cyclic load component at 20 Hz and thus is not successfully extracted. Meanwhile, the modal frequencies extracted from the estimated FRFs using APCID are 10.5 Hz, 16.4 Hz, and 22.9 Hz, respectively.

Table 4.17 has summarised the MAC values between the benchmark data and ISMA using manual impact hammer and APCID to show the correlation of mode shapes. Both excitation strategies show high and stable MAC value for the first and second natural modes and these natural modes are far from the dominant cyclic load component of 20 Hz. The third natural mode could be estimated when the APCID is used. The correlation of the mode shape with the benchmark data was high with a MAC value of 0.906 whereas for ISMA using manual impact hammer, the MAC value could not be identified. Also, mode shapes obtained are depicted in Figure 4.51, Figure 4.52, and Figure 4.53.

A higher percentage difference in damping ratio is observed for APCID for third natural modes in Table 4.18. The percentage difference between the benchmark and APCID in damping ratio estimates for the third natural mode is 14.66%. This is probably due to two reasons; (i) the harmonic disturbance could not be completely removed could cause error in the damping ratio estimates and (ii) damping ratio is estimated and

compared under two different conditions, i.e., stationary and rotating condition. Note that the modal parameters of a system depending on three factors, i.e., geometry, material properties, and boundary conditions. As the system is set to operate at 20 Hz, increases in vibration amplitude of the system possibly has led to boundary conditions change. Generally, the errors are small and it indicates a good suppression of the harmonic.

Table 4.17: Summary of Natural Frequencies and Mode Shapes Comparison between Modal Parameter Extraction Based on FRFs from a Benchmark (BM) Measurement without the Harmonic and ISMA using (A) Manual Impact Hammer and (B) APCID for 20 Hz

	Natural frequency (Hz)			Percentage of difference (%)		MAC	
Mode	BM	A	B	BM vs. A	BM vs. B	BM vs. A	BM vs. B
1	10.4	10.5	10.5	0.96	0.96	0.922	0.904
2	15.9	15.9	16.4	0	3.14	0.892	0.924
3	24.0	N/A	22.9	N/A	4.58	N/A	0.906

Table 4.18: Summary of Damping Ratios from Modal Parameter Extraction Based on FRFs from a Benchmark (BM) Measurement without the Harmonic and ISMA using (A) Manual Impact Hammer and (B) APCID for 20 Hz

	Damping Ratio			Percentage of difference (%)	
Mode	BM	A	B	BM vs. A	BM vs. B
1	0.0832	0.0949	0.0866	14.06	4.08
2	0.0448	0.0436	0.0460	2.68	2.68
3	0.0566	N/A	0.0483	N/A	14.66

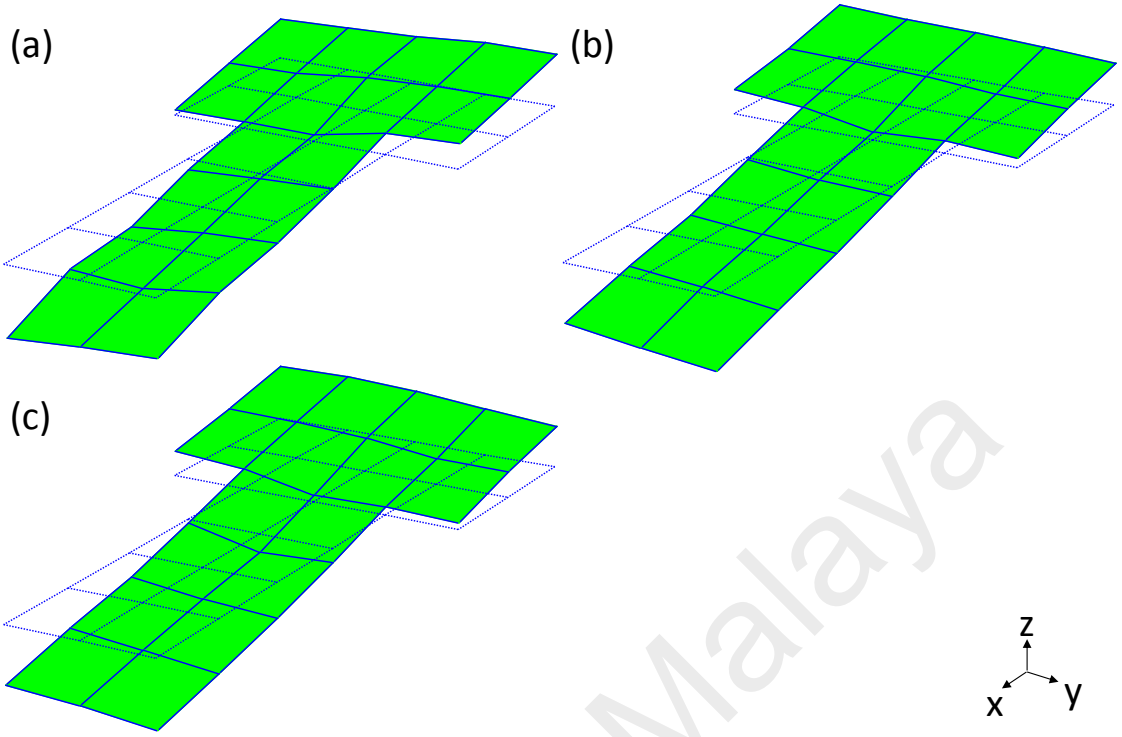

Figure 4.51: First Mode Shape (Pitching) for 20 Hz: (a) EMA, (b) Manual Impact Hammer, (c) APCID

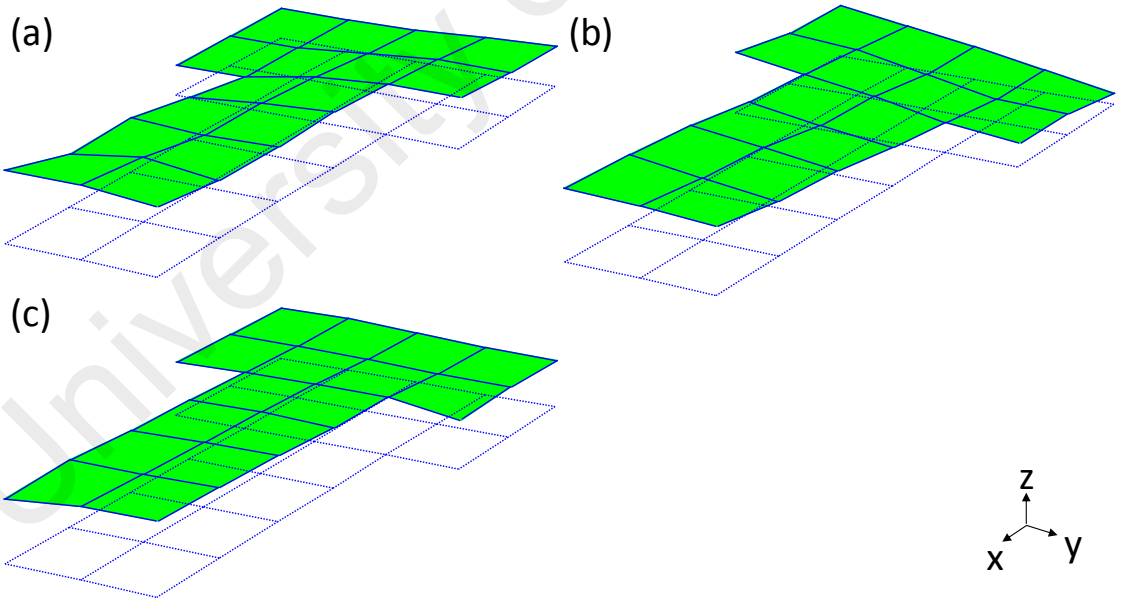

Figure 4.52: Second Mode Shape (Heaving) for 20 Hz: (a) EMA, (b) Manual Impact Hammer, (c) APCID

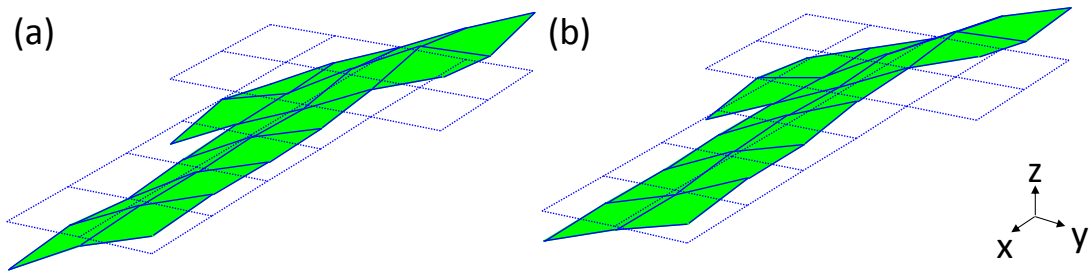

Figure 4.53: Third Mode Shape (Rolling) for 20 Hz: (a) EMA, (b) APCID

4.5.5 Modal Extraction Data from Automated Phase Controlled Impact Device and Manual Impact Hammer for 30 Hz

The modal extraction data are tabulated in Table 4.19 and Table 4.20. For ISMA using manual impact hammer, the first two natural frequencies identified are 10.6 Hz and 16.3 Hz whereas the third natural could not be identified as it is covered up by the dominant cyclic load component. In addition, the first three natural frequencies identified for ISMA using APCID are 10.4 Hz, 16.4 Hz and 22.9 Hz. Generally, the percentage of difference is less than 5% for both excitation strategies. Owing to the fact that the first and second natural mode are far away from the excitation frequency, the MAC value for this natural modes are above 0.9 showing good correlation with the benchmark EMA. Moreover, elimination of the harmonic disturbances for ISMA using APCID has led to the successful extraction of the less sensitive third natural mode with a MAC value of 0.922. The corresponding mode shapes for all the natural modes are shown Figure 4.54, Figure 4.55, and Figure 4.56. Again, the highest percentage of difference for damping ratio registered at 21.73% for third natural mode as tabulated in Table 4.20. This is probably because there is still the presence of small of amount harmonic disturbances as complete removal of harmonic disturbances may require more number of averages in addition to some effect from boundary change. Also, it is known that the dynamic characteristics of a system are governed by the geometric, material and boundary properties of the system. In this case, slight changes are boundary conditions is possible as the vibration level of the system increases due to the amplified rotational or imbalance force during operation especially

the operating frequency at 30 Hz. It is noticed that the errors are small and it indicates a good suppression of the cyclic load component and its harmonic.

Table 4.19: Summary of Natural Frequencies and Mode Shapes Comparison between Modal Parameter Extraction Based on FRFs from a Benchmark (BM) Measurement without the Harmonic and ISMA using (A) Manual Impact Hammer and (B) APCID for 30 Hz

	Natural frequency (Hz)			Percentage of difference (%)		MAC	
Mode	BM	A	B	BM vs. A	BM vs. B	BM vs. A	BM vs. B
1	10.4	10.6	10.4	1.92	0	0.916	0.903
2	15.9	16.3	16.4	2.52	3.14	0.945	0.936
3	24.0	N/A	22.9	N/A	4.58	N/A	0.922

Table 4.20: Summary of Damping Ratios from Modal Parameter Extraction Based on FRFs from a Benchmark (BM) Measurement without the Harmonic and ISMA with (A) Manual Impact Hammer and (B) APCID for 30 Hz

	Damping ratio			Percentage of difference (%)	
Mode	BM	A	B	BM vs. A	BM vs. B
1	0.0832	0.0971	0.0837	16.71	0.60
2	0.0448	0.0405	0.0456	9.60	1.79
3	0.0566	N/A	0.0455	N/A	19.61

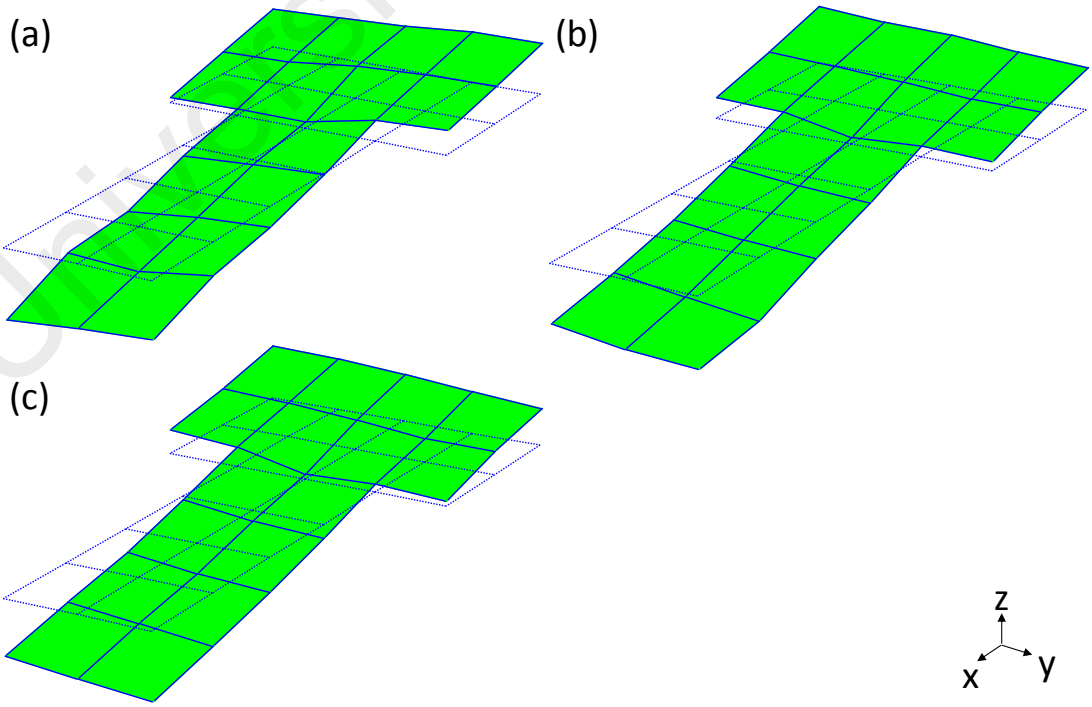

Figure 4.54: First Mode Shape (Pitching) for 30 Hz: (a) EMA, (b) Manual Impact Hammer, (c) APCID

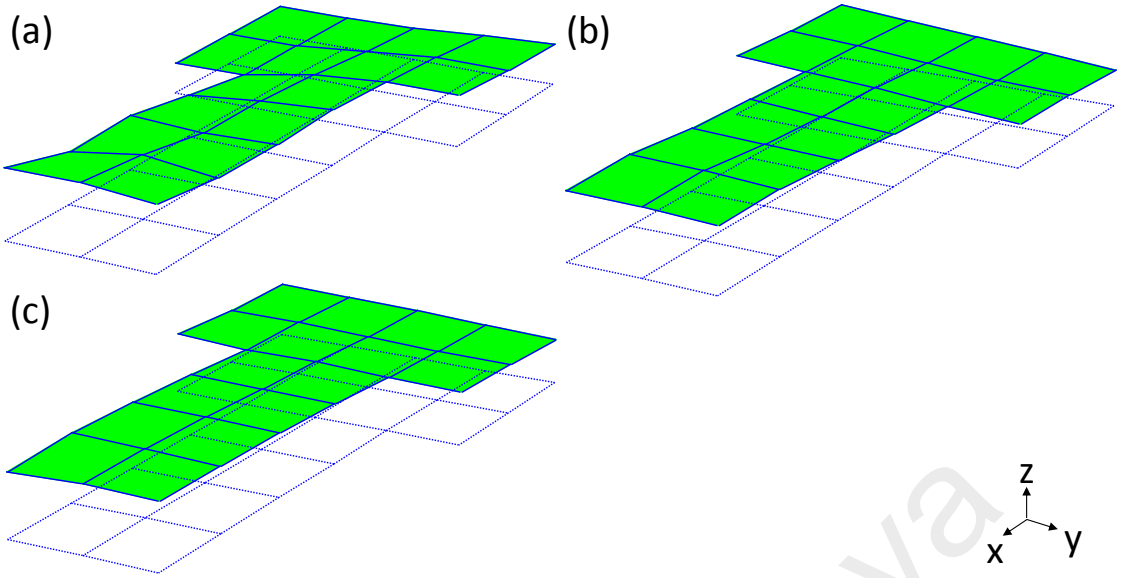

Figure 4.55: Second Mode Shape (Heaving) for 30 Hz: (a) EMA, (b) Manual Impact Hammer, (c) APCID

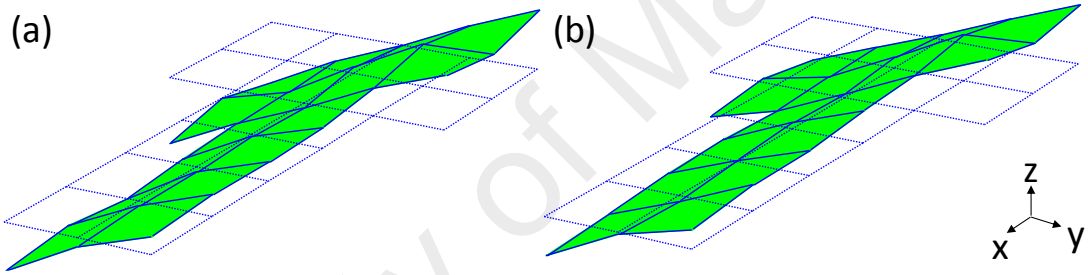

Figure 4.56: Third Mode Shape (Rolling) for 30 Hz: (a) EMA, (b) APCID

4.5.6 Summary of Impact-synchronous Modal Analysis using Automated Phase Controlled Impact Device

In summary, the effectiveness of the APCID to impart impacts at desired phase angle location is proven prior to the modal testing. It provides user to control not only on 0°, 90°, 180°, and 270° but also other possible desired phase angle. This is an additional advantage where implementation of such device in other applications which required desired phase location on impact. By implementing APCID in ISMA, the modal testing procedure during operation is thus enhanced in a way that; (i) a better FRFs estimation with high signal to noise ratio (SNR) is obtained by the appearance of the third natural mode for both 20 Hz and 30 Hz; (ii) a percentage reduction of 73.39% cyclic load component at the maximum peak of 20 Hz, 91.65% at the maximum peak of 30 Hz and

54.72% at its second harmonic, 60 Hz; (iii) minimal number of averages/impacts applied has relatively expedited the modal testing procedure; (iv) improved and high MAC values at running speed of 20 Hz and 30 Hz and (v) overall well correlation with the benchmark data.

The first attempt of applying ISMA using APCID in field testing can be found in Appendix A. The system under testing was a medium-sized water tank pump operating at 24.5 Hz. From the FRFs estimation obtained using manual impact hammer, two harmonic disturbances showing sharp peak were observed at 24.5 Hz and 49.2 Hz. By using APCID, the harmonic disturbances were reduced by 31.69% at 24.5 Hz and 75.66% at 49.2 Hz. A cleaner FRFs estimation from using APCID has shown that the case was not a problem related to resonance.

In addition to that, an enhancement of APCID in term of equipment and cost is proposed by replacing the tachometer with the in-use tri-axial accelerometer through utilising the filtered response of cyclic load component as an initiation signal to control the impact device. The accuracy was still preserved through this enhanced APCID and it is able to reduce first and second harmonics up to 93.58% and 57.78% respectively. Comparison of the modal extraction results with EMA also shows good agreement. A further description of this enhancement is given in Appendix B.

4.6 Overall Performance Comparisons with Previous Work and Classical Experimental Modal Analysis during Operation

To make a claim on this technique, it is useful to compare the overall performance of ISMA using automated impact device with previous literature as shown in Table 4.21. A ranking analysis using simple codes such as 0 for “same as”, - for “worse than” and + for “better than” has been performed. The reference here is ISMA using manual impact hammer due to the fact that the concept is proven from the previous literature. Several

criteria are chosen for comparison in order to select, or adapt, the most suitable technique for operational modal testing.

In Section 4.2, four scenarios were presented with ISMA using manual impact hammer and it was reported that synchronisation of phases between responses due to impact and periodic response of cyclic load was still possible because each impact was applied at random instance or the impact frequency is an integer multiples of the operating frequency. Thus, ISMA using automated impact device with non-synchronous impacts and APCID scores a "+" because each impact applied is always not synchronous with the harmonic disturbances. Note that among the techniques discussed, only ISMA using APCID allows users to have more control over the impacts location on periodic response of cyclic load. For this reason, a "+" score is only given to this technique in impart impact at desired phase angle criteria. Besides, impact force level is another concern while performing ISMA in the presence of dominant periodic response of cyclic load. For instance, if the excitation force is lower than the cyclic force, the FRFs estimation obtained could be severely affected by the harmonic disturbances and subsequent modal parameters identification are difficult (Ong et al., 2016). With automated impact device, an adjustable input force level can guarantee each impact has sufficient force to excite the natural modes of interest.

Previous work has shown that well correlation with the benchmark EMA can be achieved if and only if high number of averages is considered when using impact hammer, i.e., 250 averages (Rahman et al., 2014). The experimental testing can become very time-consuming; therefore APCID using feedforward control approach can be implemented as elaborated in this study in the effort of reducing the harmonic disturbances with minimal averages while enhancing the FRFs estimation. "-" scores are given to EMA in FRFs estimation and signal to noise ratio criteria as the technique is not applicable for

operational modal testing due to the fact that increasing number of averages (>250 averages) will not reduce the harmonic disturbances.

Since classical EMA is normally performed with fewer number of averages, the technique scores a "+" when compared to ISMA using manual impact hammer for man power criteria. The same score is given to ISMA using APCID as the study has shown that 20 averages are sufficient to have excellent results, which is 12.5 times lesser from previous literature. However, ISMA using automated impact device requires additional hardware, i.e., DC power supply to power up the APCID. This explains why there are "-" scores in the equipment criteria compared to other two techniques. Lastly, double impacts and overload are often the sources of human error in vibration measurement when using manual impact hammer and these errors can be easily overcome with automated impact device.

From the net score obtained, it is notable that ISMA using APCID has more advantages than others. The conclusion here is that EMA only limited to static condition and it is impractical to shut down the operating machine in today's high-technology petrochemical plants just to perform EMA as the cost of system downtime is very high. For that reason, ISMA using manual impact hammer was introduced previously but the procedure requires high number of averages which in turn may increase human errors and analysis time. ISMA using automated impact device with non-synchronous impacts was introduced in the early stage of the research. Although, the suppression of harmonic disturbances is better than by using manual impact hammer, harmonic disturbances still remain present in the FRFs estimation, especially with increasing vibration amplitude of cyclic load component. Thus, ISMA using APCID is seen to be a very good solution for the problem discussed.

Table 4.21: Ranking Analysis between EMA and ISMA using Manual Impact Hammer and APCID during Operation

Criteria	EMA	ISMA using manual impact hammer	ISMA using automated impact device with non-synchronous impacts	ISMA using APCID
Synchronisation of the impact with cyclic load	0	0	+	+
Impact condition:				
Random impacts	0	0	+	+
Impact frequency	0	0	+	+
Impact force level	0	0	+	+
Impart impact at desired phase angle	0	0	0	+
Number of averages required	+	0	0	+
FRFs estimation	-	0	+	+
Signal to noise ratio	-	0	+	+
Man power	+	0	0	+
Equipment:				
cost	0	0	-	-
set-up	0	0	-	-
Human error:				
Double impact	0	0	+	+
Overload	0	0	+	+
Sum +'s	2	0	8	11
Sum 0's	8	12	3	0
Sum –'s	2	0	2	2
Net score	0	0	6	9
Rank	3	3	2	1

CHAPTER 5: CONCLUSIONS AND RECOMMENDATIONS

5.1 Conclusions

The study on phase synchronisation effect in Impact-synchronous Modal Analysis (ISMA) using virtual instrument simulation and experimental modal testing has demonstrated the importance of phase angle with respect to impact in the determination of dynamic characteristics. Synchronisation of phases between impacts and periodic response of cyclic load should be avoided to enhance the effectiveness of ISMA. Small amount of average is sufficient to eliminate the non-synchronous components with 98.48% (simulation), 74.75% (scenario 3) and 95.22% (scenario 4) of improvement when every impact applied is not consistent with the phase angles of periodic response of cyclic load. Also, an improvement of 95.22% in the scenario 3 which is much higher than the scenario 4 indicated that there is probably a relationship tailored between phase angle of cyclic load component with respect to impact applied.

For that, an automated impact device with non-synchronous impacts is introduced to apply non-synchronous impacts in determining dynamic characteristics of an operating machine. The enhancement of the effectiveness of ISMA is demonstrated through comparison of Frequency Response Functions (FRFs) estimation obtained by a manual impact hammer and by the automated impact device with non-synchronous impacts. The percentage of reduction of harmonic disturbances can achieve 17-45%. Results show that an enhancement of FRFs estimation is obtained using the automated impact device with non-synchronous impacts, making it possible to estimate a third natural mode which, with the other two methods, is hidden by the harmonic disturbances. The cyclic load component is decreased and adjacent modes are found to be enhanced significantly. Enhanced FRFs estimation is also found to lead to more accurate modal parameters. Results show that by using the automated impact device with non-synchronous impacts, the first three natural modes are successfully determined and all three modes achieve good

correlation with benchmark Experimental Modal Analysis (EMA) results with relatively low percentage of difference in natural frequency, of less than 3%, and modal assurance criterion (MAC) values between, i.e., 0.893-0.925 for 20 Hz and 0.908-0.947 for 30 Hz.

Further improvement on FRFs estimation is done through the post-processing inconsistent phase selection assessment where a summary of the criteria for removing periodic response of cyclic load during operational modal testing is presented. The qualitatively and quantitatively validated assessment proved that the findings provide efficient means to eliminate the harmonic disturbances in providing a better FRFs estimation in operational modal testing. The assessment shows that the elimination of the harmonic disturbances is successfully achieved with a minimal number of averages, i.e., 4 averages, when the phase angles with respect to the impact are inconsistent for each impact applied. It is shown by the maximum harmonic disturbance peaks has significantly decreased by 72.96% at 20 Hz, 82.25% at 30 Hz, and 52.23% at its second harmonic, 60 Hz. Thus, it leads to a successful extraction of modal parameters and good agreement with the benchmark.

Utilising the findings from inconsistent phase selection assessment, a device namely Automated Phase Controlled Impact Device (APCID) is introduced in this paper in the effort to eliminate non-synchronous components with a minimal number of averages by feeding the phase angle information of responses from the cyclic load back to the device. It utilises the phase angle information and able to impart the impact at the correct time/phase which is always asynchronous with respect to the phase of response from cyclic load. Results showed that a cleaner FRFs estimation is obtained using the APCID, making it possible to estimate a third natural mode which is covered up by the dominant cyclic load component for ISMA using manual impact hammer. The percentage of reduction of harmonic disturbances can achieve 54-92%. Enhanced FRFs estimation for

ISMA using APCID has led to more accurate modal parameters extraction where the first three natural modes are successfully determined and reveal a good correlation with the benchmark data. This is shown by the relatively low percentage of difference in natural frequency and MAC values between, i.e., i.e., 0.904-0.924 for 20 Hz and 0.903-0.936 for 30 Hz. Therefore, ISMA using APCID has proven to be able to deliver highly accurate results which is suitable for modal testing during operation. It is a viable option for the conventional method using manual impact hammer as the modal testing procedure can be more precise, faster and more efficient.

5.2 Recommendations

This research gives a first extensive study on phase synchronisation effect as well as the effectiveness of ISMA with various excitation device on a rotating system. From the aspect of excitation device, the study has revealed the capability of automated impact device to replace manual impact hammer, from automated impact device with non-synchronous impacts to APCID. In future, ISMA using APCID can be further tested on reciprocating machines where vibration signals are more complex. In term of equipment and cost, APCID can be further enhanced, i.e., by replacing the tachometer with the in-use tri-axial accelerometer through utilising the filtered response of cyclic load component as an initiation signal to control the impact device. Parameters like digital filter characteristics on its effectiveness could be an interesting study in future progress. In the signal processing aspects, neural networks (NNs), a machine learning algorithm, can be utilised to "learn" the underlying relationship between the parameters that govern the effectiveness of ISMA based on a large number of observation. For that, an "intelligent" algorithm can be developed and optimum values for each parameter could be identified prior to perform modal testing.

Besides, ISMA using APCID can be applied to real-world applications, for example, on compressor and diesel fuel pump package in petrochemical plants. For that, a portable large scale APCID can be developed to provide higher impact force to excite medium to large size machinery. The identified dynamic characteristics can be used for later assessment, e.g., damage detection, condition based monitoring, structural dynamic modification, etc. Apart from this, the large-scale APCID should be designed in a more efficient, satisfying, and user-friendly way, typically when modal testing is to be performed in the harsh environment. It will be another breakthrough in ISMA if the control and processing part can be performed remotely, for instance, via the internet or Bluetooth. Lastly, the device can be commercialised and promoted to industry to be used with ISMA, to whether the system is in shutdown mode or operational condition.

REFERENCES

Aenlle, M. L., & Brincker, R. (2013). Modal scaling in operational modal analysis using a finite element model. *International Journal of Mechanical Sciences, 76*, 86-101.

Aenlle, M. L., Brincker, R., Pelayo, F., & Canteli, A. F. (2012). On exact and approximated formulations for scaling-mode shapes in operational modal analysis by mass and stiffness change. *Journal of Sound and Vibration, 331*(3), 622-637.

Aenlle, M. L., Fernandez, P., Brincker, R., & Fernandez-Canteli, A. (2010). Scaling-factor estimation using an optimized mass-change strategy. *Mechanical Systems and Signal Processing, 24*(5), 1260-1273.

Agneni, A., Coppotelli, G., & Grappasonni, C. (2012). A method for the harmonic removal in operational modal analysis of rotating blades. *Mechanical Systems and Signal Processing, 27*, 604-618.

Andersen, P., Brincker, R., & Kirkegaard, P. H. (1995, February 12–15). *Theory of covariance equivalent ARMAV models of civil engineering structures.* Paper presented at the Proceedings of the 14th International Modal Analysis Conference, Aalborg, Michigan, USA.

Avitabile, P. (2001). Experimental modal analysis - A simple non-mathematical presentation. *Sound and Vibration, 35*(1), 20-31.

Avitabile, P. (2017). *Modal Testing: A Practitioner's Guide* (First ed.). New Jersey, USA: JohnWiley & Sons Ltd.

Bendat, J. S., & Piersol, A. G. (1993). *Engineering Applications of Correlation and Spectral Analysis* (Second ed.): John Wiley & Sons, Inc.

Bernal, D. (2004). Modal scaling from known mass perturbations. *Journal of Engineering Mechanics-Asce, 130*(9), 1083-1088.

Bernal, D. (2011). A receptance based formulation for modal scaling using mass perturbations. *Mechanical Systems and Signal Processing, 25*(2), 621-629.

Böswald, M., Schwochow, J., Jelicic, G., & Govers, Y. (2017, May 9-12). *New concepts for ground and flight vibration testing of aircraft based on output-only modal analysis.* Paper presented at the Proceedings of the 7th International Operational Modal Analysis Conference (IOMAC 2016), Ingolstadt, Germany.

Brandt, A., Berardengo, M., Manzoni, S., & Cigada, A. (2017). Scaling of mode shapes from operational modal analysis using harmonic forces. *Journal of Sound and Vibration, 407*, 128-143.

Brandt, A., & Brincker, R. (2010). *Impact excitation processing for improved frequency response quality.* Paper presented at the Proceedings of the 28th International Modal Analysis Conference, Jacksonville, Florida, USA.

Brincker, R., Andersen, P., & Møller, N. (2000, June). *An indicator for separation of structural and harmonic modes in output-only modal testing.* Paper presented at the European COST F3 Conference on System Identification & Structural Health Monitoring, E.T.S.I. Aeronauticos, Madrid, Spain.

Brincker, R., & Ventura, C. (2015). *Introduction to Operational Modal Analysis*. Chichester, United Kingdom: John Wiley & Sons, Ltd.

Brincker, R., Zhang, L., & Andersen, P. (2000, February 7-10). *Modal identification from ambient responses using frequency domain decomposition.* Paper presented at the Proceedings of the 18th International Modal Analysis Conference, San Antonio, Texas, USA.

Brittingham, J. N., Miller, E. K., & Willows, J. L. (1980). Pole extraction from real-frequency information. *Proceedings of the Ieee, 68*(2), 263-273.

Brown, D. L., Allemang, R. J., Zimmerman, R., & Mergeay, M. (1979). Parameter estimation techniques for modal analysis. *SAE Technical Paper No. 790221*.

Brownjohn, J. M. W., & Pavic, A. (2007). Experimental methods for estimating modal mass in footbridges using human-induced dynamic excitation. *Engineering Structures, 29*(11), 2833-2843.

Cara, J. (2016). Computing the modal mass from the state space model in combined experimental-operational modal analysis. *Journal of Sound and Vibration, 370*, 94-110.

Couch, R. N., Radcliffe, E. J., & Caldwell, R. A. (2016). A novel method to correlate a rocket launcher finite element model using experimental modal test measurements and identification algorithms. *Shock & Vibration, Aircraft/Aerospace, Energy Harvesting, Acoustics & Optics, 9*, 153-166.

Devriendt, C., De Sitter, G., Vanlanduit, S., & Guillaume, P. (2009). Operational modal analysis in the presence of harmonic excitations by the use of transmissibility measurements. *Mechanical Systems and Signal Processing, 23*(3), 621-635.

Devriendt, C., De Troyer, T., De Sitter, G., & Guillaume, P. (2012). Transmissibilty-based operational modal analysis for flight flutter testing using exogenous inputs. *Shock and Vibration, 19*(5), 1071-1083.

Ding, Y. L., Li, A. Q., & Liu, T. (2008). Environmental variability study on the measured responses of Runyang Cablestayed Bridge using wavelet packet analysis. *Science in China Series E-Technological Sciences, 51*(5), 517-528.

Dion, J. L., Stephan, C., Chevallier, G., & Festjens, H. (2013). Tracking and removing modulated sinusoidal components: A solution based on the kurtosis and the Extended Kalman Filter. *Mechanical Systems and Signal Processing, 38*(2), 428-439.

Dobson, B. J. (1985, January 28-31). *Modal analysis using dynamic stiffness data.* Paper presented at the Proceedings of the 3rd International Modal Analysis Conference, Orlando, Florida, USA.

Dobson, B. J. (1987). A straight-line technique for extracting modal properties from frequency-response data. *Mechanical Systems and Signal Processing, 1*(1), 29-40.

Doebling, S. W., & Farrar, C. R. (1996, May 20-22). *Computation of structural flexibility for bridge health monitoring using ambient modal data.* Paper presented at the Proceedings of the 11th ASCE Engineering Mechanics Conference, Ft. Lauderdale, Floride, USA.

Ewins, D. J. (1984). *Modal Testing: Theory and Practice* (First ed.). United Kingdom, UK: Research Studies Press.

Ewins, D. J. (2000). *Modal Testing: Theory, Practice, and Application* (Second ed.). Baldock, England: Research Studies Press.

Ewins, D. J., & Gleeson, P. T. (1982). A method for modal identification of lightly damped structures. *Journal of Sound and Vibration, 84*(1), 57-79.

Fan, P. Q., Wang, Y. S., & Zhao, L. L. (2015). Modal analysis of a truck cab using the least squares complex exponent test method. *Advances in Mechanical Engineering, 7*(3).

Fayyadh, M. M., & Razak, H. A. (2013). Damage identification and assessment in RC structures using vibration data: A review. *Journal of Civil Engineering and Management, 19*(3), 375-386.

Felber, A. J. (1994). *Development of a hybrid bridge evaluation system.* (Doctor of Philosophy), University of British Columbia, Vancouver, Canada.

Fernandez, P., Reynolds, P., & Lopez-Aenlle, M. (2011). Scaling mode shapes in output-only systems by a consecutive mass change method. *Experimental Mechanics, 51*(6), 995-1005.

Fillod, R., Lallement, G., Piranda, J., & Raynaud, J. (1985, January 28-31). *Global method of modal identification.* Paper presented at the Proceedings of the 3rd International Modal Analysis Conference, Orlando, Florida, USA.

Fu, Z. F., & He, J. (2001). *Modal Analysis* (First ed.). Oxford, United Kingdom: Butterworth-Heinemann.

Garcia-Perez, A., Amezquita-Sanchez, J. P., Dominguez-Gonzalez, A., Sedaghati, R., Osornio-Rios, R., & Romero-Troncoso, R. J. (2013). Fused empirical mode decomposition and wavelets for locating combined damage in a truss-type structure through vibration analysis. *Journal of Zhejiang University-Science A, 14*(9), 615-630.

Gaukroger, D. R., Skingle, C. W., & Heron, K. H. (1973). Numerical analysis of vector response loci. *Journal of Sound and Vibration, 29*(3), 341-353.

Giraldo, D. F., Song, W., Dyke, S. J., & Caicedo, J. M. (2009). Modal identification through ambient vibration: Comparative study. *Journal of Engineering Mechanics-Asce, 135*(8), 759-770.

Guillaume, P., De Troyer, T., Devriendt, C., & De Sitter, G. (2006, September 18-20). *OMAX - A combined experimental-operational modal analysis approach.* Paper presented at the Proceedings of ISMA2006: International Conference on Noise and Vibration Engineering, Leuven, Belgium.

Hameed, A. F., & Pavic, A. (2016). Multi-shaker modal testing and modal identification of hollow-core floor system. *Dynamics of Civil Structures, Volume 2: Proceedings of the 34th IMAC, A Conference and Exposition on Structural Dynamics 2016* (pp. 331-340). Cham: Springer International Publishing.

He, L., Huang, G., Wu, H. Y., & Lei, Y. L. (2014). Modal testing and analysis of z-axis supporting plate for high-speed PCB NC drilling machine. *Frontiers of Manufacturing and Design Science Iv, Pts 1-5* (Vol. 496-500, pp. 1016-1019). Switzerland: Trans Tech Publications Ltd.

He, L. Z., Yu, P., Zhang, T., & Guo, R. (2014). Inertia parameters identification of motor assembly for electric vehicles based on modal test method. *Mechanical Engineering, Materials Science and Civil Engineering Ii* (Vol. 470, pp. 534-538). Switzerland: Trans Tech Publications Ltd.

Hou, W. L., Zhou, H., & Wang, S. L. (2013). Acoustic modal test and finite element analysis on vehicle cavity. *Measurement Technology and Its Application, Pts 1 and 2* (Vol. 239-240, pp. 32-36). Switzerland: Trans Tech Publications Ltd.

Hwang, J. S., Kim, H. J., & Kim, J. K. (2006). Estimation of the modal mass of a structure with a tuned-mass damper using H-infinity optimal model reduction. *Engineering Structures, 28*(1), 34-42.

Ibrahim, S. R., & Mikulcik, E. C. (1973). A time domain modal vibration test technique. *The Shock & Vibration Bulletin, 43*(4), 21-37.

Ibrahim, S. R., & Mikulcik, E. C. (1976). The experimental determination of vibration parameters from time responses. *The Shock & Vibration Bulletin, 46*(5), 187-196.

Ibrahim, S. R., & Mikulcik, E. C. (1977). A method for the direct identification of vibration parameters from the free response *The Shock and Vibration Inform. Ctr. Shock and Vibration Bull. Part. 4* (pp. 183-198). United States: NASA.

Jacobsen, N. J., Andersen, P., & Brincker, R. (2006, September 18-20). *Using enhanced frequency domain decomposition as a robust technique to harmonic excitation in operational modal analysis.* Paper presented at the Proceedings of ISMA2006: International Conference on Noise and Vibration Engineering, Leuven, Belgium.

James, G. H., Carne, T. G., & Lauffer, J. P. (1992, February 3-7). *Modal testing using natural excitation.* Paper presented at the Proceedings of the 10th International Modal Analysis Conference, San Diego, California, USA.

Jannifar, A., Zubir, M. N. M., & Kazi, S. N. (2017). Development of a new driving impact system to be used in experimental modal analysis (EMA) under operational condition. *Sensors and Actuators a-Physical, 263*, 398-414.

Juang, J. N., & Pappa, R. S. (1985). An eigensystem realization-algorithm for modal parameter-identification and model-reduction. *Journal of Guidance Control and Dynamics, 8*(5), 620-627.

Juang, J. N., & Suzuki, H. (1988). An eigensystem realization algorithm in frequency domain for modal parameter identification. *Journal of Vibration Acoustics Stress and Reliability in Design, 110*(1), 24.

Ka-Veng., Y., L., B. J., & S., K. L. (2002). Probabilistic approach for modal identification using non-stationary noisy response measurements only. *Earthquake Engineering & Structural Dynamics, 31*(4), 1007-1023.

Khatibi, M. M., Ashory, M. R., Malekjafarian, A., & Brincker, R. (2012). Mass-stiffness change method for scaling of operational mode shapes. *Mechanical Systems and Signal Processing, 26*, 34-59.

Lauwagie, T., Van Assche, R., Van der Straeten, J., & Heylen, W. (2006, September 18-20). *A comparison of experimental, operational, and combined experimental-operational parameter estimation techniques.* Paper presented at the Proceedings of ISMA2006: International Conference on Noise and Vibration Engineering, Leuve, Belgium.

Le, T. P., & Argoul, P. (2015). Distinction between harmonic and structural components in ambient excitation tests using the time-frequency domain decomposition technique. *Mechanical Systems and Signal Processing, 52-53*, 29-45.

Lee, J., Wang, S., Pluymers, B., Desmet, W., & Kindt, P. (2015). A modified complex modal testing technique for a rotating tire with a flexible ring model. *Mechanical Systems and Signal Processing, 60-61*, 604-618.

Leuridan, J. (1984). *Some direct parameter model identification methods applicable for multiple input modal analysis.* (Doctor of Philosophy), University of Cincinnati, Ohio, USA.

Leuridan, J., & Vold, H. (1983). A time domain linear model estimation technique for multiple input modal analysis *The Winter Annual Metting of the America Socity of Mechanical Engineers* (pp. 51-62). Boston, Massachusetts, USA.

Li, Z. J., Li, A. Q., & Zhang, J. A. (2010). Effect of boundary conditions on modal parameters of the Run Yang Suspension Bridge. *Smart Structures and Systems, 6*(8), 905-920.

Magalhaes, F., Cunha, A., & Caetano, E. (2012). Vibration based structural health monitoring of an arch bridge: From automated OMA to damage detection. *Mechanical Systems and Signal Processing, 28*, 212-228.

Maia, N. M. M., & Silva, J. M. M. (1997). *Theoretical and Experimental Modal Analysis*. Taunton, Somerset, UK: Research Studies Press.

Mansour, G., Tsongas, K., & Tzetzis, D. (2016). Modal testing of epoxy carbon-aramid fiber hybrid composites reinforced with silica nanoparticles. *Journal of Reinforced Plastics and Composites, 35*(19), 1401-1410.

Manzato, S., Devriendt, C., Weijtjens, W., Di Lorenzo, E., Peeters, B., & Guillaume, P. (2014). Removing the influence of rotor harmonics for improved monitoring of offshore wind turbines. *Dynamics of Civil Structures, Volume 4: Proceedings of the 32nd IMAC, A Conference and Exposition on Structural Dynamics, 2014* (pp. 299-312). Cham: Springer International Publishing.

Mikota, G., Manhartsgruber, B., Kogler, H., & Hammerle, F. (2017). Modal testing of hydraulic pipeline systems. *Journal of Sound and Vibration, 409*, 256-273.

Mishra, A. K., & Chakraborty, S. (2015). Determination of material parameters of FRP plates with rotational flexibility at boundaries using experimental modal testing and model updating. *Experimental Mechanics, 55*(5), 803-815.

Modak, S. V., Rawal, C., & Kundra, T. K. (2010). Harmonics elimination algorithm for operational modal analysis using random decrement technique. *Mechanical Systems and Signal Processing, 24*(4), 922-944.

Mohanty, P., & Rixen, D. J. (2004a). A modified Ibrahim time domain algorithm for operational modal analysis including harmonic excitation. *Journal of Sound and Vibration, 275*(1-2), 375-390.

Mohanty, P., & Rixen, D. J. (2004b). Modified SSTD method to account for harmonic excitations during operational modal analysis. *Mechanism and Machine Theory, 39*(12), 1247-1255.

Mohanty, P., & Rixen, D. J. (2004c). Operational modal analysis in the presence of harmonic excitation. *Journal of Sound and Vibration, 270*(1-2), 93-109.

Mohanty, P., & Rixen, D. J. (2006). Modified ERA method for operational modal analysis in the presence of harmonic excitations. *Mechanical Systems and Signal Processing, 20*(1), 114-130.

Motte, K., Weijtjens, W., Devriendt, C., & Guillaume, P. (2015). Operational modal analysis in the presence of harmonic excitations: A review. *Dynamics of Civil Structures, Vol 2*, 379-395.

Ong, Z. C. (2013). *Development of impact-synchronous modal analysis technique on motor-driven structure during operation* (Doctor of Philosophy), University of Malaya, Malaysia.

Ong, Z. C., Kor, M. A. M. A., & Brandt, A. (2015, May 12-14). *Experimental validation of phase synchronisation effects in optimising impact-synchronous time averaging.* Paper presented at the 6th International Operational Modal Analysis Conference (IOMAC 2015), Gijon, Spain.

Ong, Z. C., & Lee, C. C. (2015). Investigation of impact irofile and isolation effect in automated impact device design and control for operational modal analysis. *Journal of Dynamic Systems Measurement and Control-Transactions of the Asme, 137*(9).

Ong, Z. C., Lim, H. C., Khoo, S. Y., Rahman, A. G. A., & Ismail, Z. (2016). An experimental investigation on the effects of exponential window and impact force

level on harmonic reduction in impact-synchronous modal analysis. *Journal of Mechanical Science and Technology, 30*(8), 3523-3532.

Orlowitz, E., & Brandt, A. (2017). Comparison of experimental and operational modal analysis on a laboratory test plate. *Measurement, 102*, 121-130.

Overschee, P. a. D. M., B. (1996). *Subspace Identification for Linear Systems: Theory, Implementation, Applications*. Netherlands: Kluwer Academic Publishers.

Parloo, E., Verboven, P., Guillaume, P., & Van Overmeire, M. (2002). Sensitivity-based operational mode shape normalisation. *Mechanical Systems and Signal Processing, 16*(5), 757-767.

Peeters, B., Cornelis, B., Janssens, K., & Van der Auweraer, H. (2007, May 1-2). *Removing disturbing harmonics in operational modal analysis.* Paper presented at the 2nd International Operational Modal Analysis Conference (IOMAC 2007), Copenhagen, Denmark.

Peeters, B., & De Roeck, G. (2000). Reference based stochastic subspace identification in civil engineering. *Inverse Problems in Engineering, 8*(1), 47-74.

Peeters, B., Van der Auweraer, H., Guillaume, P., & Leuridan, J. (2004). The PolyMAX frequency-domain method: A new standard for modal parameter estimation? *Shock and Vibration, 11*(3-4).

Phillips, A. W., & Allemang, R. J. (2003). An overview of MIMO-FRF excitation/averaging/processing techniques. *Journal of Sound and Vibration, 262*(3), 651-675.

Pintelon, R., Peeters, B., & Guillaume, P. (2008). Continuous-time operational modal analysis in the presence of harmonic disturbances. *Mechanical Systems and Signal Processing, 22*(5), 1017-1035.

Pintelon, R., Peeters, B., & Guillaume, P. (2010). Continuous-time operational modal analysis in the presence of harmonic disturbances-The multivariate case. *Mechanical Systems and Signal Processing, 24*(1), 90-105.

Porras, J. A., de Sebastian, J., Casado, C. M., & Lorenzana, A. (2012). Modal mass estimation from output-only data using oscillator assembly. *Mechanical Systems and Signal Processing, 26*, 15-23.

Rahman, A. G. A., Ismail, Z., Noroozi, S., & Ong, Z. C. (2014). Enhancement of impact-synchronous modal analysis with number of averages. *Journal of Vibration and Control, 20*(11), 1645-1655.

Rahman, A. G. A., Ong, Z. C., & Ismail, Z. (2011a). Effectiveness of impact-synchronous time averaging in determination of dynamic characteristics of a rotor dynamic system. *Measurement, 44*(1), 34-45.

Rahman, A. G. A., Ong, Z. C., & Ismail, Z. (2011b). Enhancement of coherence functions using time signals in modal analysis. *Measurement, 44*(10), 2112-2123.

Randall, R. B., Gao, Y., & Swevers, J. (1999, September 16 - 18). *Updating modal models from response measurements.* Paper presented at the Proceedings of the International Seminar on Modal Analysis, Leuven, Belgium.

Randall, R. B., Peeters, B., Antoni, J., & Manzato, S. (2012, September 17-19). *New cepstral methods of signal pre-processing for operational modal analysis.* Paper presented at the Proceedings of International Conference on Noise and Vibration Engineering (ISMA2012)/International Conference on Uncertainty in Structural Dynamics (USD2012), Leuven, Belgium.

Reynders, E., Degrauwe, D., De Roeck, G., Magalhaes, F., & Caetano, E. (2010). Combined experimental-operational modal testing of footbridges. *Journal of Engineering Mechanics-Asce, 136*(6), 687-696.

Reynders, E., Degrauwe, D., Schevenels, M., De Roeck, G., Van den Broeck, P., Dekkers, K., . . . Cunha, A. (2008, September 15-17). *OMAX testing of a bow-string and a stress-ribbon footbridge.* Paper presented at the Proceedings of ISMA2008: International Conference on Noise and Vibration Engineering, Leuven, Belgium.

Richardson, M. H. (1986, February 3-6). *Global frequency and damping estimates from frequency response measurements.* Paper presented at the Proceedings of the 4th International Modal Analysis Conference, Los Angeles, California, USA.

Richardson, M. H., & Formenti, D. L. (1982, November 8-10). *Parameter estimation from frequency response measurements using rational fraction polynomials.* Paper presented at the Proceedings of the 1st International Modal Analysis Conference, Orlando, Florida, USA.

Richardson, M. H., & Formenti, D. L. (1985, January 28-31). *Global curve fitting of frequency response measurements using the rational fraction polynomial method.* Paper presented at the Proceedings of the 3rd International Modal Analysis Conference, Orlando, Florida, USA.

Rossmann, S. (1999). *Development of force controlled modal testing on a rotor supported by magnetic bearing.* (Master of Science Degree), The Imperial College of Science, Technology and Medicine, University of London, London.

Schmerr, L. W. (1982, November 8-10). *A new complex exponential frequency domain technique for analysing dynamic response data.* Paper presented at the Proceedings of the 1st International Modal Analysis Conference, Orlando, Florida, USA.

Sharma, A., Brown, D. L., Allemang, R. J., & Phillips, A. W. (2016, January 25-28). *An alternative MIMO FRF estimation method using pneumatic exciters.* Paper presented at the 34th IMAC Conference and Exposition on Structural Dynamics, Orlando, Florida, USA.

Spitznogle, F. R., Barrett, J. M., Black, C. I., Ellis, T. W., & LaFuze, W. L. (1971). Representation and analysis of sonar signals. volume I. Improvements in the complex exponential signal analysis computational algorithm: Texas Instruments Inc Dallas Equipment Group.

Spitznogle, F. R., & Quazi, A. H. (1970). Representation and analysis of time - limited signals using a complex exponential algorithm. *The Journal of the Acoustical Society of America, 47*(5A), 1150-1155.

Thibault, L., Marinone, T., Avitabile, P., & Van Karsen, C. (2012). *Comparison of modal parameters estimated from operational and experimental modal analysis approaches.* Paper presented at the Proceedings of the 30th International Modal Analysis Conference, Jacksonville, Florida, USA.

Timoshenko, S., Young, D. H., & Weaver, W. (1974). *Vibration problems in engineering*. New York: John Wiley.

Turker, T., & Bayraktar, A. (2017). Vibration based modal testing of a scaled reinforced concrete building for construction stages. *Bulletin of Earthquake Engineering, 15*(8), 3399-3416.

Vanderauweraer, H., & Leuridan, J. (1987). Multiple input orthogonal polynomial parameter-estimation. *Mechanical Systems and Signal Processing, 1*(3), 259-272.

Vandiver, J. K., Dunwoody, A. B., Campbell, R. B., & Cook, M. F. (1982). A mathematical basis for the random decrement vibration signature analysis technique. *Journal of Mechanical Design-Transactions of the Asme, 104*(2), 307-313.

Vold, H., Kundrat, J., & Rocklin, G. T. (1986, February 3-6). *The numerical implementation of a multi-input modal estimation method for mini-computers.* Paper presented at the Proceedings of 4th International Modal Analysis Conference, Orlando, Florida, USA.

Vold, H., Kundrat, J., Rocklin, G. T., & Russell, R. (1982). A multi-input modal estimation algorithm for mini-computers. *SAE Technical Paper No. 820194*.

Wang, F., Ma, S. C., Wei, W., Zhang, Y., & Zhang, Z. Y. (2017). Frequency sweep test and modal analysis of watermelon during transportation. *International Journal of Food Engineering, 13*(5).

Wang, H., Mao, J. X., Huang, J. H., & Li, A. Q. (2016). Modal identification of sutong cable-stayed bridge during typhoon haikui using wavelet transform method. *Journal of Performance of Constructed Facilities, 30*(5).

Wang, H., Zou, K. G., Li, A. Q., & Jiao, C. K. (2010). Parameter effects on the dynamic characteristics of a super-long-span triple-tower suspension bridge. *Journal of Zhejiang University-Science A, 11*(5), 305-316.

Weijtjens, W., De Sitter, G., Devriendt, C., & Guillaume, P. (2014). Operational modal parameter estimation of MIMO systems using transmissibility functions. *Automatica, 50*(2), 559-564.

Weijtjens, W., Lataire, J., Devriendt, C., & Guillaume, P. (2014). Dealing with periodical loads and harmonics in operational modal analysis using time-varying transmissibility functions. *Mechanical Systems and Signal Processing, 49*(1-2), 154-164.

Wickramasinghe, V., Chen, Y., Zimcik, D., Tremblay, P., Dahl, H., & Walkty, I. (2013). Modal survey test and model correlation of the CASSIOPE spacecraft. *Experimental Techniques, 37*(6), 15-23.

William, T. T., & Marie, D. D. (1998). *Theory of Vibration with Applications* (Fifth ed.): New Jersey: Prentice Hall.

Wong, K.-Y. (2004). Instrumentation and health monitoring of cable-supported bridges. *Structural Control and Health Monitoring, 11*(2), 91-124.

Yan, S., Li, B., Li, F., & Li, B. C. (2017). Finite element model updating of liquid rocket engine nozzle based on modal test results obtained from 3-D SLDV technique. *Aerospace Science and Technology, 69*, 412-418.

Yu, L. L., & Song, H. W. (2017). Scaling mode shapes in output-only structure by a mass-change-based method. *Shock and Vibration*.

Zaghlool, S. A. (1980). Single-station time-domain (SSTD) vibration testing technique: Theory and application. *Journal of Sound and Vibration, 72*(2), 205-234.

Zhang, L., & Kanda, H. (1986). The algorithm and application of a new multi-input-multi-output modal parameter identification method. *Shock and Vibration Bulletin*, 11-17.

Zhang, L., Kanda, H., Brown, D., & Allemang, R. (1985). A polyreference frequency domain method for modal parameter identification. *ASME paper*(85-DET), 106.

Zhang, L., Kanda, H., & Lembregts, F. (1986, February 3-6). *Some applications of a frequency domain polyreference modal parameter identification method.* Paper presented at the Proceedings of the 4th International Modal Analysis Conference, Los Angeles, California, USA.

Zhang, L. M., Wang, T., & Tamura, Y. (2010). A frequency-spatial domain decomposition (FSDD) method for operational modal analysis. *Mechanical Systems and Signal Processing, 24*(5), 1227-1239.

Zhou, J. H., Chui, Y. H., Gong, M., & Hu, L. (2017a). Comparative study on measurement of elastic constants of wood-based panels using modal testing: choice of boundary conditions and calculation methods. *Journal of Wood Science, 63*(5), 523-538.

Zhou, J. H., Chui, Y. H., Gong, M., & Hu, L. (2017b). Elastic properties of full-size mass timber panels: Characterization using modal testing and comparison with model predictions. *Composites Part B-Engineering, 112*, 203-212.

Zhu, W. D., Zheng, N. A., & Wong, C. N. (2006). A Stochastic Model for the Random Impact Series Method in Modal Testing. *Journal of Vibration and Acoustics, 129*(3), 265-275.

LIST OF PUBLICATIONS AND PAPERS PRESENTED

1. Ong, Z. C., Lim, H. C., Khoo, S. Y., Rahman, A. G. A., & Ismail, Z. (2016). ***An experimental investigation on the effects of exponential window and impact force level on harmonic reduction in impact-synchronous modal analysis***. Journal of Mechanical Science and Technology, 30(8), 3523-3532. doi: 10.1007/s12206-016-0712-6
2. Ong, Z. C., Lim, H. C., Khoo, S. Y., Ismail, Z., Kong, K. K., & Rahman, A. G. A. (2017). ***Assessment of the phase synchronization effect in modal testing during operation.*** Journal of Zhejiang University-Science A, 18(2), 92-105. doi: 10.1631/jzus.A1600003
3. Ong, Z.C., Lim, H.C., & Brandt, A. (2018). ***Automated impact device with non-synchronous impacts: a practical solution for modal testing during operation.*** Journal of Zhejiang University-Science A. 19(6), 452-460
4. Lim, H.C., Ong, Z.C., & Brandt, A. (2018). ***Implementation of phase controlled impact device for enhancement of frequency response function in operational modal testing.*** Journal of the Franklin Institute. 355 (1), 291-313 doi: https://doi.org/10.1016/j.jfranklin.2017.11.031
5. Ong, Z.C., Lim, H.C., Brandt, A., Ismail, Z., & Khoo, S. Y. (2018). ***An inconsistent phase selection assessment for harmonic peaks elimination in operational modal testing.*** Archive of Applied Mechanics (Under Review, AAM-18-0208)
6. Lim, H.C., Ong, Z.C., Ismail, Z., & Khoo, S. Y. (2017). ***A performance study of controlled impact timing on harmonics reduction in operational modal testing.*** Journal of Dynamic Systems, Measurement, and Control (Under Review, DS-17-1338)
7. Lim, H.C., & Ong, Z.C. (2016). ***Development of adaptive phase control impact device for enhancement of frequency response function in operational modal testing.*** Proceedings of Isma2016 International Conference on Noise and Vibration Engineering and Usd2016 International Conference on Uncertainty in Structural Dynamics, 2849-2857.

PATENT

1. APPARATUS FOR PERFORMING MODAL ANALYSIS ON OBJECT (Auto Impact Device (AID) with non-synchronous time interval). (PI 2015701296)
2. APPARATUS FOR PERFORMING MODAL ANALYSIS (Adaptive Phase Control Impact Device (APCID)) (PI 2016701968)